

***Actinide Analysis and
Leaching of Samples
Collected from the Glovebox
Excavator Method Project for
OU 7-13/14***

*Gary S. Groenewold
William F. Bauer
Robert V. Fox
Bruce J. Mincher
Anita K. Gianotto*

**Idaho
Completion
Project**

Bechtel BWXT Idaho, LLC

April 2005

ICP/EXT-04-00439
Revision 0
Project No. 23378

Actinide Analysis and Leaching of Samples Collected from the Glovebox Excavator Method Project for OU 7-13/14

**Gary S. Groenewold
William F. Bauer
Robert V. Fox
Bruce J. Mincher
Anita K. Gianotto**

April 2005

**Idaho Completion Project
Idaho Falls, Idaho 83415**

**Prepared for the
U.S. Department of Energy
Assistant Secretary for Environmental Management
Under DOE Idaho Operations Office
Contract DE-AC07-99ID13727**

ABSTRACT

This report presents the results of analysis and actinide leaching studies of waste and soil samples collected during a waste retrieval demonstration (Glovebox Excavator Method Project) in Pit 9, which is part of the Subsurface Disposal Area. The Subsurface Disposal Area is a radioactive waste landfill located in the Radioactive Waste Management Complex at the Idaho National Laboratory in southeastern Idaho. Samples of both soil and waste were intentionally collected from the waste zone to ensure acquisition of actinide-contaminated material. Although actinide content of Pit 9 has been inferred from disposal records and confirmed by subsurface gamma probes, data from direct analysis of samples from this or other burial sites within the SDA are not available. Hence the samples from the Pit 9 waste retrieval presented a unique opportunity to measure actinide contamination, leaching, and speciation in material that has been buried more than 30 years.

Nearly all of the soil and waste samples were contaminated with plutonium, and most had elevated levels of uranium, americium, or neptunium. The $^{239}\text{Pu}/^{240}\text{Pu}$ and $^{239}\text{Pu}/^{241}\text{Am}$ isotope ratios indicated that much of the actinide contamination was derived from weapons-grade plutonium originating from Rocky Flats Plant. The most contaminated soil samples were collected (a) from soil caked to graphite mold fragments, and (b) after rupture of a jar containing graphite mold scarfings which contaminated the excavation area. Leaching of plutonium at ambient pH generated operational distribution coefficients (K_d) of about 10^3 mL/g for organic waste, 10^4 to 10^5 mL/g for low-contamination soil, and about 10^6 mL/g for highly contaminated soil, respectively. The K_d values are consistent with sequential aqueous extraction results that showed large percentages of plutonium in the nonextractable fraction. High K_d values were also measured for americium. Leaching studies of uranium and neptunium showed enhanced aqueous partitioning at pH values of ≤ 4 . Complete leaching as a function of pH and ionic strength and studies of sequential aqueous extraction were reported for uranium, neptunium, plutonium, and americium.

SUMMARY

This report presents the results of actinide analysis and aqueous leaching studies of waste and soil samples collected for the Operable Unit 7-13/14 Retrieved Waste and Soil Characterization Project during the Glovebox Excavator Method Project, a waste retrieval demonstration conducted at Pit 9, which is part of the Subsurface Disposal Area (SDA). The SDA is a radioactive waste landfill located in the Radioactive Waste Management Complex at the Idaho National Laboratory in southeastern Idaho. Although actinide content of Pit 9 has been inferred from disposal records and confirmed by probes that measure gamma activity from within the burial, little information has been available from direct analysis of samples from burial sites within the SDA. These samples from Pit 9 represent a unique opportunity to examine samples that have been buried more than 30 years for actinide contamination, leaching, and operational speciation. The data acquired from this study have many potential uses, which include providing contamination information and distribution coefficient (K_d) values, which can be compared with values being used for actinide release from the source term and the surrounding soil.

In early 2004, the Glovebox Excavator Method Project retrieved approximately 75 m³ of soil and waste material from the SDA. During waste retrieval, a total of 36 interstitial soil samples (i.e., soil residing between waste materials) and eight waste samples were collected. The sample collection process was secondary to the waste retrieval, which used a backhoe in an enclosure designed to mitigate release of radioactive particulates. Sample collection was biased toward acquisition of contaminated material, and was not conducted to provide a spatially representative characterization of the site.

For the purpose of facilitating communication of the actinide concentration results, the 36 interstitial soil samples were grouped into five categories based on appearance and on the results of the actinide analyses:

1. Clean or nearly clean (four samples)
2. Low-contamination (13 samples)
3. Mixed soil-waste (nine samples)
4. Soil scraped from graphite (one sample)
5. Soil after rupture of graphite scarfings jar (nine samples).

The last category emerged as a result of the backhoe intentionally rupturing a plastic jar containing graphite scarfings, which caused a fine dusting of scarfings across the excavation. After this event, apparently clean soil samples had high actinide concentrations and thus constituted a separate category of samples. Eight waste samples were categorized as:

6. Organic waste
7. Unknown waste type I
8. Unknown waste type II.

Actinide concentrations in the clean soil were below detection limits for all isotopes except for ^{240}Pu , which suggested that both clean soil could be acquired without mixing from the excavation process, and that there was low-plutonium contamination of unknown origin above fallout levels. Other soil samples varied from apparently clean to obviously mixed with waste, but all had detectable ^{239}Pu in concentrations that ranged from the detection limit (about 20 ng/g) to about 700 ng/g. Many also contained ^{235}U , ^{238}U , ^{240}Pu , and ^{241}Am at lower concentrations, particularly those that were mixed with waste. The $^{239}\text{Pu}/^{240}\text{Pu}$ and $^{239}\text{Pu}/^{241}\text{Am}$ isotope ratios in these samples were similar to the ratios for samples contaminated with actinide elements from the jar rupture, and were characteristic of weapons-grade plutonium. The highest concentrations of transuranic actinide elements were measured in one soil sample that was scraped from graphite mold fragments and in soil samples collected after the jar rupture.

Actinide concentrations in the waste samples were variable; for example, ^{239}Pu ranged from 80 to 4,900 ng/g. Uranium concentrations were high in six of the eight waste samples (to 220,000 ng/g ^{238}U). Isotope ratios suggested a Rocky Flats Plant origin for several of these samples, and also indicated a different process origin for two of the organic waste samples, three of the unknown waste samples, and three or four of the mixed waste-soil samples. Higher fractions of ^{241}Am also suggested that these samples were derived from other processes.

Actinide leaching was dependent on pH and nature of the sample matrix, but was independent of ionic strength (I). The results produced two generalizations. First, K_d values were largest for (a) soil samples scraped from graphite mold fragments, and (b) soil samples contaminated from the jar rupture. Somewhat smaller K_d values were measured for the low-contamination soil samples, and K_d values were smallest for the waste samples. Second, actinide distribution coefficients K_d decreased one to two orders of magnitude at acidic pH values (<4).

Uranium and neptunium displayed decreased K_d values at near neutral pH, which were most pronounced for the waste samples; hence, these actinide elements are those most likely to dissolve. Plutonium leaching was characterized by K_d values of about 10^3 mL/g in organic waste samples, 10^4 to 10^5 mL/g in low-contamination soil samples, and about 10^6 mL/g in soil samples that were contaminated by graphite molds and by the jar rupture. The results suggested that any plutonium that dissolves from the organic waste will be aggressively adsorbed by the adjacent soil, and further that leaching from the soil contaminated by the graphite mold or the jar rupture is very unlikely unless significant changes in chemistry occur. Leaching of americium is also likely to be very limited; K_d values of about 10^5 mL/g were measured at ambient pH.

Sequential aqueous extraction (SAE) experiments were used to characterize actinide contamination in terms of five categories of operational speciation: (1) cation exchangeable, (2) carbonate bound, (3) oxidizable, (4) reducible, and (5) residual. Uranium displayed an impressive range of operational speciation, depending on the pH and the nature of the sample. Large percentages of uranium were contained in the residual fraction in natural soil samples, low-contamination soil samples, and the highly plutonium-contaminated soil samples from the jar rupture event. In other samples, the

oxidizable fraction was frequently the most important, which suggested that uranium is susceptible to oxidation and subsequent dissolution.

A large percentage of the plutonium in low-contamination soil samples resided in the oxidizable SAE fraction, which suggested that plutonium species present in the IV oxidation state were susceptible to oxidation to Pu(V) or Pu(VI) species that are more soluble. A large percentage of oxidizable plutonium was also measured in the mixed soil-waste samples, although large percentages were also measured in the reducible or residual fractions, depending on the individual sample. The largest percentage of the plutonium in the soil sample scraped from graphite was in the residual fraction, although a substantial percentage was oxidizable. Plutonium in the soil samples contaminated by the jar rupture overwhelmingly resided in the residual fraction, which was consistent with the very high K_d values measured for these samples. In two of the three waste samples, plutonium was also primarily in the residual fraction. In the third organic waste sample, plutonium resided mainly in the reducible fraction, which suggested binding to iron oxide in that sample.

Americium in the soil sample scraped from graphite and in the organic waste samples was predominantly in the residual SAE fraction, although the reducible and oxidizable fractions were also substantial. The tendency for nonleachable americium species was even greater in the soil samples contaminated by the jar rupture, with nearly all of the americium residing in the residual. Limited SAE studies for neptunium showed that in the soil sample scraped from graphite and in organic waste samples, the largest percentage of neptunium was found in the oxidizable fraction, although the carbonate-bound fraction was also substantial. These results are consistent with the more extensive leaching behavior of neptunium.

CONTENTS

ABSTRACT.....	iii
SUMMARY	v
ACRONYMS.....	xv
1. INTRODUCTION.....	1
1.1 Purpose	3
1.2 Scope	3
1.3 Site Background	4
1.3.1 Location and Description	4
1.3.2 Physical Characteristics.....	4
1.3.3 Surface and Subsurface Geology	5
1.4 Document Organization.....	6
2. BACKGROUND AND OVERVIEW	8
2.1 Pit 9 Background	8
3. DESCRIPTION OF SAMPLE CHARACTERIZATION	11
3.1 Observation of Excavation and Sample Collection Activities	11
3.2 Gamma Spectroscopy Screening of Samples	11
3.3 Visual Inspection of Samples and Subsampling.....	11
3.4 Total Actinide Analyses	11
3.5 Actinide Leaching	12
3.6 Sequential Aqueous Extraction	12
3.7 Surface Characterization	12
4. DESCRIPTION OF SAMPLE COLLECTION	13
4.1 Excavation	13
4.2 Field Observations.....	14
4.2.1 Potential Mixing and Cross-Contamination from Excavator Operation	17
4.3 Sample Collection	17

4.3.1	Waste Samples	17
4.3.2	Interstitial Soil Samples	18
4.3.3	Benchmark Soil Samples	18
4.4	Sample Categorization.....	18
5.	PHOTOGRAPHIC SAMPLE CATEGORIZATION.....	20
6.	GAMMA SPECTROSCOPY SCREENING.....	24
7.	TOTAL ACTINIDE ANALYSES	27
7.1	Concentrations of Actinide Elements in Interstitial Soil and Waste Samples.....	31
7.2	Isotope Ratios of Actinide Elements in Interstitial Soil and Waste Samples.....	33
8.	LEACHING.....	39
8.1	Distribution Coefficients (K_d) at Ambient pH.....	40
8.2	Distribution Coefficients (K_d) as a Function of pH and I	43
8.3	Uranium K_d as a Function of pH and I	43
8.4	Plutonium K_d as a Function of pH and I	46
8.5	Americium K_d as a Function of pH and I	48
8.6	Neptunium K_d as a Function of pH and I	49
8.7	Thorium K_d as a Function of pH and I	50
8.8	Lead K_d as a Function of pH and I	51
9.	SEQUENTIAL AQUEOUS EXTRACTION.....	53
9.1	Operational Speciation of Uranium.....	54
9.2	Operational Speciation of Plutonium	58
9.3	Operational Speciation of Americium.....	61
9.4	Operational Speciation of Neptunium	63
10.	SURFACE CHARACTERIZATION.....	64
10.1	Negative Ion SIMS spectra.....	64
10.2	Positive Ion SIMS Spectra.....	67
10.3	Development of Empirical Method for Identification of Sample Type.....	68

11.	SUMMARY OF PROJECT SAMPLE MANAGEMENT	69
11.1	Handling of Retrieved Waste and Soil Characterization Project Samples	69
11.2	Handling of Retrieved Waste Soil Characterization Project Sample Waste	70
12.	SUMMARY	71
12.1	Caveats Related to Sample Collection.....	71
12.2	Actinide Contamination.....	71
12.3	Aqueous Partitioning of Actinide Contaminants.....	73
12.4	Operational Speciation	74
13.	REFERENCES	75
	Appendix A—Elemental Analyses and Soluble Soil Cations of Six Uncontaminated RWMC Soil Samples	79
	Appendix B—Field Observations Sampling Guidance	83
	Appendix C—Sample Descriptions	91
	Appendix D—Gamma Spectroscopy Screening.....	157
	Appendix E—Total Actinide Analyses.....	165
	Appendix F—Leaching Studies	179
	Appendix G—Sequential Aqueous Extraction	195
	Appendix H—Surface Characterization Using Ion Trap Secondary Ion Mass Spectrometry	203
	Appendix I—Glovebox Excavator Method Project Sample Repackaging	211

FIGURES

1.	Map of the Idaho National Laboratory showing the location of the Radioactive Waste Management Complex and other major facilities.....	2
2.	Map of the Radioactive Waste Management Complex showing the location of the Subsurface Disposal Area.	5
3.	Fan-shaped excavation area showing the location of probes, adapted from DOE-ID (2004).	13
4.	Schematic diagram of the vertical profile of the Pit 9 excavation, adapted from DOE-ID (2004).	14
5.	Photographs of two samples initially categorized as clean soil: upper left and upper right, Sample T09; lower left and lower right, Sample T32.	20

6.	Photographs of two typical mixed soil-waste samples: upper left and upper right, Sample T07; lower left and lower right, Sample T27.	21
7.	Photographs of a probable organic sludge: upper left and upper right, Sample R04; a mixed soil-waste sample: lower left and lower right, Sample R20.	22
8.	Photographs of two unknown waste samples: upper left and upper right, Sample P03; lower left and lower right, Sample P04, which contains pieces of concrete.	23
9.	Comparison of ^{241}Am activity determined by gamma spectroscopy and ICP-MS for interstitial soil samples and samples representing inorganic and organic sludge.	25
10.	Plots of (A) $[^{239}\text{Pu}]$ versus $[^{241}\text{Am}]$, and (B) the $^{239}\text{Pu}/^{241}\text{Am}$ isotope ratio versus $[^{241}\text{Am}]$. Lines have been drawn to highlight the difference in the $^{239}\text{Pu}/^{241}\text{Am}$ ratio for different sample types. ...	35
11.	^{239}Pu concentration versus ^{237}Np concentration in soil and waste samples. Lines have been drawn to highlight the difference in the $^{239}\text{Pu}/^{237}\text{Np}$ ratio for different sample types.	38
12.	Average K_d values for the leaching of ^{238}U with low-ionic-strength leachate (deionized water) and high-ionic-strength leachate (100 mM NaCl) as a function of pH for interstitial soil samples and organic waste.	44
13.	Uranium K_d values (triangular data points, left-hand y axis) and $^{238}\text{U}/^{235}\text{U}$ ratios (square data points, right-hand y axis) as a function of pH for the interstitial soil sample T03.	45
14.	Uranium K_d values (triangular data points, left-hand y-axis) and $^{238}\text{U}/^{235}\text{U}$ ratios (square data points, right-hand y-axis) as a function of pH for the high-plutonium interstitial soil samples.	46
15.	Average K_d values for leaching ^{239}Pu with low-ionic-strength leachate (deionized water) and high-ionic-strength leachate (100 mM NaCl) as a function of pH for interstitial soil samples and organic waste.	47
16.	Average K_d values for leaching ^{241}Am with low-ionic-strength leachate (deionized water) and high-ionic-strength leachate (100 mM NaCl) as a function of pH for interstitial soil samples and organic waste samples. Gaps in data sets represent measurements for which ^{241}Am was below detection limits.	48
17.	Average K_d values for the leaching of ^{237}Np with low-ionic-strength leachate (deionized water) and high-ionic-strength leachate (100 mM NaCl) as a function of pH for interstitial soil samples and organic waste samples. Gaps in data sets represent measurements for which ^{237}Np was below detection limits.	49
18.	Average K_d values for the leaching of ^{232}Th with low-ionic-strength leachate (deionized water) and high-ionic-strength leachate (100 mM NaCl) as a function of pH for interstitial soil samples and organic waste samples. Gaps in data sets represent measurements for which ^{232}Th was below detection limits.	50
19.	Average K_d values for the leaching of lead with low-ionic-strength leachate (deionized water) and high-ionic-strength leachate (100 mM NaCl) as a function of pH for interstitial soil samples and organic waste samples.	51

20.	SAE dissolution profile for ^{238}U present in blank INL soil plutonium-spiked blank, and an average of overburden soil samples W09, W13, and W15.....	54
21.	SAE dissolution profile for ^{238}U present in low-contamination soil samples T08, T09, and T10.....	55
22.	SAE dissolution profile for ^{238}U and ^{235}U present in interstitial soil samples T03, T05, T07, and T17.	56
23.	SAE dissolution profile for ^{238}U and ^{235}U present in the highly plutonium-contaminated interstitial soil samples.	57
24.	SAE dissolution profile for ^{238}U and ^{235}U present in probable organic waste samples R04, R20, and R23.	58
25.	Plutonium-SAE dissolution profiles for the spiked soil, and the low-contamination soil samples T08, T09, and T10. Data are plotted together with data from SAE analysis of plutonium-spiked INL blank soil.	59
26.	Plutonium-SAE dissolution profiles for mixed soil-waste samples T03, T05, T07, and T17.....	59
27.	Plutonium-SAE dissolution profiles for high-plutonium soil samples.....	60
28.	Plutonium-SAE dissolution profiles for probable organic sludge samples R04, R20, and R23.....	61
29.	Americium-SAE dissolution profiles for interstitial soil samples T27, T32, and T34.....	62
30.	Americium-SAE dissolution profiles for probable organic sludge samples R04 and R20.....	62
31.	Neptunium-SAE dissolution profiles for probable organic sludge sample R20 and interstitial soil sample T27.....	63
32.	Averaged negative ion SIMS spectra: (a) overburden soil samples, (b) organic waste samples R20 and R23, (c) organic waste sample R04.....	65
33.	Anion spectra of unknown waste samples P01, P02, P03, P04, and P05.....	66
34.	Averaged positive ion SIMS spectra of (a) overburden soil samples and (b) organic waste samples R20 and R23.	67
35.	Photograph of RWSC sample P9GT04016G (left), wrapped in radioactive material handling sack (right).....	69
36.	Photograph of Drum #1 contents (left) and lid (right) before shipment to storage facility.	70

TABLES

1.	Percentage compositions of actinides derived from Rocky Flats Plant and reactor-grade plutonium, (DOE/RFP-CO 2003; Carlson et al. 2005) and the changes in this composition at T = 0, 30, 50, and 100 years.	9
2.	Sample categories based on visual field and visual laboratory observations.	15
3.	Ranges of actinide and lead concentrations for categories of interstitial soil and waste samples. All values are reported in units of ng/g. Values underlined are above or below the significance criteria for that isotope (equal to the mean $\pm t_{(p=0.01)} \times$ standard deviations of the blank INL soil samples). Values in red are greater than the significance criteria, and those in blue samples are less than. Results for individual samples are provided in Appendix E, Table E-1.	29
4.	Ranges of ambient pH and K_d values for categories of down-selected samples. Measurements were conducted using low I leachate solutions. Since there was a single sample for the category “soil scraped from graphite” (T27), the average value was provided with the error bars for that measurement.	42

ACRONYMS

ICP-MS	inductively coupled plasma mass spectrometry
INL	Idaho National Laboratory
INTEC	Idaho Nuclear Technology and Engineering Center
OU	Operable Unit
RFP	Rocky Flats Plant
RI/FS	remedial investigation/feasibility study
RWMC	Radioactive Waste Management Complex
SAE	sequential aqueous extraction
SDA	Subsurface Disposal Area
SIMS	secondary ion mass spectrometry
SRPA	Snake River Plain Aquifer
WAG	Waste Area Group

Actinide Analysis and Leaching of Samples Collected from the Glovebox Excavator Method Project for OU 7-13/14

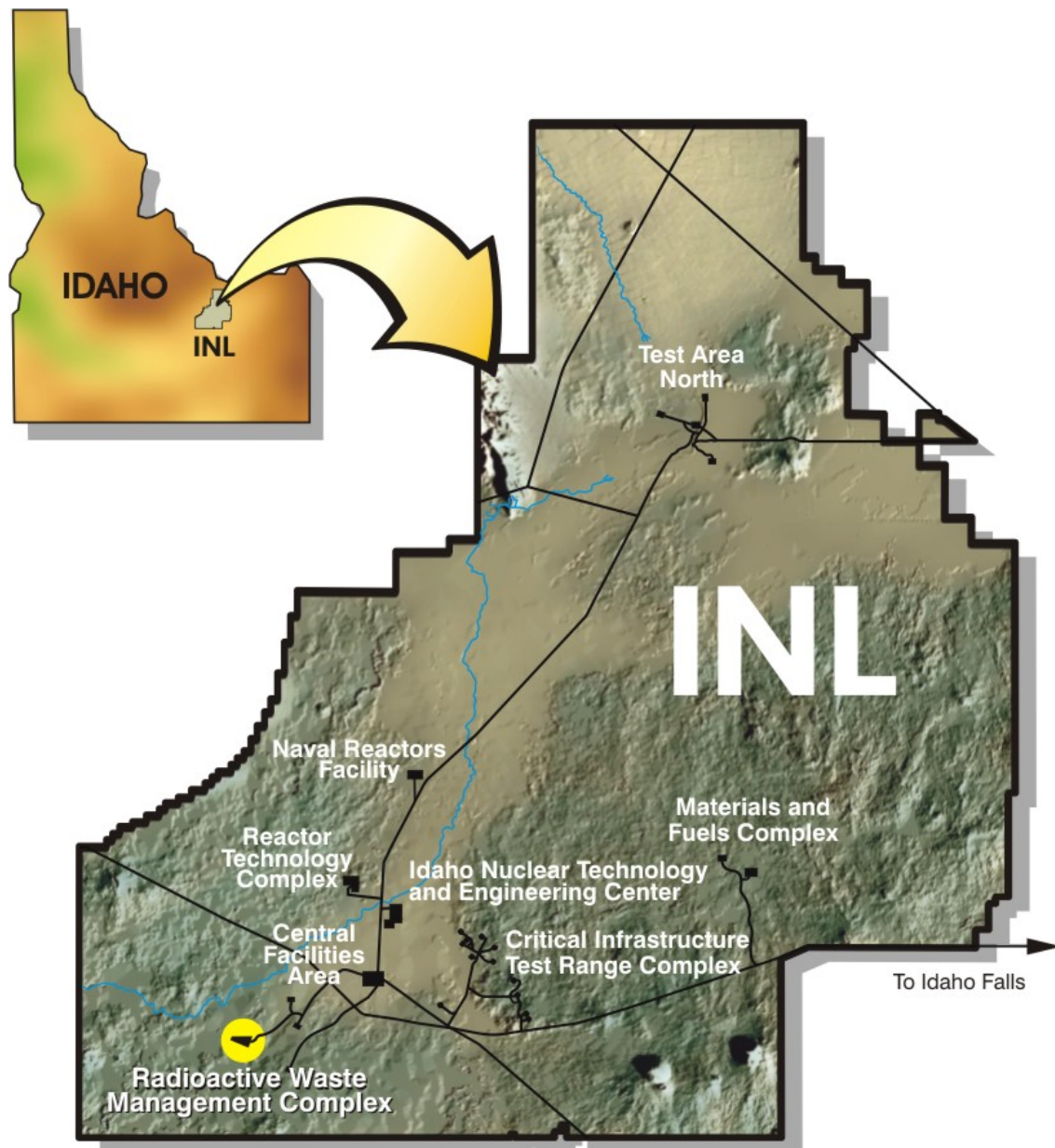
1. INTRODUCTION

This report presents the results of analysis and characterization of waste and soil samples collected for the Retrieved Waste and Soil Characterization Project during the waste retrieval demonstration in Pit 9 by the Operable Unit (OU) 7-10 Glovebox Excavator Method Project^a (DOE-ID 2004). Pit 9 is part of the Subsurface Disposal Area (SDA), which is a radioactive waste landfill located in the Radioactive Waste Management Complex (RWMC) at the Idaho National Laboratory (INL) in southeastern Idaho (see Figure 1). During the waste retrieval project, the opportunity arose for collection of samples of both soil and waste from the waste zone. Samples were collected on behalf of OU 7-13/14, the comprehensive remedial investigation/feasibility study for the RWMC. Although probable actinide content of Pit 9 had been inferred from disposal records and confirmed by probes that measure gamma activity from within the burial site (DOE-ID 2004; Holdren et al. 2002), little information has been available from direct analysis of samples from this or other burial sites within the SDA. These samples from Pit 9 presented a unique opportunity to examine samples that have been buried more than 30 years for actinide contamination, leaching, and operational speciation.

The sampling effort at Pit 9 was aimed at acquiring waste and interstitial soil samples specifically to identify the actinide isotopes present, their concentrations, and their dissolution behavior. A total of 36 interstitial soil samples, three organic sludge samples, five unknown waste samples, and seven benchmark soil samples (from the overburden and outside the fence line) were collected and analyzed for actinides using inductively coupled plasma-mass spectrometry (ICP-MS). A subset of 26 interstitial soil samples, three waste samples, and four benchmark soil samples were tested for actinide leaching behavior. A reduced subset of 10 interstitial soil samples, three waste samples, and four overburden soil samples were studied to determine operational speciation using sequential aqueous extraction (SAE). Samples in the subsets were selected to span a range of sample categories and contaminant concentrations. In addition, the surface chemistry of all samples was interrogated using secondary ion mass spectrometry (SIMS).

The objective of the Glovebox Excavator Method Project was to demonstrate waste retrieval, and because of radioactivity considerations, did not overtly support sample acquisition. Thus, sample acquisition was opportunistic, and not designed to generate a statistically defensible description of the extent of actinide contamination, either from a concentration or from a spatial perspective. Because the composition and structure of the SDA subsurface is extremely variable, production of a statistically valid understanding of the spatial distribution of the actinide contamination is beyond the present scope. Instead, sample collection was biased toward acquisition of actinide-contaminated material to understand better the source chemistry. This will enable comparisons of:

a. The samples were taken during operations of the OU 7-10 Glovebox Excavator Method Project, which retrieved 75 m³ of buried waste from the SDA during December 2003 and January 2004 (DOE-ID 2004). The purpose of the Glovebox Excavator Method Project was to demonstrate the feasibility of waste retrieval, provide information on any contaminants of concern present in the underburden, and characterize waste zone material for safe and compliant storage pending a decision on final disposition. The Glovebox Excavator Method Project operated under the *Federal Facility Agreement and Consent Order for the Idaho National Engineering Laboratory* (DOE-ID 1991) and the "Comprehensive Environmental Response, Compensation, and Liability Act of 1980 (CERCLA/Superfund)" (42 USC § 9601 et seq., 1980).



G1468-01

Figure 1. Map of the Idaho National Laboratory showing the location of the Radioactive Waste Management Complex and other major facilities.

- Actinide elements present in the samples that have historical disposal records
- Measured isotope ratios with those expected from weapons fabrication with those derived from other processes
- Leaching parameters with values used in transport modeling, and derived from previous laboratory and field studies.

The studies provide contaminant concentration values from materials from an actual radioactive waste disposal pit; there are few such measurements in the literature, and none associated with Pit 9 or any part of the SDA.

Nearly all of the soil and waste samples were contaminated with plutonium, and most had elevated levels of uranium, americium, or neptunium. The $^{239}\text{Pu}/^{240}\text{Pu}$ and $^{239}\text{Pu}/^{241}\text{Am}$ isotope ratios were consistent with actinide contamination derived from weapons-grade plutonium originating from the Rocky Flats Plant (RFP).^b The most contaminated soil samples were collected: (a) from soil caked to graphite mold fragments, and (b) after rupture of a jar containing graphite mold scarfings^c that contaminated the excavation area. Leaching of plutonium at ambient pH generated distribution coefficients (K_d) of about 10^3 mL/g for organic waste, 10^4 to 10^5 mL/g for low-contamination soil, and about 10^6 mL/g for highly contaminated soil, respectively. The highest values were consistent with SAE results that showed large percentages of plutonium in the nonextractable fraction. High K_d values were also measured for americium. Leaching studies of uranium and neptunium showed enhanced aqueous partitioning at modest acidic solution pH values. Complete leaching as a function of pH and ionic strength, and SAE studies were reported for uranium, neptunium, plutonium, and americium.

1.1 Purpose

The purpose of this study is to provide detailed data on contaminant identity, contaminant concentration, and distribution coefficient (K_d) values for the source term and for the surrounding soil specific to the Pit 9 burial. The data can be compared with values currently used in fate and transport modeling supporting the remedial investigation/feasibility study (RI/FS) for Waste Area Group (WAG) 7,^d OU 7-13/14. A secondary intention is to provide speciation information on the actinides in the waste and soil that provide a starting point for future chemistry investigations. Note that samples collected from a single location within one of ten pits containing RFP waste may not be representative of other locations.

1.2 Scope

The sample characterization project consists of measuring the actinide content, concentration, leachability, and operational speciation in 36 interstitial soil samples, five unknown waste samples, three organic sludge samples, six overburden soil samples collected during the demonstration excavation (Glovebox Excavator Method Project) in Pit 9, and one soil blank sample collected outside the RWMC fence line. The samples for this study were biased since they were collected from the freshest material in the excavation (Salomon 2003) rather than statistically representative samples. The biased grab sampling was directed during the excavation on the basis of waste form appearance, by field representatives trained to recognize original descriptions of the waste as interred 35–50 years previously. A down-selected set of samples was used to evaluate leaching and operational speciation. Results of the following activities are included in this report:

b. The Rocky Flats Plant is located 26 km (16 mi) northwest of Denver, Colorado. In the mid-1990s, it was renamed the Rocky Flats Environmental Technology Site. In the late 1990s, it was again renamed, to its present name, the Rocky Flats Plant Closure Project. Most of the transuranic waste buried in the Subsurface Disposal Area originated at the Rocky Flats Plant.

c. “Scarfings” refer to fragments of graphite molds that constitute a portion of the waste.

d. Each of 10 WAGs identified by the FFA/CO is subdivided into OUs. The RWMC is identified as WAG 7 and originally contained 14 OUs. Operable Unit 7-13 (transuranic pits and trenches RI/FS) and OU 7-14 (WAG 7 comprehensive RI/FS) were ultimately combined into the OU 7-13/14 comprehensive RI/FS for WAG 7.

- Description of sample collection
- Photographic sample categorization
- Gamma spectroscopy screening
- Total actinide analyses
- Actinide leaching
- Sequential aqueous extraction
- Surface characterization.

1.3 Site Background

1.3.1 Location and Description

The INL is a U.S. Department of Energy-managed reservation that historically has been devoted to energy research and related activities. The laboratory was originally established in 1949 as the National Reactor Testing Station before being renamed, and early in its history was used for subsurface disposal of nuclear waste because of its remote location and perceived lack of risk to human population and the environment. Waste interment activities were localized at RWMC, which is located in the southwestern quadrant of INL (see Figure 1) and encompasses a total of 72 ha (177 acres). The RWMC contains the SDA, which was originally established in 1952 and covered 5.2 ha (13 acres) that was used for shallow land disposal of radioactive waste. In 1958, the landfill was expanded to 35.6 ha (88 acres). Relocating the security fence in 1988 to outside the dike surrounding the landfill established the current size of the SDA at 39 ha (97 acres) (see Figure 2).

The particular burial pit that is the subject of this report is Pit 9, OU 7-10 within the SDA. The OU 7-10 project was conceived as a demonstration to retrieve waste and contaminated soil, and Pit 9 was chosen as the demonstration site because it was the pit that was most recently used, and therefore has the most complete disposal records (Eisenbud and Gesell 1997). To provide perspective, the excavated retrieval area from which samples in this study were collected was approximately 1% of Pit 9, and Pit 9 is one of several pits containing transuranic waste (Vejvoda 2005). The putative inventory of contaminants in Pit 9 is based on available shipping records, process knowledge, and written correspondence at INL. RFP was the most important source of transuranic waste buried in Pit 9. The mission of the RFP was production of plutonium components for nuclear weapons, and hence much of the waste generated contained actinide contaminants. It has been estimated that approximately 3,115 m³ (110,000 ft³) of the waste generated at RFP was shipped to the INL (DOE-ID 2004).

1.3.2 Physical Characteristics

The Snake River Plain Aquifer (SRPA) underlies the SDA at an approximate depth of 177 m (580 ft) and flows generally northeast to southwest, and is considered to be one of the most productive in the United States (Geslin et al. 2002). Infiltration of water occurs episodically from rain, flood, and snowmelt because the Snake River Plain is an arid environment with an average annual precipitation of only 23 cm/year (9 in./year). However, the SDA is situated in a natural topographic depression that tends to hold precipitation and to collect additional run-off from the surrounding slopes. Surface water either eventually evaporates or infiltrates into the vadose zone (i.e., the unsaturated subsurface) and underlying aquifer. Historically, the SDA has been flooded by local run-off at least three times because of a combination of snowmelt, rain, and warm winds (Becker et al. 1996). Dikes and drainage channels were constructed around the perimeter of the SDA in 1962 in response to the first flooding event. Height of the

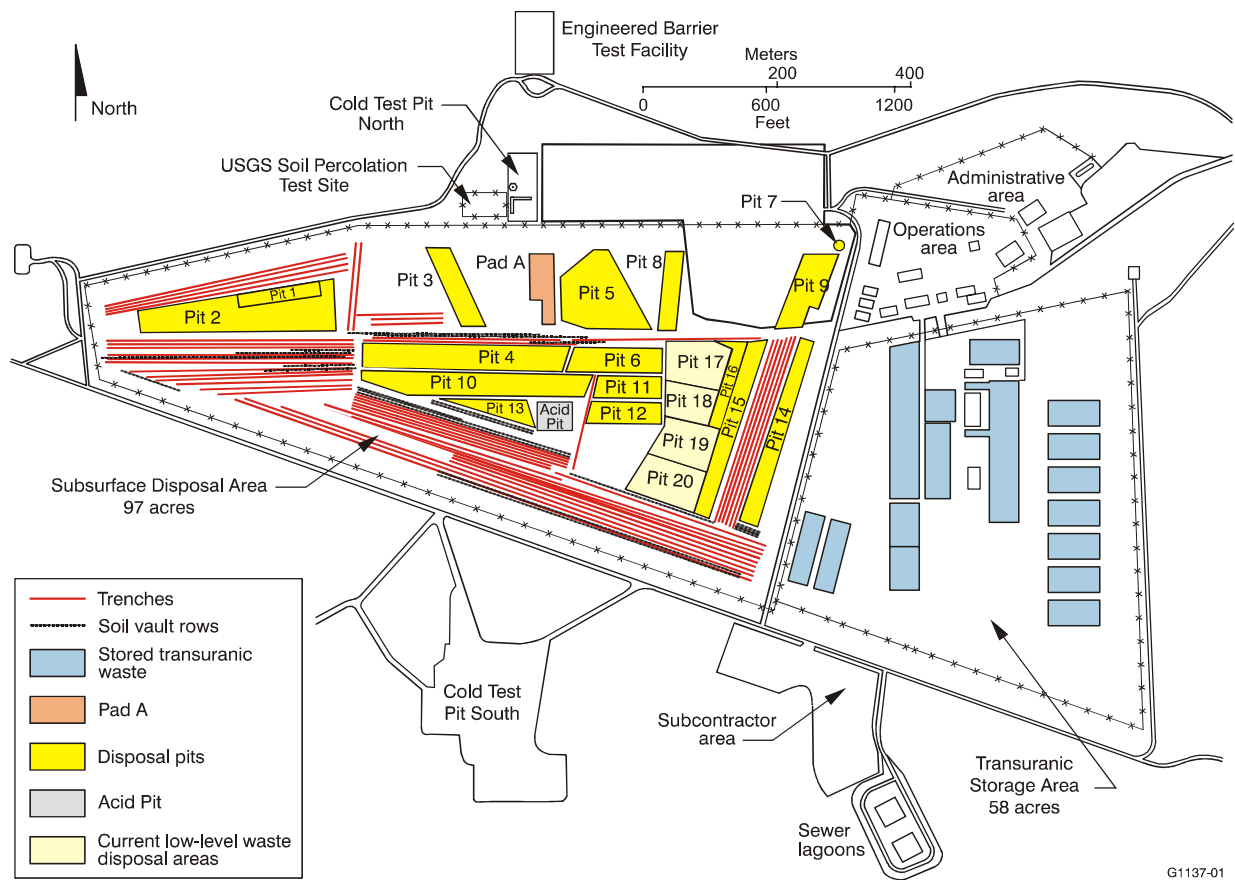


Figure 2. Map of the Radioactive Waste Management Complex showing the location of the Subsurface Disposal Area.

dike was increased and the drainage channel was enlarged, following a second flood in 1969. The dike was breached by accumulated snowmelt in 1982, resulting in a third inundation of the SDA. Significant flood-control improvements were subsequently implemented, which included increasing height and width of the dike, deepening and widening the drainage channel, and contouring the surface to eliminate formation of surface ponds within the SDA (Becker et al. 1996; Becker et al. 1998; Holdren et al. 2002).

Under typical conditions, the soil horizon at the SDA is unsaturated most of the year and underlying formations are characterized as a vadose zone. The deep vadose zone is considered to be the principal protector of the aquifer, and comprises surficial sediments (approximately 10 m) that overlie alternating layers of fractured basalt and sedimentary deposits called interbeds. The waste at the SDA was interred in the surficial sediments, which are the result of fluvial, lacustrine, and aeolian deposition and have little stratigraphic layering.

1.3.3 Surface and Subsurface Geology

The potential for interaction of actinide elements with surficial soil in and around the SDA makes the nature of this soil an important consideration. The surficial soil ranges from calcareous silty-loams to calcareous silty-clays and is typical of soil found in the western United States. INL surficial soil contains an unusually high concentration of clay-sized ($<2 \mu\text{m}$) quartz particles. Sediment mineralogy by X-ray diffraction typically shows about 50–75% quartz, 10–25% plagioclase and potassium-feldspar, 10–25% clay minerals, $<5\%$ olivine and pyroxene diopside, and $<5\%$ calcite (Bartholomay 1990; Bartholomay,

Knobel, and Davis 1989; Bartholomay 1995; Liszewski, Rosentreter, and Miller 1997; Liszewski et al. 1998; Mincher et al. 2003; Rightmire and Lewis 1987; Rosentreter et al. 1999). Individual samples can deviate from the average by up to a factor of four, depending on the location and depth of the sample: for example, a sample collected from the 18-ft level near the SDA contained about 70% clay, 25% quartz, and 5% feldspars.

The composition of the clay fraction is of particular interest because it can strongly bind cations, and would be expected to be a strong retarding factor in the movement of actinide elements in the subsurface. The clay fraction in the SDA soil is principally a mixed illite-smectite that comprises approximately 50–70% of the clay minerals, with kaolinite, illite, and calcium and sodium-rich smectites comprising the remaining fraction. In general, clays with higher smectite content would be expected to provide stronger cation binding resulting from the availability of inter-sheet sites from which cation desorption is very slow.

RWMC surficial sediments are practically devoid of organic matter, which is an important consideration since previous SAE studies (Mincher 2004) have shown that plutonium tends to localize with the “organic” fraction (Asbury 2001; Ibrahim and Morris 1997; Komosa 1999; Komosa 2002; Litaor 1996; Mincher 2001; Mincher 2003). Soil carbonates vary widely, from 0.1 wt% to as high as 30 wt%, which is consistent with soil pH values ranging from 7.5 to 8.2. Cation exchange capacities ranging from 10 to 25 milliequivalents per 100 g have been measured. These observations are consistent with the elemental analyses and analyses of soil exchangeable cations (Tables A-1 and A-2, Appendix A), which show that Ca^{2+} , Mg^{2+} , Na^{+} , K^{+} are present, but that Cs^{+} and Ba^{2+} are also surprisingly important. Soluble soil anions include high levels of soluble NO_3^{-} salts, and sedimentary SO_4^{2-} is probably due to the presence of gypsum. Depending on location and depth, surface area (specific surface) for bulk soil samples can vary from 15 to 36 m^2/g . The average pore size is 26 angstroms.

The soil also contains substantial iron, which is known to foster cation adsorption. A combination of SAE and Mössbauer spectroscopy indicated about 75% of the sedimentary iron is associated with illite clay, while about 15% is associated with hematite and about 10% is associated with poorly crystalline, small-particulate iron oxide minerals (e.g., ferrihydrite). These data were consistent with the reactive surfaces of INL SDA sediments being dominated by illite clays and quartz, with iron oxides being a relatively minor constituent.

1.4 Document Organization

This report contains thirteen sections. A summary of each section follows:

- Section 1 contains introductory information about this report and INL.
- Section 2 summarizes background information on buried radionuclides at Pit 9.
- Section 3 provides a summary description of the sample characterization activities.
- Section 4 details the sample collection process.
- Section 5 includes the results of the photographic inspections that were combined with the field observations and field categorizations.
- Sections 6 through 10 address the following studies, respectively: gamma spectroscopy, total actinide analyses, leaching behavior, SAE, and SIMS.

- Section 11 describes the management of the waste materials that were produced by the analysis and leaching studies;
- Section 12 summarizes the report
- Section 13 lists all the references cited in this report.
- Appendix A contains elemental analyses of soluble soil cations.
- Appendix B provides field observations from the excavation of Pit 9 as they apply to the samples analyzed.
- Appendix C provides complete sample descriptions.
- Appendix D includes the gamma spectroscopy screening results.
- Appendix E contains the complete compilation of actinide measurements by ICP-MS and calculated isotope ratios for all samples.
- Appendix F presents the data for the ratio of the concentration of the contaminant sorbed to the concentration in the aqueous phase ($K_d = C_{\text{solid}}/C_{\text{aqueous}}$).
- Appendix G summarizes the SAE results.
- Appendix H reviews the surface characterization procedure and data.
- Appendix I provides details for unaltered sample material and sample waste repackaging.

2. BACKGROUND AND OVERVIEW

Pit 9 is located within the SDA, a radioactive waste landfill with shallow subsurface disposal units consisting of pits, trenches, and soil vaults in rows. Contaminants in the landfill include hazardous chemicals and radionuclides derived from many sources, and include fission and activation products from reactor operations, and actinide elements from weapons manufactured at RFP. Pit 9 received a variety of defense- and reactor-related waste from RFP and INL that included uranium, neptunium, plutonium, and americium isotopes. Probable actinide content of Pit 9 has been inferred from disposal records and confirmed from probes that measure gamma activity from within the burial site. However, there is very little information from direct analysis of samples from this or other burial sites within the SDA because of a historical lack of sampling campaigns aimed at acquiring waste and interstitial soil samples specifically for physical and chemical characterization of interred material.

In the more than 30 years since Pit 9 was first used, it has been subjected to infiltrating water resulting from spring snowmelt and percolating rainwater. Because the infiltrating water may percolate all the way to the SRPA, Pit 9 may represent a contamination threat arising from actinide solubilization and transport. As noted in the Pit 9 Interim Action Record of Decision, analytical results indicated that minute amounts of anthropogenic radionuclides had migrated from the SDA toward the SRPA (DOE-ID 1993). A total of 352 vadose zone core samples collected during well drilling were analyzed for $^{239/240}\text{Pu}$ between 1971 and 2000 (Holdren et al. 2002). Twenty-nine positive detections, including duplicates, were identified; however, nine of those were suspect because of well drilling and sampling methods used in the early 1970s (see Section 4.5.5 of Holdren et al. [2002]). Many of the positive detections were duplicate samples and no trends were apparent. Thus, a consistent picture of actinide mobility is not evident.

Concern over actinide mobility was reflected in the *Ancillary Basis for Risk Analysis* (Holdren et al. 2002), which concluded that in the short term, mobile chlorinated solvents, nitrates, and long-lived fission and activation products posed the most imminent risks to the SRPA. Several hundred years in the future, however, the actinides uranium and ^{237}Np were shown to contribute the majority of risk. In addition, plutonium isotopes are classified as special-case contaminants of concern to acknowledge uncertainties about plutonium mobility in the environment and to reassure stakeholders that risk management decisions for the SDA will be fully protective. Refined modeling and risk assessment for OU 7-13/14 are currently underway in accordance with the Second Addendum to the Work Plan (Holdren and Broomfield 2004). Results may or may not corroborate the conclusions in the *Ancillary Basis for Risk Analysis* (Holdren et al. 2002).

2.1 Pit 9 Background

Waste was initially disposed of at the SDA using a variety of containers, including steel drums, cardboard cartons, and wooden boxes. However, the actual condition of the drums and other items used for waste containment (e.g., plastic bags, plastic bottles, boxes, and liners) after more than 30 years of interment was unknown before retrieval activities. Earlier retrieval efforts from other locations in RWMC and Pit 9 found evidence of deteriorating drums as well as some leaking containers indicating unabsorbed or desorbed free liquid in drums (Holdren et al. 2002). Radioactive waste from off-site sources other than RFP included military and other defense agencies, universities, commercial operations, and the Atomic Energy Commission. However, the primary off-site contributor was RFP, which shipped transuranic waste to the SDA between 1954 and 1970. Initially, waste was stacked in pits and trenches. However, beginning in 1963, waste was dumped at random to minimize radiation exposure of personnel. Figure 2 provides a map of RWMC showing the location of pits, trenches, and soil vaults in the SDA.

At RFP, nuclear weapons components were manufactured between 1952 and 1989 from weapons-grade plutonium, highly enriched uranium (>90% ^{235}U), beryllium, and stainless steel (Vejvoda 2005). At one time there was more than 14 tons of plutonium and as much as 7.4 tons of highly enriched uranium located at RFP. Waste from RFP has the potential for substantial quantities of actinide elements, chlorinated solvents like carbon tetrachloride, and absorbents like calcium silicate (ICP 2004). Much of the waste generated from operations at RFP was shipped to Idaho. Until 1970, RFP waste was buried in shallow pits and trenches at the SDA.

Clues to the origin of contamination can be generated using isotope ratios of the actinide contaminants. The relevant major isotopes of uranium are ^{234}U , ^{235}U , ^{236}U , and ^{238}U , and these have sufficiently long half lives to ensure that the uranium isotope ratios have changed very little in the last 30-plus years. The relevant plutonium isotopes are ^{238}Pu , ^{239}Pu , ^{240}Pu , ^{241}Pu , and ^{242}Pu . Weapons-grade plutonium from RFP is expected to be >93% ^{239}Pu , with the majority of the rest ^{240}Pu . Like the uranium isotope ratios, the $^{239}\text{Pu}/^{240}\text{Pu}$ ratio (typically 16–17) has varied very little in this time period. However, ^{241}Pu has a short half life ($t_{1/2}=14.4$ yr), and undergoes conversion to ^{241}Am by β decay; ^{241}Am subsequently produces ^{237}Np by α decay. Depending upon the actual quantity of ^{241}Pu originally present in the waste, ^{241}Am and ^{237}Np should be detectable since only 10–20% of the original ^{241}Pu remains. Isotopic ratios expected from weapons-grade and reactor-grade plutonium are presented in Table 1, after 0, 30, and 50 years, which shows the possibility of differentiating the origins of actinide contamination.

Table 1. Percentage compositions of actinides derived from Rocky Flats Plant and reactor-grade plutonium, (DOE/RFP-CO 2003; Carlson et al. 2005) and the changes in this composition at T = 0, 30, 50, and 100 years.

Plutonium Source	^{238}Pu	^{239}Pu	^{240}Pu	^{241}Pu	^{242}Pu	^{241}Am	^{237}Np	^{234}U	^{235}U	^{236}U
[RFP]										
T = 0 yr	0.010	93.790	5.800	0.360	0.030					
T = 30 yr	0.008	93.694	5.781	0.085	0.030	0.270	0.008	0.002	0.081	0.018
T = 50 yr	0.007	93.651	5.769	0.032	0.030	0.313	0.017	0.003	0.135	0.030
T = 100 yr	0.005	93.522	5.738	0.003	0.030	0.317	0.043	0.005	0.269	0.061
Reactor Grade										
T = 0 yr	4.900	56.600	23.200	13.900	1.300					
T = 30 yr	3.865	56.542	23.126	3.280	1.299	10.409	0.307	1.030	0.049	0.073
T = 50 yr	3.301	56.499	23.067	1.252	1.299	12.095	0.667	1.593	0.081	0.122
T = 100	2.223	56.414	22.949	0.113	1.299	12.253	1.643	2.666	0.162	0.243

The isotopic composition of the waste from RFP differs substantially from the actinide isotopic signature expected from atmospheric fallout. Eisenbud and Gesell (1997) report that the $^{239}\text{Pu}/^{240}\text{Pu}$ atom ratio in fallout is about 6.13, whereas Beasley and coworkers (Beasley et al. 1998) report 5.56. These $^{239}\text{Pu}/^{240}\text{Pu}$ values are radically different from those expected for weapons-grade plutonium (>15) and reactor-grade plutonium (<4.26). In terms of total deposition for atmospheric plutonium, estimates from the literature are up to 1.5 pg cm^{-2} to 3 pg cm^{-2} , in references Eisenbud and Gesell (1997) and Hardy (1973), respectively. This is consistent with Beasley et al. (1998), who noted an areal inventory for plutonium at 81 Bq m^{-2} , which converts to only 0.26 pg cm^{-2} , however. The values were also consistent with the general values reported by Myasoedov and Pavlotskaya (1989), which were $0.7\text{--}17 \text{ pg cm}^{-2}$ for $^{239+240}\text{Pu}$, which corresponded to a bulk concentration of $0.03\text{--}2 \text{ ng/g (m/m)}$.

Substantial actinide quantities were detected that corresponded to signal at m/z 238, which is mostly uranium.^e An understanding of background levels of plutonium and uranium at these isotopic masses is necessary to arrive at this conclusion, since ^{238}Pu is also present from fallout. Beasley et al. (1998) measured activity ratios (gamma spectroscopy) of ^{238}Pu : $^{239+240}\text{Pu}$ on the order of 0.030 at INL, which originated from fallout. Given that a $^{239+240}\text{Pu}$ activity of 81 Bq m^{-2} , this would suggest 2.4 Bq m^{-2} for ^{238}Pu , which would correspond to about 0.4 fg cm^{-2} , which is close to the value reported for Salt Lake (0.6 fg cm^{-2}) (Hardy 1973). These would correspond to bulk values of only $0.00002\text{--}0.00003 \text{ ng/g}$. Even though most of the deposited plutonium would be expected to be near the surface, this is vastly lower than the uranium (Litaor and Ibrahim 1996; Eisenbud and Gesell 1997).

e. The mass to charge ratio (m/z) of an atomic or molecular ion is obtained by dividing the atomic or molecular mass of an ion m by the number of charges z that the ion bears.

3. DESCRIPTION OF SAMPLE CHARACTERIZATION

This section provides an overview of each of the sample characterization steps, which consisted of observations during sample collection, photographic inspection, gamma spectroscopy, measurement of actinide content and concentration, measurement of leachability, determination of operational speciation, and surface analysis. These characterizations were conducted for the entire set, or selected subsets, of 36 soil and eight putative waste samples that were collected during the retrieval demonstration at Pit 9.

3.1 Observation of Excavation and Sample Collection Activities

The excavation of the radioactive waste and soil materials from Pit 9 was conducted to demonstrate retrieval operations, not sample collection. However, sample collection was accommodated during the course of excavation operations. To provide guidance and record observations during sample collection, field representatives from OU 7–13/14 recorded observations of sample location, appearance, and related excavation activities. This enabled excavation activities and sample appearance at the time of acquisition to be compared and contrasted with actinide concentration values, leaching characteristics, and speciation determinations observed later in the laboratory.

3.2 Gamma Spectroscopy Screening of Samples

Samples had the potential to contain substantial quantities of plutonium, which could have exceeded (1) facility limits at INL laboratories at the Reactor Technology Complex and (2) radiological safety limits in the analysis laboratories. To ensure these outcomes did not occur, samples from Pit 9 were initially shipped to radiological laboratories at INL's Idaho Nuclear Technology and Engineering Center (INTEC) for gamma spectroscopy. The results of those tests enabled samples to be shipped to the analysis laboratories at the Reactor Technology Complex.

The results of the gamma spectroscopy are reported in full detail for two reasons. First, they provide an independent, qualitative validation for the results that were generated using dissolution and ICP-MS analyses. Second, the efficacy of gamma spectroscopy for characterizing samples having contaminants that are principally alpha emitters can be evaluated by comparing results to those produced in subsequent laboratory analyses.

3.3 Visual Inspection of Samples and Subsampling

A preliminary categorization of waste and soil samples resulted in classifications of waste, mixed waste-soil, and unmixed soil. Categorization was based on direct visual inspection of each sample in the laboratory cross-referenced with visual descriptions of sample collection obtained from the OU 7-13/14 field representative logbooks (Olson 2004). Further refinement of the samples into categories occurred as more laboratory data became available.

3.4 Total Actinide Analyses

Each of the samples were subsampled in triplicate and then dissolved using an aggressive sodium peroxide fusion procedure. Fused materials were dissolved in water, acidified, filtered, and the resulting solution analyzed using ICP-MS. These analyses identified actinide elements present, and quantified their concentrations.

Total actinide analysis using mass spectrometry produced isotope-specific measurements. Isotope abundance ratios were calculated for individual samples and used for

- Evaluation of sample similarity or dissimilarity
- Comparison with values expected from RFP
- Validation or adjustment of sample categorization.

Isotopic ratios from visually mixed or unmixed samples that are the same as those from waste samples constitute strong evidence for a similar origin and for waste-soil mixing occurring during excavation and sample collection. Alternatively, the measurement of different ratios can indicate either multiple origins or the operation of fractionation processes.

3.5 Actinide Leaching

A subset of interstitial soil and waste samples was subjected to aqueous leaching as a function of pH and ionic strength (*I*). In this context, interstitial refers to soil collected from between waste materials in the excavation. At any given set of pH and *I* conditions, a distribution coefficient K_d can be calculated, which for this report is operationally defined as the ratio of the actinide fraction in the solid phase to the fraction in solution. The K_d coefficients are usually rigorously derived from controlled systems in which only adsorption and desorption processes in equilibrium are operating. In real-world samples, this is never the case, yet “operational K_d ” measurements such as those determined herein are useful for quantitatively describing the tendencies of the contaminants to sorb or leach. K_d can be very sensitive to relatively small changes in acidity or concentrations of other solutes. For this reason it is important to further bound the uncertainty of the measured K_d values for actinides by evaluating variations due to changes that might occur in the pore water, and variations in pH and ionic strength are both conceivable.

3.6 Sequential Aqueous Extraction

Aqueous partitioning of actinides from soil and waste matrices is strongly influenced by the explicit chemical forms present—e.g., oxidation states, oxide forms, salts, ligand complexes, adsorbates, and particulates—in which a given element can exist. This envelope of possibilities is referred to as the speciation of the element, and it is important because different species will display vastly different partitioning behavior.

In practice, explicitly determining metal speciation is difficult in systems where the metal concentration is low, or for which a large number of species is present. In many cases, systems are complex to the extent that precise molecular-level speciation can only be determined using accelerator-based synchrotron spectroscopy studies, which are not practical for most field investigations that have large numbers of samples, or for which samples present substantial radioactive or toxic hazards. An alternative strategy is to use SAE, which produces what is termed operational speciation. Operational speciation describes characteristics that can be used to draw conclusions about chemical interactions despite the lack of explicit metal speciation. The laboratory approach for measuring operational speciation is to perform leaching studies using increasingly aggressive solutions designed to selectively remove adsorbed metals from ion-exchangeable sites, the carbonate fraction, the oxidizable fraction (oxidizable actinides, or organic bound), iron and manganese oxides, and strongly binding oxide lattices.

3.7 Surface Characterization

Surface characterization of soil and waste samples was provided by using a simple, instrumental surface technique derived from past INL expertise in SIMS. SIMS identifies chemical features associated with the waste or soil samples.

4. DESCRIPTION OF SAMPLE COLLECTION

This section briefly describes the Pit 9 excavation to provide the context of sample collection; Appendix B provides further detail.

4.1 Excavation

The retrieval demonstration area was located within the larger 12.2×12.2 -m (40×40 -ft) area of interest that had been previously identified (LMITCO 1998). The samples were collected from a fan-shaped area defined by the reach of the excavator (backhoe), with a 6-m (20-ft) radius and an angular extent of 145 degrees (see Figure 3). As depicted in Figure 3, the probes are designated by colored geometric points. The probes were equipped with gamma sensors that identified radiologically hot zones within the pit before excavation (DOE-ID 2004).

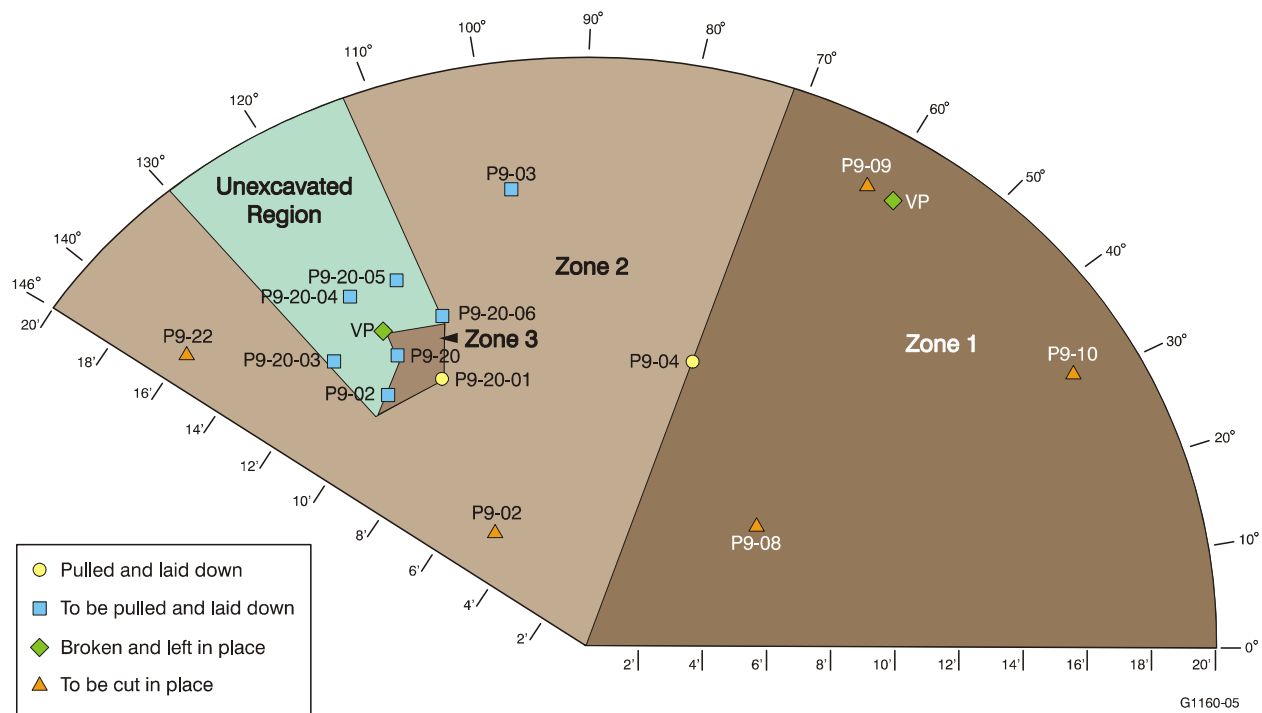


Figure 3. Fan-shaped excavation area showing the location of probes, adapted from DOE-ID (2004).

Initially, about 1.1 m (3.5 ft) of overburden soil from the excavation area (see Figure 4) was removed. Soil from across the excavation area was then removed to a depth of 1.1 m (3.5 ft) below ground surface. Waste was encountered at approximately 1.8 m (6 ft) below the ground surface. Figure 4 is a schematic diagram (not to scale) depicting the location of the overburden, waste zone, and underburden regions of the recent excavation at Pit 9.

Excavator operators acquired scoops of waste zone materials using the excavator bucket and placed those materials in transfer carts lined with a soil bag. The reach, angle, and depth were recorded after every scoop and before placement of the waste zone materials into a transfer cart. The loaded transfer cart was then brought into the glove box, where the material was visually evaluated by field representatives to identify the general waste types that made up the cart load. At some junctures in the excavation, field representatives were able to provide guidance to the excavator operator, and were thus able to influence scoop collection. Field representatives supervised collection of samples, which were then transferred from

the carts to jars. Remaining tray contents were then removed by closing the soil bag and then lowering it by hoist into a drum.

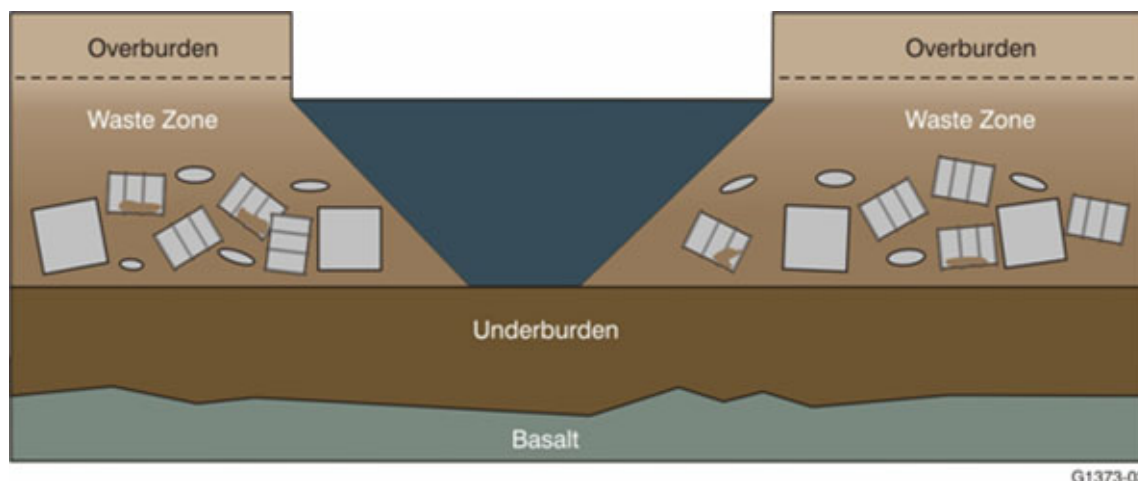


Figure 4. Schematic diagram of the vertical profile of the Pit 9 excavation, adapted from DOE-ID (2004).

4.2 Field Observations

Field representatives visually identified possible waste materials, interstitial soil, and uncontaminated soil. The objective was to collect sludge and interstitial soil samples that were not mixed or minimally mixed as a result of the action of the excavator. In addition, sludge samples having no cross-contamination with either soil or water were sought to evaluate actinide content, concentration, and leaching behavior without influences from an external source. Field representatives were trained before the excavation to visually identify waste forms (i.e., soil, sludge, debris, or miscellaneous materials) and to become familiar with the expected locations and conditions of the buried waste. When probable waste was encountered, identification was further refined by visually identifying type of sludge, debris (e.g., graphite or plastics), or miscellaneous item(s) (e.g., nitrates or material from high-efficiency particulate air filters) present in the scoop. In broad terms, possible sludge types included organic sludge (referred to as Series 743 sludge, which consisted of silicates that had been used to absorb organic liquids with plutonium), and inorganic sludge (Series 741 sludge, which consisted of a dark red to tan material having the consistency of loose peanut butter). The visual data collected during the excavation enabled identification of the material from which samples were collected. The visual data from the field were later combined with laboratory photographic examination data for each sample (Table 2). The visual observations (both field and laboratory) were combined with the analytical measurements of actinide concentrations to generate sample categories in order to streamline communication of a large volume of data (see Section 4.4).

Table 2. Sample categories based on visual field and visual laboratory observations.

Sample Number	Sample Designation	Acquisition Date	Field Category	Summarized Field Descriptions	Lab Description	Appearance Category
P9GW04013A P9GW09013A P9GW12013A P9GW13013A P9GW15013A P9GW21013A	W04 W09 W12 W13 W15 W21	1/27/2004 1/27/2004 1/27/2004 1/27/2004 1/29/2004 1/29/2004	Overburden	None provided	Medium brown-gray soil, fine grained, large clods, no debris or sludge.	Clean soil
P9GT09016G P9GT10016G P9GT13016G P9GT21016G P9GT22016G P9GT24016G P9GT28016G P9GT32016G P9GT34016G	T09 T10 T13 T21 T22 T24 T28 T32 T34	2/13/2004 2/14/2004 2/17/2004 2/17/2004 2/17/2004 2/17/2004 2/19/2004 2/19/2004 2/19/2004	Interstitial soil, appears clean	Moist to very moist medium brown soil, some with off-white chunks of possible calcite. Sample generally collected near a drum. Bags, debris, and corroding drums were proximate to the sample location. Typically, no evidence of sludge was present.	Medium brown, fine particulate soil, with no sludge or debris.	Clean soil
P9GT08016G P9GT11016G P9GT12016G P9GT14016G P9GT15016G P9GT16016G P9GT18016G P9GT20016G P9GT23016G P9GT25016G P9GT26016G P9GT29016G P9GT30016G P9GT31016G P9GT33016G P9GT35016G P9GT36016G	T08 T11 T12 T14 T15 T16 T18 T20 T23 T25 T26 T29 T30 T31 T33 T35 T36	2/13/2004 2/14/2004 2/14/2004 2/17/2004 2/17/2004 2/17/2004 2/17/2004 2/17/2004 2/17/2004 2/17/2004 2/17/2004 2/19/2004 2/19/2004 2/19/2004 2/19/2004 2/19/2004 2/19/2004	Interstitial soil, visually clean with <1% sludge	Moist to very moist medium brown soil, some with off-white chunks of calcite. Sample generally collected near a drum. Bags, debris, and corroding drums were proximate to the sample location. No evidence of sludge.	Medium brown, fine particulate soil with visible traces of sludge, a small quantity of rust flecks, and small off-white calcite chunks or small particles of unidentified debris.	Clean-to-mostly-clean soil

Table 2. (continued).

Sample Number	Sample Designation	Acquisition Date	Field Category	Summarized Field Descriptions	Lab Description	Appearance Category
P9GT01016G P9GT02016G P9GT03016G P9GT04016G P9GT05016G P9GT06016G P9GT07016G P9GT17016G P9GT19016G	T01 T02 T03 T04 T05 T06 T07 T17 T19	2/2/2004 2/2/2004 2/8/2004 2/8/2004 2/8/2004 2/8/2004 2/11/2004 2/17/2004 2/17/2004	Soil mixed with rust, debris, and organic sludge from near drum	Predominantly soil (est. 99%), with bits of rusted drum collected from a scoop that contained a 4-in. ball of stained material possibly sludge. Blackish material noted near dig face, probably not graphite. Drums nearby, with bits of plastic.	Dark brown particulate soil, with minor rust, debris, and or small pea-sized particulates of unidentified material. Some soil appeared mixed 50:50 with tan to off-white clods of unidentified amorphous materials that are probable organic sludge.	Mixed soil-unknown waste
P9GT27016G	T27	2/17/2004	Soil scraped directly from graphite mold piece	Moist fine grained soil scraped from flat pieces of a graphite mold. Severely corroded drums of graphite pieces caked with soil were excavated.	Medium brown cloddy soil, with flecks of dark gray material present (graphite perhaps). No other evidence for contamination.	Mixed soil-rust-graphite
P9GR04012G P9GR20012G P9GR23012G	R04 R20 R23	2/1/2004 2/2/2004 2/12/2004	Organic sludge	Moist clay-like solid with a minor amount of adhering soil. Moderate yellow color with red flecks of rust. Loose soil mixed with probable organic sludge collected from a disintegrated drum with an intact liner.	Very little or no soil. Off-white to tan-gray putty-like solid, moist clay-like consistency with a very small amount of rust-colored inclusions.	Probable organic sludge
P9GP01015G P9GP02015G P9GP03015G P9GP04015G P9GP05015G	P01 P02 P03 P04 P05	2/1/2004 2/1/2004 2/2/2004 2/2/2004 2/2/2004	Inorganic sludge	Gray clumpy solid, with orange and white regions. Fibrous inclusions in the sample. From a zone containing numerous pieces of heavily corroded drums.	Gray solid with significant regions of rust-to-brown coloration. Numerous dark particulate inclusions. Fibrous material also observed. The samples varied from solid hard concrete pieces to soil-rust-carbonate coating on solid chunks.	Unknown waste material
a. Chunks of off-white calcite, chunks of concrete, and drum rust were not confirmed analytically. The information is provided as a visual interpretation only.						

4.2.1 Potential Mixing and Cross-Contamination from Excavator Operation

The backhoe excavation of Pit 9 had consequences for sample collection activities. Since exact locations of barrels and other waste in the excavation zone could not be predicted, any given scoop could contain waste, soil, or a mixture of the two. Note that the objective of the Glovebox Excavator Method Project was to demonstrate retrieval of waste from Pit 9: the project presented opportunities for sample acquisition, but was not designed for collection of unmixed samples. On account of the radioactivity of the waste zone, more delicate hand excavation was not performed; in fact, the excavation was conducted in an enclosed structure to minimize spread of radioactive contamination. The probability of cross-contamination of samples from the excavator itself was high because the excavator bucket was not cleaned between scoops. Further surface cross-contamination of low-lying materials could have occurred from contamination rolling downhill from a higher elevation in the waste zone. During the excavation effort, fine, powdery drum contents were released and appeared to disperse and then settle throughout the containment structure; in particular, this occurred on February 18, 2004, which strongly influenced the analytical results of those samples collected after that date (see Sections 6 and 7). Thus, when evaluating analytical results, the probability that many samples were cross-contaminated during excavation events must be acknowledged.

These operational considerations affected collection of both waste and interstitial soil samples. Preferred soil samples were envisioned as those that were undisturbed from the time of drum emplacement and backfilling without significant incidental surface cross-contamination resulting from later excavation events. Even though the probability of incidental surface cross-contamination to soil samples was high due to excavation methods, new soil was continuously being uncovered, and in several instances, large chunks of intact soil and previously undisturbed soil (since the time of drum emplacement) were encountered. These were carefully selected for excavation, placed by backhoe into a fresh transfer cart liner (i.e., soil bag), then sampled using clean spatulas. In some cases, intact soil chunks were carefully broken open in the packaging glove-box system line and the internal surfaces were sampled, creating the strong possibility that some soil samples were not cross-contaminated by the excavation. Field visual- and laboratory-photographic identifications were corroborated with laboratory analysis data to the greatest extent possible.

Some waste samples could also be free of cross-contamination because intact and pliable plastic drum liners were frequently encountered in the upper waste zone even though the steel drums were severely corroded. Relatively undisturbed sludge, still possessing an organic sheen, was encountered and samples free of soil were acquired. On the other hand, some sludge samples collected from deeper in the waste zone were observed to be saturated with water because plastic drum liners had been compromised due to brittleness. Other sludge samples were clearly mixed with soil during excavation.

4.3 Sample Collection

The samples collected are described and categorized in the paragraphs below and in Table 2. The sample identification scheme employed 10 alphanumeric characters (Salomon 2003); however, for the purposes of this report, samples are uniquely identified using characters in positions four through six of the full sample name. To simplify discussion, samples are identified using only these designations (e.g., sample P9GP01015G will be referred to as P01 in Table 2).

4.3.1 Waste Samples

Samples P01 through P05 were labeled as inorganic sludge to justify sample acquisition. They had a light whitish appearance with some having yellow or orange coloration, and resembled evaporated salt solutions. These samples were collected from waste zones containing heavily corroded drums.

Samples R04, R20, and R23 were identified as organic sludge, and were thought to have originally been calcium or sodium silicate that had been used to absorb solvents containing actinides and other radionuclides. R04 and R20 were described as tan-orange solids with streaked red inclusions the origins of which are unknown. R23 was notably different, a gray putty-like substance that would retain its shape when molded with a gloved hand.

4.3.2 Interstitial Soil Samples

Interstitial soil is defined in this context as soil surrounding buried drums and waste in the waste zone (i.e., excludes overburden and underburden soil). The interstitial soil samples were designated T01 through T36. Many of the soil samples contained foreign inclusions ranging from small millimeter-sized particulates to chunks several inches in diameter. In some cases the inclusions were probably organic sludge; in other cases the inclusions were probably vermiculite or other absorbent, rust, graphite, paper, pieces of plastic drum liner, or other debris. Soil samples containing white mineral inclusions were frequently encountered, and closer visual scrutiny suggested that these were indigenous, perhaps calcite or quartz, and contained no foreign inclusions. Examples of this sample type were T03 through T05 and T14 through T21. Samples T01, T02, and T07 were similar, except that the orange inclusions were noted to be either flecks of rust or orange and red organic sludge mixed into the samples. Many of the soil samples contained no evidence of sludge inclusions at the time of sampling. Samples in this category include T06, T08 through T13, and T22 through T36.

4.3.3 Benchmark Soil Samples

Six uncontaminated soil samples were collected from the soil overlying the waste zone before excavation of any waste for use as benchmarks for the study. Overburden soil was expected to be uncontaminated and suitable for use as an analytical baseline, (i.e., benchmark samples). These samples were designated W04, W09, W12, W13, W15, and W21. The origin and history of the overburden materials, before placement over Pit 9, is unknown. The approximate year of placement can be surmised from historical records; however, the history and origin before the date of placement are unknown. Overburden materials likely arise from several geographic locations in and around the RWMC vicinity and may constitute a mixture of various surficial sediments, some or all of which may have been exposed to radionuclides during any or all of the three different SDA flooding events. Chemical modifications or amendments to (i.e., addition of dust suppressants) the overburden soil are also unknown. Based on the total actinide analysis, uranium in the overburden materials is primarily attributed to natural sources, although some of the uranium could be attributed to fallout or some other source (e.g., flooding). In addition to the overburden, a blank soil collected from an area just outside the RWMC fence line was included because a substantial amount of information on this sample had been generated before the present study (Fox and Mincher 2003; Mincher 2003; Mincher 2004). The concentrations of radionuclides in these samples were measured at or below background levels for typical INL soil (Sections 6 and 7).

4.4 Sample Categorization

Samples were grouped into categories to facilitate interpretation of the analytical and leaching information that was generated. Four iterative sample categorizations evolved during the course of these investigations:

- First, visual data from the field was combined with visual (photographic) inspection conducted in the laboratory to generate a single category based on appearance (right-hand column, Table 2). The results of the total actinide analyses showed that sample categorization solely on the basis of appearance could in some instances result in incongruous groupings, and compelled a second iteration.

- Second, results of the analyses (Section 7) were combined with the appearance categories. This produced groupings that are referred to as postanalysis categories (see Table 3, Section 7) that were used to interpret analytical measurements, and the SAE results (Section 9).
- Third, a categorization was used to describe leaching behavior of the samples (see legends, Figures 11–18, Section 8): this grouping actually resulted in a reduction of the number of soil categories, and splitting of the “organic waste” samples into two categories.
- Fourth, a categorization was performed based on the results of the surface analyses (Section 10). However, as noted, these characterizations were strongly influenced by organic surface contaminants that were not necessarily related to the sample. The surface categories developed were specific to the surface analyses in Section 10.

5. PHOTOGRAPHIC SAMPLE CATEGORIZATION

Visual inspection was performed after the samples were received in the laboratory. The inspection consisted of photographing all samples in the sample jars, then transferring a portion of each to a Petri dish, where sample texture was investigated by probing material with a scoopula. Samples were photographed again in the Petri dish. The results of the photographic inspections were combined with the field observations and field categorizations (Table 2) to produce a combined categorization based on appearance (“appearance category”) for each sample. The appearance category was subsequently refined to “postanalysis” categories as noted in Sections 4.4 and 7.

The following photographs provide typical examples of the appearance categories (the complete photographic atlas of the samples is provided in Appendix C). Examples of visually clean soil samples are shown in Figure 5, for samples T09 and T32, and these are similar to photos for other visually clean soil samples and benchmarks. Two samples are presented here because the contamination levels are radically different, despite their similar appearance. In fact, the difference between these samples motivated the second iteration of sample grouping, which led to formation of the postanalysis categories.



Figure 5. Photographs of two samples initially categorized as clean soil: upper left and upper right, Sample T09; lower left and lower right, Sample T32.

Figure 6 shows examples of mixed soil-waste samples. Sample T07 (see Figure 6, upper left and upper right) was collected near a drum that was thought to contain organic sludge waste. Small bits of probable rust were observed in the sample, together with whitish inclusions. Distinguishing between the calcite, dried, clodded clay, and organic sludge is difficult photographically; however, some materials displayed putty-like consistency when probed with a scoopula, which suggested that they were an organic sludge. The appearance of T07 was typical for most of the mixed waste-soil samples; the difference between these categories is not quantitative but rather a matter of degree based on the discretion of the individual doing the categorization.

Sample T27 (see Figure 6, lower left and lower right) was included because it was scraped from large pieces of graphite molding. The soil looks clean, but flecks of black graphite are present in the sample; this is most evident in the photo of the sample remaining in the jar.

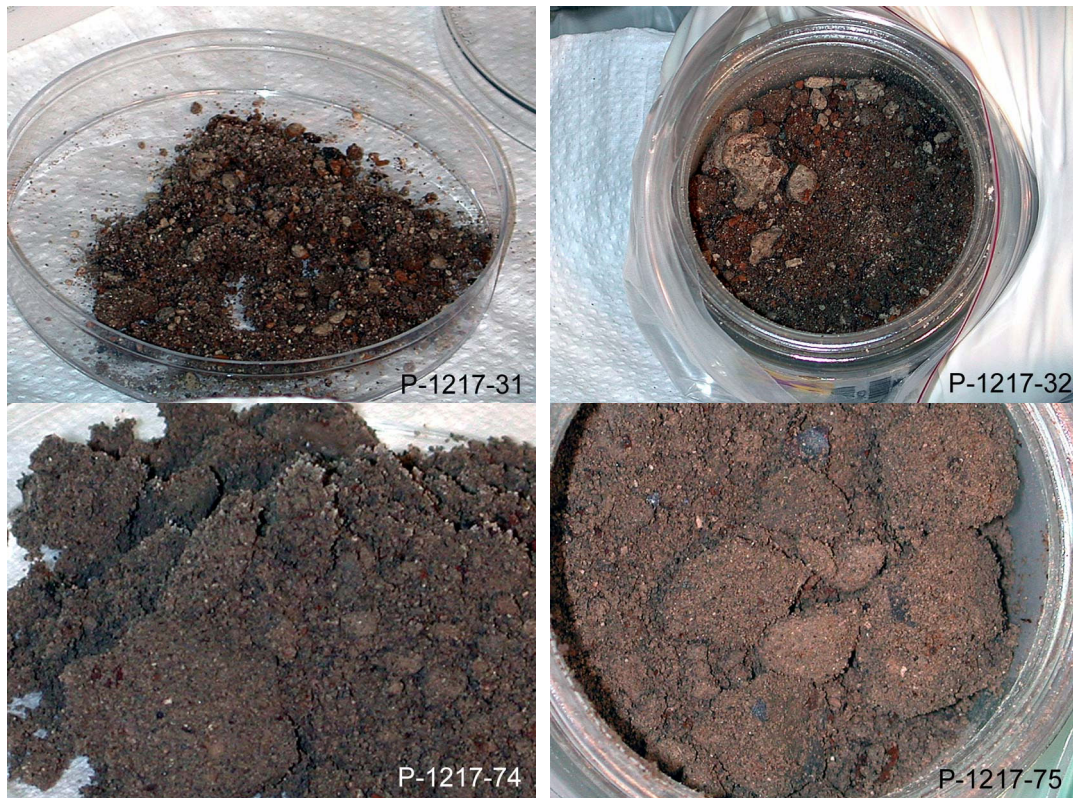


Figure 6. Photographs of two typical mixed soil-waste samples: upper left and upper right, Sample T07; lower left and lower right, Sample T27.

Figure 7 (upper left and upper right) shows photographs of sample R04 that was identified as an organic sludge and was similar to R23. The sample is a light, tan-gray solid with reddish inclusions, and has a putty-like consistency. When this sample was excavated, it was noted that the plastic drum liner was intact, which suggested that the waste sample had not been exposed to the subsurface environment during interment. Figure 7, lower left and lower right, shows sludge that is mixed with soil; here reddish material appears to be rust, but in fact has the consistency of putty. This suggests that it might be sludge, arising from silicate adsorbent that had been exposed to red organic oil; however, identification was speculative.

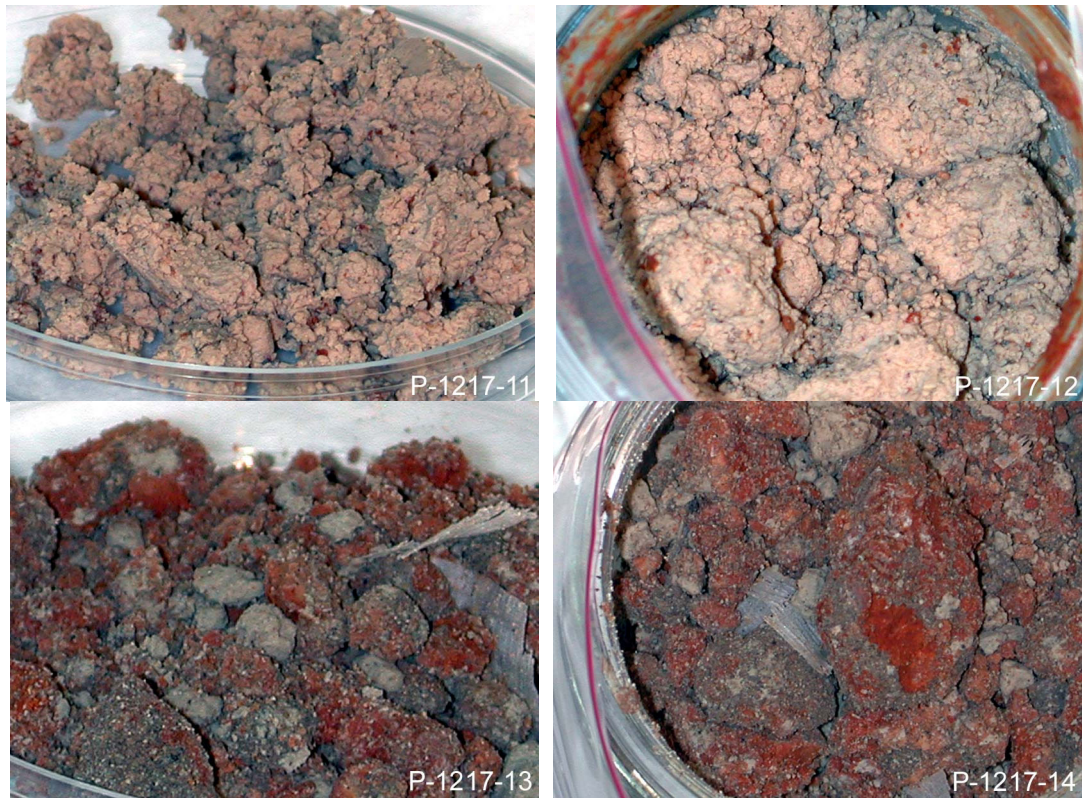


Figure 7. Photographs of a probable organic sludge: upper left and upper right, Sample R04; a mixed soil-waste sample: lower left and lower right, Sample R20.

Several unknown waste materials were collected (P01 through P05), and examples are shown in Figure 8. The material appeared to consist of salt-like material with fibrous inclusions. In some instances, reddish material like the organic sludge was included, and in others pieces of concrete were observed.

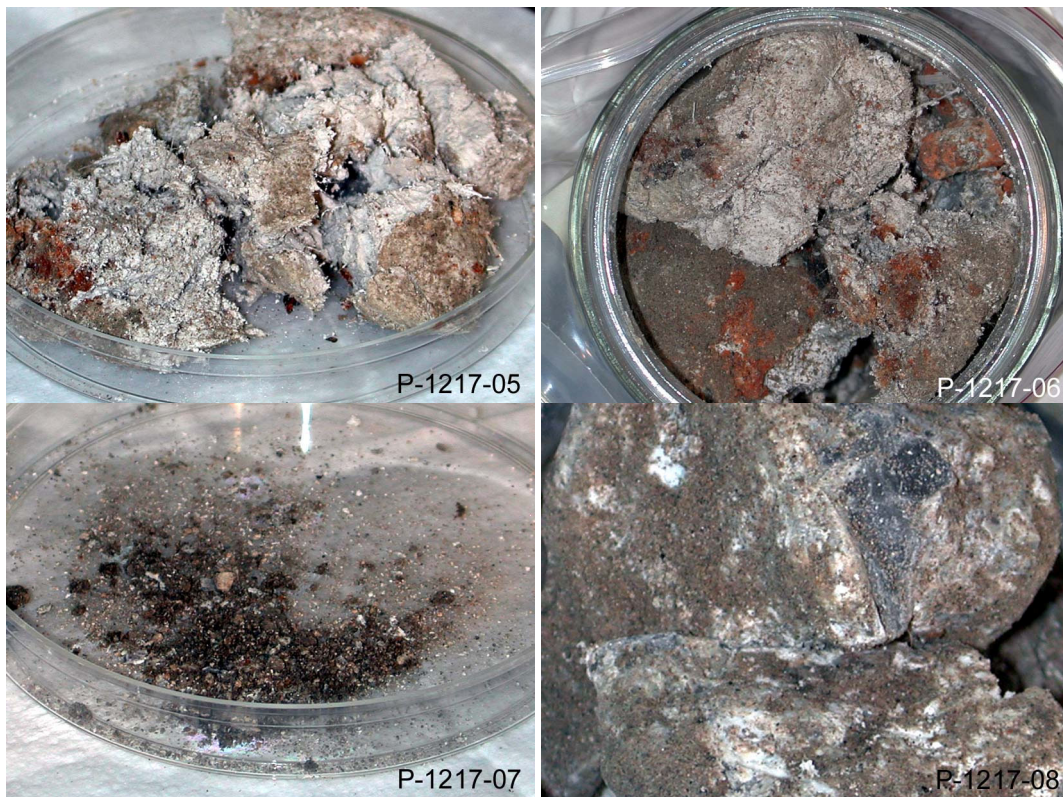


Figure 8. Photographs of two unknown waste samples: upper left and upper right, Sample P03; lower left and lower right, Sample P04, which contains pieces of concrete.

6. GAMMA SPECTROSCOPY SCREENING

Gamma spectroscopy was performed on all samples, principally to ensure that radionuclide inventory limits at the ICP-MS laboratory were not exceeded. The gamma spectroscopy measurements are not as sensitive as are the ICP-MS analyses for ^{239}Pu , but are sometimes more sensitive to ^{241}Am , and so are reported here. In addition, the gamma spectroscopy analyses use a significantly larger sample size than do the ICP-MS analyses. Thus by comparing the two sets of results, the heterogeneity of the samples may be qualitatively assessed and the results cross-validated.

Gamma spectroscopy was performed by configuring a 30-g sample into a puck geometry and then counting (Hill 2003; Hill 2004; ACMM-3993). Gamma-emitting radionuclides that would produce measurable values include ^{241}Am , ^{239}Pu , and ^{240}Pu ; the gamma energies from the plutonium isotopes are very similar and are not resolvable, hence are reported as a single value, designated $^{239+240}\text{Pu}$. Results of the analyses are presented in Appendix D, Table D-1, with subsequently generated ICP-MS results for ^{241}Am and ^{239}Pu , which were included for comparison. The ICP-MS results are presented in detail in Section 7 and Appendix E.

Overall, the correlation between the results of the gamma spectrometry and the ICP-MS analyses was good, as shown in Figure 9 for ^{241}Am . The diagonal line in Figure 9 is what would be expected for a perfect 1:1 correlation between the two techniques. The strong correlation was encouraging because the following factors can produce different results depending on measurement technique used:

- The high degree of heterogeneity may produce different results from analysis of different aliquots of the same sample.
- The aliquot size used in the ICP-MS is (0.1–0.5 g) is much smaller than that used for gamma spectroscopy (about 30 g), and hence is more susceptible to aliquot variability.
- Plutonium is difficult to quantify accurately at lower activity levels by gamma spectroscopy because of background issues.
- Overestimation of ^{241}Am can be caused by possible ^{241}Pu isobaric interference as measured by ICP-MS. This interference is estimated to be 10–20% if the original waste contained only ^{241}Pu .

The most notable feature in Table D-1 is that soil samples having sample numbers greater than T26 were appearance categorized as “clean” or “mostly clean.” These samples had dramatically higher concentrations than for samples less than T26 ($^{239+240}\text{Pu}$ concentrations were in the thousands of nCi/g, and ^{241}Am concentrations were as high as 1,000 nCi/g irrespective of sample appearance). The majority of the contamination in samples T28 through T36 probably occurred on February 18, 2004, when a large jar of powdered material was ruptured by the backhoe, producing a cloud of fine particulates that eventually settled. Thus the high activities for the samples collected after that date (samples T28 through T36 were collected on February 19) were most likely attributable to particle contamination from this event. Overburden samples (benchmark), mixed waste-soil samples, and waste-bearing samples were collected before this event and hence were not affected by it.

Sample T27 was collected before the rupture of the scarfings jar, but also contained elevated concentrations of ^{241}Am and plutonium. This soil sample was scraped from pieces of soil-caked graphite molds that were originally used at RFP to shape plutonium components. The ^{239}Pu and ^{241}Am concentrations measured were similar to those for soil samples acquired after the scarfings jar was ruptured.

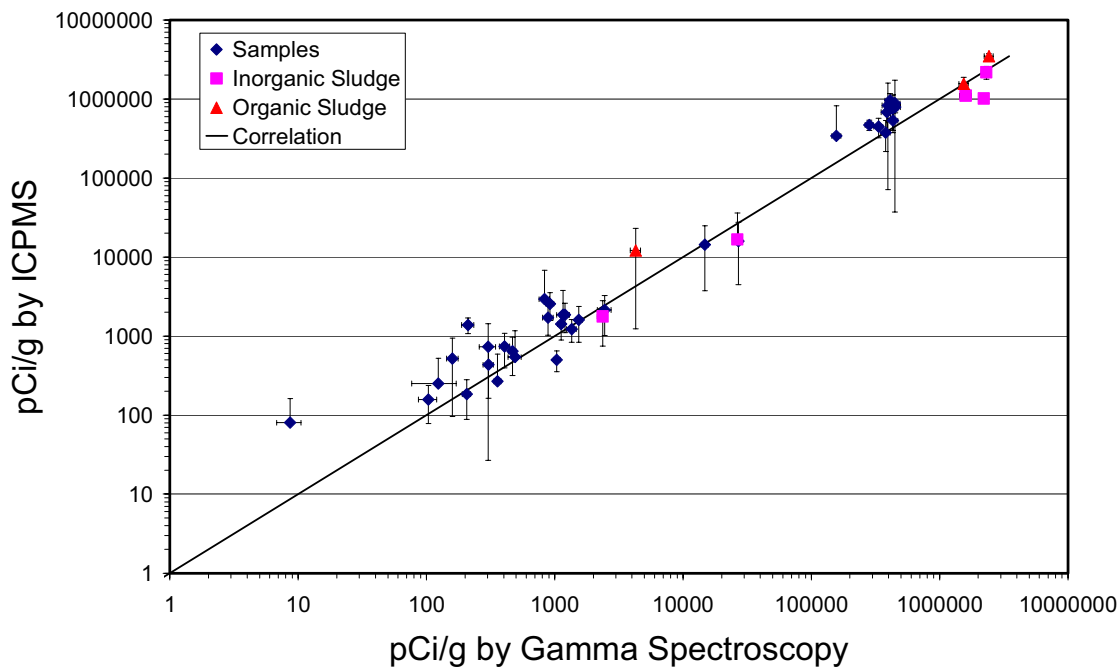


Figure 9. Comparison of ^{241}Am activity determined by gamma spectroscopy and ICP-MS for interstitial soil samples and samples representing inorganic and organic sludge.

For the interstitial soil samples collected before February 18 and categorized as “clean,” nondetectable concentrations of ^{239}Pu and concentrations of ^{241}Am just slightly above atmospheric fallout levels were found in T13, T22, and T24. “Clean” soil samples T9, T10, and T21 showed ^{239}Pu values from 1 to 3 nCi/g, and similar values for ^{241}Am : low values but still one to two orders of magnitude above those expected from atmospheric fallout.

For soil samples collected before February 18 that were categorized as “mostly clean,” sample T26 contained no detectable plutonium and ^{241}Am was only slightly above fallout background. The remainder of the samples (T08, T11, T12, T14–16, T18, T20, T23, T25) were found to contain ^{241}Am ranging from 0.1 to 2 nCi/g by gamma spectroscopy, but no plutonium. ICP-MS did detect ^{239}Pu at values ranging from 1 to 5 nCi/g, with sporadic detections of ^{241}Am . Variations between the two forms of analyses reflect both relative sensitivities to the two elements and differences arising from sample heterogeneity as mentioned above. Sample T15 is worth noting because it contained 21 nCi/g ^{239}Pu . In general, the samples contained significantly more ^{239}Pu than ^{241}Am , although sample T11 was nearly the opposite, in that it contained much more ^{241}Am than ^{239}Pu , suggesting that the associated waste may be from a different generating process.

Gamma spectroscopy of samples categorized as “mixed soil-waste” showed ^{241}Am significantly above background; this was validated by ICP-MS. Concentrations varied widely, ranging from 1 to 900 nCi/g. In contrast, gamma spectroscopy did not detect ^{239}Pu in any of these samples except for T07, but plutonium significantly above background was detected in each sample using ICP-MS. In T01, T02, T03, and T05, ^{241}Am was more abundant compared to ^{239}Pu , which contrasts sharply with other “mixed” samples and with the “clean” and “mostly clean samples.”

^{241}Am concentrations of about 2,000 nCi/g were measured for two of the three samples categorized as organic waste (R04 and R20), but the third (R23) was significantly smaller at only 4 nCi/g. In contrast,

^{239}Pu was not detected using gamma spectroscopy, but was present in abundance via ICP-MS. The ^{241}Am was more abundant than ^{239}Pu in R04 and R20, but not in R23, again suggesting a different waste-generating process.

Materials originally identified as inorganic sludge showed large differences in ^{241}Am by gamma spectroscopy: samples P02, P04, and P05 (which later became unknown waste type II) had concentrations on the order of 2000 nCi/g, with variable plutonium, depending on whether gamma spectroscopy or ICP-MS was used. About 9,000 and 5,000 nCi/g were measured for ^{239}Pu using gamma spectroscopy for P02 and P04, respectively, but the same values measured by ICP-MS were only 100 and 50 nCi/g. This difference is most likely due to significant heterogeneities in these samples, a conclusion that is supported by the photographic evidence. Subsampling for the ICP-MS analysis (normally about 250 mg) did not reproduce the high concentration of plutonium in the sample, suggesting that there are even higher concentrations at some locations within the sample. For P05, which also had between 1,000 and 2,000 nCi/g ^{241}Am , no plutonium was detected using gamma spectroscopy, whereas nearly 60 nCi/g was detected using ICP-MS.

Unknown waste samples P01 and P03 (which later became unknown waste type I) were much lower in ^{241}Am , having about 2 and 20 nCi/g by both gamma spectroscopy and ICP-MS. ^{239}Pu was not detected by gamma spectroscopy for either sample, but was present at about 5 nCi/g as detected by ICP-MS in each case. As in the case of the organic waste, the americium was more abundant than the plutonium in most cases.

In addition to ^{241}Am and $^{239+240}\text{Pu}$, other radioisotopes (^{137}Cs , ^{144}Ce , ^{152}Eu , ^{233}Pa , ^{234}Pa , ^{237}U , ^{237}Np , and ^{239}Np) were observed at lower intensity. For completeness, these data are included in Table D-2 in Appendix D. The other isotopes are primarily fission and decay products with relatively short half-lives and, consequently, high activity. The detection of ^{237}U is interesting as it has a half-life of only 6.75 days. The ^{237}U is seen in the samples with high plutonium and americium content and the source of the ^{237}U can only be the small fraction ($<<1\%$) of ^{241}Pu decay events that emit an alpha particle. This would imply that in some cases, a significant portion of ^{241}Pu activity remains, even though the overall ^{241}Pu activity is expected to be only 10–25% of its initial value when the waste was buried.

7. TOTAL ACTINIDE ANALYSES

Concentrations of actinide isotopes and lead were measured for all 36 of the interstitial soil samples, three organic waste samples, five unknown waste samples, and seven benchmark soil samples. The samples were subsampled in triplicate because only 0.1–0.5 g of material could be dissolved using the sodium peroxide fusion procedure (Appendix E). The solutions resulting from each of the triplicates were then analyzed using ICP-MS, which provided mass-explicit measurements having high analytical accuracy and precision that enabled calculation of isotope ratios. The excellent minimum detection limits achievable using the ICP-MS permitted detection of longer-lived products of lower abundance radionuclides—such as ^{237}Np and ^{235}U —that arise from decay of more abundant isotopes.

The target analytes of this study were isotopes of uranium (isotopes at m/z 233, 234, 235, 236, and 238, of which 234, 235, and 238 occur naturally), neptunium (m/z 237), plutonium (m/z 239, 240, 241, and 242) and americium (m/z 241). The ion at m/z 241 certainly contains contributions from both ^{241}Pu and ^{241}Am in most samples. However, ^{241}Pu has a short half-life and arises from neutron capture from ^{240}Pu , which is not expected to be a prevalent process; thus most of the signal at m/z 241 is thought to be ^{241}Am . In addition, m/z 232, 206, 207 and 208 were analyzed: the former corresponds to ^{232}Th , which is a naturally occurring radionuclide that provides a convenient benchmark for evaluating analytical performance and type of sample. Thorium thus behaves as a built-in reference for determining if the analysis is representative of an actual soil sample. In the background soil, the mean thorium concentration was $10,970 \pm 640$ ng/g. This value is very close to the average of 10,700 ng/g found in most soil. The ions at m/z 206, 207, and 208 correspond to lead isotopes at those masses. Lead was included because it could be present above background levels as a result of radioactive waste disposal.

The actinide concentrations measured for the interstitial soil were compared with background concentration levels generated by analysis of soil collected from the soil overlying the waste zone (see Section 4.3.3, Benchmark Soil Samples) and from Spreading Area B located approximately 1 mile south of RWMC. ^{233}U , ^{234}U , ^{236}U , ^{237}Np , ^{239}Pu , ^{240}Pu , ^{241}Pu , ^{241}Am or ^{242}Pu were not detected in any of those samples (Table 3 below and Table E-1 in Appendix E). Agreement was good between the measured concentrations of the natural isotopes and natural concentrations.

Concentrations of the anthropogenic isotopes measured in soil and waste samples were considered significant if the values were greater than the product of the Student's 99% confidence interval ($t_{(p=0.01)}$) (Ullman 1972; Miller and Miller 1988) and the standard deviation of the background signal of the mass spectrometer at each of the respective masses; this constituted the significance criteria referred to in Table 3 and Table E-1. This calculation provided an upper bound for the minimum detectable concentrations for the anthropogenic isotopes. For those isotopes occurring in nature but also possibly arising from waste disposal (i.e., lead isotopes, ^{232}Th , ^{235}U , and ^{238}U) a concentration measured in a sample was considered significant if it was outside of the range of the mean $\pm t_{(p=0.01)}$ times the standard deviation of the background soil.

Table E-1 holds an exhaustive listing of the mean concentrations for each isotope for each of the samples, while Table 3 provides a condensed summary of the data, providing ranges of concentrations measured for postanalysis categories of samples. An evaluation of the data grouped by the visually-defined appearance categories (see Table 2) suggested that a more functional categorization could be generated by also considering the ICP-MS results (particularly the ^{239}Pu and ^{241}Am concentrations, see Table 3). This caused samples T27 through T36 to be separately categorized, reflecting high levels of contamination. Secondly, it separated the unknown waste samples into two categories reflecting different contamination levels. These second-tier groupings are referred to as postanalysis categories. These categories are found in the total actinide analyses sections (Table 3, Section 7, and Table E-1,

Appendix E) and in the sequential aqueous extraction sections (Section 9 and Table G-1, Appendix G). The postanalysis categories are listed below:

- **Clean soil**, which had a clean appearance with very little actinide contamination
- **Low-contamination soil**, which had a very clean appearance, and modest actinide contamination
- **Mixed soil-waste**, which visually contained evidence for waste material, and had variable contaminant concentrations by ICP-MS
- **Soil scraped from graphite**, which consisted of one sample, T27
- **Soil after rupture of graphite scarfings jar**, which consisted of samples T28–T36, and appeared clean, but in fact was heavily contaminated
- **Unknown waste type I**, which contained low levels of americium and plutonium
- **Unknown waste type II**, which contained substantially higher levels of americium and plutonium
- **Organic waste**, which contained three samples that had similar appearances, but in fact displayed significantly different contaminant concentrations
- **Overburden blank**, which constituted the benchmark samples for the studies.

The actinide concentrations presented in Tables 3 and E-1 are coded to indicate significance relative to background. Underlined values indicate that the measured concentration is outside the significance criteria: values in red are greater than the significance criteria, while values in blue are less than the value. Ranges of values are reported in Table 3, which are the high and low values measured for a given isotope for the samples in that postanalysis category. Individual concentration measurements with their standard deviations are reported in Table E-1: large values stemmed from differences of up to an order of magnitude between concentrations from individual aliquots from the same sample, which is consistent with significant sample heterogeneity as indicated by the photographs (Appendix C) and by differences between the gamma spectroscopy and ICP-MS results. Given the relatively small aliquot size (0.1–0.5 g), this degree of variability is not surprising.

Difficulties in reducing the data by grouping samples into categories were underscored by using principal component analysis. Because of the high degree of heterogeneity in the samples, repeated efforts to systematically group the samples using this approach coupled with a cluster analysis technique produced a greater number of categories than those listed. Strict application of principal component analysis ignored similarities derived from the appearance of the samples and from knowledge of the details of sample collection. With this additional qualitative information, similar subgroupings to those above could be obtained from the principal component analysis score plots which largely grouped the samples along two lines; those associated with graphite and those associated with the organic and unknown waste.

Table 3. Ranges of actinide and lead concentrations for categories of interstitial soil and waste samples. All values are reported in units of ng/g. Values underlined are above or below the significance criteria for that isotope (equal to the mean $\pm t_{(p=0.01)} \times$ standard deviations of the blank INL soil samples). Values in red are greater than the significance criteria, and those in blue samples are less than. Results for individual samples are provided in Appendix E, Table E-1.

Field Sample	Postanalysis Category	Total Lead (mean)	²³² Th	²³⁴ U	²³⁵ U	²³⁶ U	²³⁷ Np	²³⁸ U	²³⁹ Pu	²⁴⁰ Pu	²⁴¹ Am, ²⁴¹ Pu	²⁴² Pu
T13, T22, T24, T26	Clean Soil	<u>14,800</u> — 22,300	9,300 — 13,060	<0.48	23.3 — <u>38.7</u>	<1.0	<3.6	2,970 — <u>4,560</u>	<19	<0.19 — <u>0.95</u>	<0.15	<0.048
T08–T12, T14–T16, T18, T20–T21, T23, T25	Low-Contamination Soil	17,700 — <u>26,000</u>	9,900 — 13,100	<0.48 — <u>0.81</u>	25.7 — <u>78</u>	<1.0	<3.6	3,280 — <u>5,630</u>	21 — <u>86</u> (T15 had a value of 340)	<u>0.35</u> — <u>4.2</u>	<0.15 — <u>0.9</u>	<0.048 — <u>0.48</u>
T01–T07, T17, T19	Mixed Soil-Waste	22,600 — <u>260,000</u>	<u>2,200</u> — 11,300	0.67 — <u>6.9</u>	<u>20</u> — <u>580</u>	<1.0 — <u>24</u>	<3.6 — <u>19</u>	<u>5,430</u> — <u>45,000</u>	21 — <u>700</u>	<u>0.85</u> — <u>43</u>	<u>0.36</u> — <u>260</u>	<0.048 — <u>0.24</u>
T27	Soil Scraped from Graphite	<u>32,000</u> — <u>35,500</u>	10,540 — 10,780	<u>0.94</u> — <u>1.90</u>	<u>52.8</u> — <u>98</u>	<u>6.09</u> — <u>16</u>	<u>6.9</u> — <u>17</u>	3,420 — 3,520	<u>31,100</u> — <u>78,000</u>	<u>1,469</u> — <u>3,500</u>	<u>137</u> — <u>300</u>	<u>4.88</u> — <u>11</u>
T28–T36	Soil after Rupture of Graphite Scarfings Jar	20,500 — <u>60,000</u>	9,940 — <u>13,600</u>	0.68 — <u>1.99</u>	<u>62</u> — <u>90</u>	<u>6.4</u> — <u>14.0</u>	<u>5.8</u> — <u>14.8</u>	3,290 — <u>4,470</u>	<u>30,000</u> — <u>63,000</u>	<u>1,260</u> — <u>3,100</u>	<u>109</u> — <u>240</u>	<u>4.2</u> — <u>10.5</u>
P01, P03	Unknown Waste Type I	<u>2,250</u> — <u>2,780</u>	<u>1,000</u> — <u>1,020</u>	<0.48	<u>13.3</u> — 23	<1.0	<3.6	<u>1,500</u> — 2,400	<u>80</u> — <u>90</u>	<0.19 — <u>0.25</u>	<u>0.52</u> — <u>4.9</u>	<0.048
P02 ^a , P04, P05	Unknown Waste Type II	<u>75,200</u> — <u>115,000</u>	<u>3,870</u> — <u>6,100</u>	<u>5.8</u> — <u>12.3</u>	<u>441</u> — <u>880</u>	<u>29.7</u> — <u>56.8</u>	<u>23</u> — <u>56</u>	<u>54,500</u> — <u>102,000</u>	<u>700</u> — <u>1,650</u>	<u>35</u> — <u>99</u>	<u>300</u> — <u>630</u>	<u>0.4</u> — <u>0.59</u>

Table 3. (continued).

Field Sample	Postanalysis Category	Total Lead (mean)	²³² Th	²³⁴ U	²³⁵ U	²³⁶ U	²³⁷ Np	²³⁸ U	²³⁹ Pu	²⁴⁰ Pu	²⁴¹ Am, ²⁴¹ Pu	²⁴² Pu
R04 ^b , R20 ^c , R23	Organic Waste	<u>122,700</u> — <u>290,000</u>	<u>1,074</u> — <u>3,320</u>	<u>7.55</u> — <u>35</u>	<u>772</u> — <u>2,400</u>	<u>3.66</u> — <u>160</u>	<3.6 — <u>137</u>	<u>19,500</u> — <u>220,000</u>	<u>870</u> — <u>4,900</u>	<u>25</u> — <u>179</u>	<u>3.5</u> — <u>1,800</u>	<u>0.17</u> — <u>2.5</u>
W04, W09, W12, W13, W15, W21, Blank	Overburden Blank	19,000 — 21,700	10,120 — 11,860	<0.48	21.4 — 29.2	<1.0	<3.6	2,890 — 3,435	<19	<0.19	<0.15	<0.048
<p>a. ²³³U was measured in P02 at 2.73 ± 0.21 ng/g.</p> <p>b. For sample R04, two mean values were used, one including all replicates and the other where one very high replicate was eliminated. ²³³U was measured in R04 at levels of 7.1± 5.9 µg/g when all values were used and 3.73 ± 0.82 µg/g when the high replicate was dropped.</p> <p>c. ²³³U was measured in R20 at 2.47 ± 0.49 ng/g.</p>												

7.1 Concentrations of Actinide Elements in Interstitial Soil and Waste Samples

Clean Soil Samples: T13, T22, T24, and T26. Four samples collected on February 17 showed only traces of actinide contamination. Traces of ^{240}Pu at concentrations slightly above method background were found in some samples, slightly elevated uranium was found in sample T26, and slightly elevated ^{235}U was found in sample T24. The $^{238}\text{U}/^{235}\text{U}$ isotope ratios were in the 119–134 range in samples T13, T22, and T26, which are consistent with isotopic ratios occurring in the overburden and blank soil samples. The exception was T24, which had a $^{238}\text{U}/^{235}\text{U}$ ratio of 114.3 ± 3.7 indicating slight enrichment with ^{235}U . The elevated ^{240}Pu measurements are significant and suggest low-level contamination that is not detected for other plutonium isotopes because ^{240}Pu has a detection limit that is 100 times lower than the most abundant isotope (^{239}Pu) and the relative abundance of ^{242}Pu is low. Nevertheless, these samples were significantly less contaminated than other interstitial soil samples from Pit 9. This conclusion is consistent with the measured concentrations of ^{232}Th , which were in accord with those expected for natural soil. Analyses of “clean” samples showed it was possible to collect interstitial soil samples with minimal incidental contamination.

Low-Contamination Soil Samples: T08–12, T14–16, T18, T20–21, T23, and T25. Analysis of 13 samples categorized by appearance as “clean” or “clean-to-mostly clean” consistently showed evidence for low-level contamination from several actinide isotopes. Detectable ^{239}Pu and ^{240}Pu were measured in every sample, with all samples having ^{240}Pu , and 11 of 13 having ^{239}Pu determinations above the significance criteria. Significant detection of ^{241}Am occurred in 9 of 13 samples, and elevated uranium in 6 of 13 samples. The samples having elevated uranium also showed $^{238}\text{U}/^{235}\text{U}$ atom ratios indicating some isotopic enrichment, which is also consistent with contamination. ^{239}Pu concentrations ranged from 21 to 86 ng/g (compared to a detection limit of 19), except for T15, which had a value of 340 ± 520 ng/g. The high average and large variance in T15 indicated that one of the aliquots contained a significant waste inclusion, again underscoring the heterogeneity of the sample. ^{241}Am was measured as high as 0.9 ng/g. The concentrations measured for both ^{239}Pu and ^{241}Am are orders of magnitude higher than those expected from fallout (0.2 pg/g for ^{239}Pu , and about 0.02 pg/g for ^{241}Am) (Beasley et al. 1998), thus excluding fallout as a possible source of the contamination. The concentrations of ^{232}Th indicate that these samples are principally soil.

Mixed Soil-Waste Samples: T01–07, T17, T19. Analysis of nine samples categorized as “mixed soil-waste” showed more variability than the rest of the interstitial soil samples, which was consistent with their more varied visual appearance. However, general comments on contamination can be made based on the ICP-MS results. The naturally occurring uranium isotopes 235 and 238 were significantly elevated for all samples, and ^{234}U was elevated for all but T05. The $^{238}\text{U}/^{235}\text{U}$ atom ratio was augmented in all samples, and as low as 29.3 ± 1.1 in sample T19, compared with a $^{238}\text{U}/^{235}\text{U}$ atom ratio of 139 ± 14 found in the overburden soil samples. The other fissionable nucleus, ^{239}Pu , ranged from 21 ng/g to 700 ng/g, and all values were greater than the significance criterion except T05. All samples had significant ^{240}Pu and ^{241}Am concentrations. All samples had significantly elevated lead except for T03, consistent with a sizeable waste content. ^{232}Th was within normal ranges in all soil samples except for T07, T17, and T19, which had significantly less ^{232}Th than expected for soil, indicating a high waste content. Indeed, noticeable chunks of “organic waste” (see below) were visible in T17 and T19.

Soil Sample Scraped from Graphite: T27. A single sample was collected by scraping soil caked to graphite surfaces, with the expectation that this unique assemblage of soil in close contact with a graphite fragment for an extended time period would have a high probability of containing significant actinide contamination. Analysis of multiple subsamples showed significantly high concentrations for all actinides, except for the naturally occurring ^{232}Th and ^{238}U , which had values consistent with normal soil.

The ^{239}Pu concentration averaged 78,000 ng/g when results from all subsamples were included; one subsample was unusually high, and when this was discarded from the data set, an average of 31,000 ng/g was calculated. This latter value was probably more representative of the ^{239}Pu concentration in the soil. The results clearly show that soil in contact with graphite molds can have exceptionally high actinide concentration levels.

Soil Samples After Rupture of Graphite Scarfings Jar: T28–T36. As noted above, on February 18, 2004, a jar thought to be holding graphite scarfings was intentionally ruptured by the backhoe, sending a plume of particulate “scarfings fallout” and graphite dust throughout the excavation enclosure (Olson 2004). Samples collected after that time were originally categorized, based on appearance, as either “clean” or “clean-to-mostly clean” interstitial soil samples, but both the gamma spectroscopy and ICP-MS data showed very high levels of actinide contamination associated with those samples. As a result, they were assigned to a separate category. The ICP-MS results for those samples were indistinguishable from those for T27, the soil caked to graphite, which suggested that contamination in the soil caked to graphite and in the soil contaminated by the scarfings fallout had similar origins (i.e., particulate derived from graphite molds). This conclusion draws strong support from the $^{240}\text{Pu}/^{239}\text{Pu}$ ratio discussed below, which is consistent with the presence of weapons-grade plutonium.

There are alternative explanations for the high ^{239}Pu concentrations measured in samples T28 through T36, which were collected from the bottom of what was known as the waste zone, near the P9-20 probe cluster (see Figure 3). That area of the pit contained numerous steel drums of graphite mold pieces, and 4-liter poly jars of plutonium-laden scarfings. Although the poly jars themselves were retrieved intact (except for the one that was intentionally ruptured), not all of the mold pieces were enclosed in intact plastic drum liners or poly jars. Loose, plutonium-contaminated graphite pieces from severely corroded drums located close to where the scoop was acquired, or that were located higher in the excavation zone, may have caused incidental contamination. Alternatively, episodic infiltration by water could have led to contamination of those samples.

However, the most obvious explanation for the high contamination levels in samples T28 through T36 was that they were contaminated with a visible dust cloud that affected most of the containment structure after a container of graphite scarfings was intentionally ruptured. Samples T28 through T36, which were collected only a few hours later, displayed a high degree of similarity with each other and with soil scraped from graphite (T27), which strongly indicates uniform contamination from plutonium-laden dust from graphite waste. Samples T28 through T36 were collected near the bottom of the P9-20 cluster, it is certain that those samples were contaminated by the jar rupture event.

Unknown Waste Type I Samples: P01, P03. Two unknown waste samples were similar in appearance, namely white debris encrusted with white salt material. The samples contained ^{239}Pu at concentrations modestly above background (i.e., 4 times higher), and variable ^{241}Am (3 to 30 times background). Uranium isotopes were measured at concentrations at or below those encountered in soil; $^{238}\text{U}/^{235}\text{U}$ isotope ratios indicated modest enrichment of ^{235}U . ^{232}Th and lead were depleted compared to soil, indicating that most of the sample was indeed a waste material with little soil.

Unknown Waste Type II Samples: P02, P04, P05. Three other unknown waste samples also had similar contamination, namely high values for the plutonium isotopes (^{239}Pu ranging to about 1,000 ng/g), ^{237}Np , and ^{241}Am . Uranium was also present at concentrations well in excess of those expected in soil, but with $^{238}\text{U}/^{235}\text{U}$ isotope ratios showing only slight ^{235}U enrichment compared to natural abundance. The high concentrations of neptunium and americium suggest this material may have different origins.

Organic Waste Samples: R04, R20, R23. Based on appearance, these waste samples were believed to be similar; when the actinide concentrations were compared, R04 and R20 were similar, but R23 was unique. All three samples had significant concentrations of uranium that were much greater than those expected for naturally occurring soil. R04 and R20 had $^{238}\text{U}/^{235}\text{U}$ ratios that reflected slight ^{235}U enrichment (110 ± 13 and 103.1 ± 3.2), but R23 showed a significantly lower value at 25.55 ± 0.78 , indicating significant enrichment. All three samples showed significant neptunium, plutonium, and americium, with R23 having the lowest values. Also significant in those samples were the high concentrations of lead, ranging to 290,000 ng/g (consistent with waste), while ^{232}Th was depleted, indicating lack of soil in those samples. The organic waste was thought to be a mixture of sodium silicate with organic oil and solvent, which is consistent with little or no thorium in the samples.

7.2 Isotope Ratios of Actinide Elements in Interstitial Soil and Waste Samples

The isotope ratios of actinide elements in the soil and waste samples can provide information regarding waste generating processes. In contrast to the wide variability seen in the concentration data in Table E-1 (Appendix E), the isotope ratios for the same samples (Table E-2) are generally much more precise provided the concentrations of both isotopes in the ratio are significantly above the detection limit. Improved precision enables more detailed comparisons of isotope ratios between aliquots and samples, despite variable absolute concentrations within a sample. Comparison of isotope ratios from different samples can suggest different or similar process or location origins. In this section, a variety of ratios were measured for many of the samples; the salient observation was that the $^{239}\text{Pu}/^{241}\text{Am}$ ratios roughly divided the samples into two categories, namely, those related to weapons-grade plutonium contamination and those related to waste materials. The division was largely substantiated by the other isotope ratios that were measured.

Ratios of interest in this study were:

- **$^{232}\text{Th}/^{238}\text{U}$:** The m/z 232/238 ratio can identify excursions from background concentrations in soil, since both isotopes are prevalent in the environment. The normal range for the 232/238 ratio is in the 3–4 range; values lower than this indicate less thorium (due to no soil in the sample) or the presence of additional uranium.
- **$^{238}\text{U}/^{235}\text{U}$:** The ratio of m/z 238/235 identified samples containing enriched fissionable uranium. A natural $^{238}\text{U}/^{235}\text{U}$ atom ratio in soil is approximately 137.8, which is consistent with the value of 139 ± 14 found for the overburden samples, and with the value of 137.2 ± 8.7 measured for the Spreading Area B blank soil. A decrease in the m/z 238/235 ratio is an indication of isotopic enrichment of ^{235}U , which can be encountered in samples containing radioactive waste.
- **$^{239}\text{Pu}/^{240}\text{Pu}$:** The m/z 239/240 ratio is one of the most useful for identifying the source of contamination because it varies dramatically depending on origin (Borrentzen 2005). Plutonium used in the manufacture of nuclear weapons can have values from as low as 15 to values approaching 100. The ratio calculated for RFP plutonium after 30 years should be approximately 16.2 (Table 1); this calculation accounts for slow changes in the ratio arising from faster decay of ^{240}Pu . In contrast, $^{239}\text{Pu}/^{240}\text{Pu}$ values ranging from 2.4 to 5 are typical of commercial reactor fuel. Intermediate between these values is atmospheric fallout, which has a ratio of about 5.6 to 6.1. At a waste site such as Pit 9, intermediate values could arise in samples having contributions from multiple processes.

- **$^{239}\text{Pu}/^{241}\text{Am}$:** The ratio of these two isotopes can also be used to differentiate weapons material from reactor fuel. A ratio of 341 can be calculated for RFP plutonium after 30 years; the ^{241}Am is formed from beta decay of ^{241}Pu that is present as a minor isotope, and tends to increase over time. The ratio calculated for reactor fuel after 30 years is only 5.4.

Isotope Ratios for Clean Soil Samples: T13, T22, T24, and T26. $^{232}\text{Th}/^{238}\text{U}$ ratios for all four of these samples were within normal range for soil, indicating that these samples were mostly clean. $^{238}\text{U}/^{235}\text{U}$ was normal for all except T24, which was slightly enriched in ^{235}U .

The diagnostic $^{239}\text{Pu}/^{240}\text{Pu}$ ratio could not be calculated for T22 or T24 because the low concentration of ^{239}Pu could not be precisely measured in those samples. ^{239}Pu was detected in T13 and T26, although concentrations were below the significance criteria, and the $^{239}\text{Pu}/^{240}\text{Pu}$ ratios for those samples were 16.7 and 18, respectively. These values are consistent with those expected for weapons-grade plutonium from RFP, and are in very good agreement with ratios for the soil scraped from graphite (T27) and with the ratios from the soil after the rupture of the graphite scarfings jar. The isotope ratio similarity suggests that the low ^{239}Pu and ^{240}Pu detections in those samples are valid, and that the sources of contamination are the same.

$^{239}\text{Pu}/^{241}\text{Am}$ ratios could not be calculated for these samples because ^{241}Am was not detected in these samples.

Isotope Ratios for Low-Contamination Soil Samples: T08–12, T14–16, T18, T20–21, T23, and T25. Analysis of the 13 samples categorized by appearance as “clean” or “clean-to-mostly clean” showed $^{232}\text{Th}/^{238}\text{U}$ ratios consistent with the soil as the main constituent. T15, T16, T20, and T21 had significantly lower ratios caused by elevated ^{238}U in those samples. For those samples the $^{238}\text{U}/^{235}\text{U}$ ratio was also depressed, indicating that the uranium was enriched in the fissile isotope. T14 and T18 also showed lower $^{238}\text{U}/^{235}\text{U}$ ratios. Hence in general, this group of samples had elevated overall uranium concentrations that were modestly enriched in the ^{235}U isotope (see Table E-2, Appendix E).

The $^{239}\text{Pu}/^{240}\text{Pu}$ ratios for those samples ranged from 16.2 to 54, and all but two were clustered between 16.2 and 22.7, consistent with weapons-grade plutonium from RFP. $^{239}\text{Pu}/^{240}\text{Pu}$ ratios for T15 and T16 were 54 and 28, respectively, indicating plutonium highly enriched in the fissile isotope in these two samples.

$^{239}\text{Pu}/^{241}\text{Am}$ ratios ranged from 42 to 470 for “low-contamination soil” samples (ratios were not calculated for T14, T16, and T18 because ^{241}Am was not detected). These ratios for low-contamination soil samples were fairly consistent with those calculated for T27 and the soil after rupture (the “high-plutonium” soil samples). A correlation between $[\text{}^{239}\text{Pu}]$ and $[\text{}^{241}\text{Am}]$ established for the high-plutonium soil samples could be extrapolated to the low-concentration soil (see Figure 10A, diamond data points in left-hand oval), which suggested that the contamination had a similar process origin. In contrast, the $^{239}\text{Pu}/^{241}\text{Am}$ ratios of the low-contamination and high-plutonium soil samples were dissimilar to those measured for waste or soil mixed with waste.

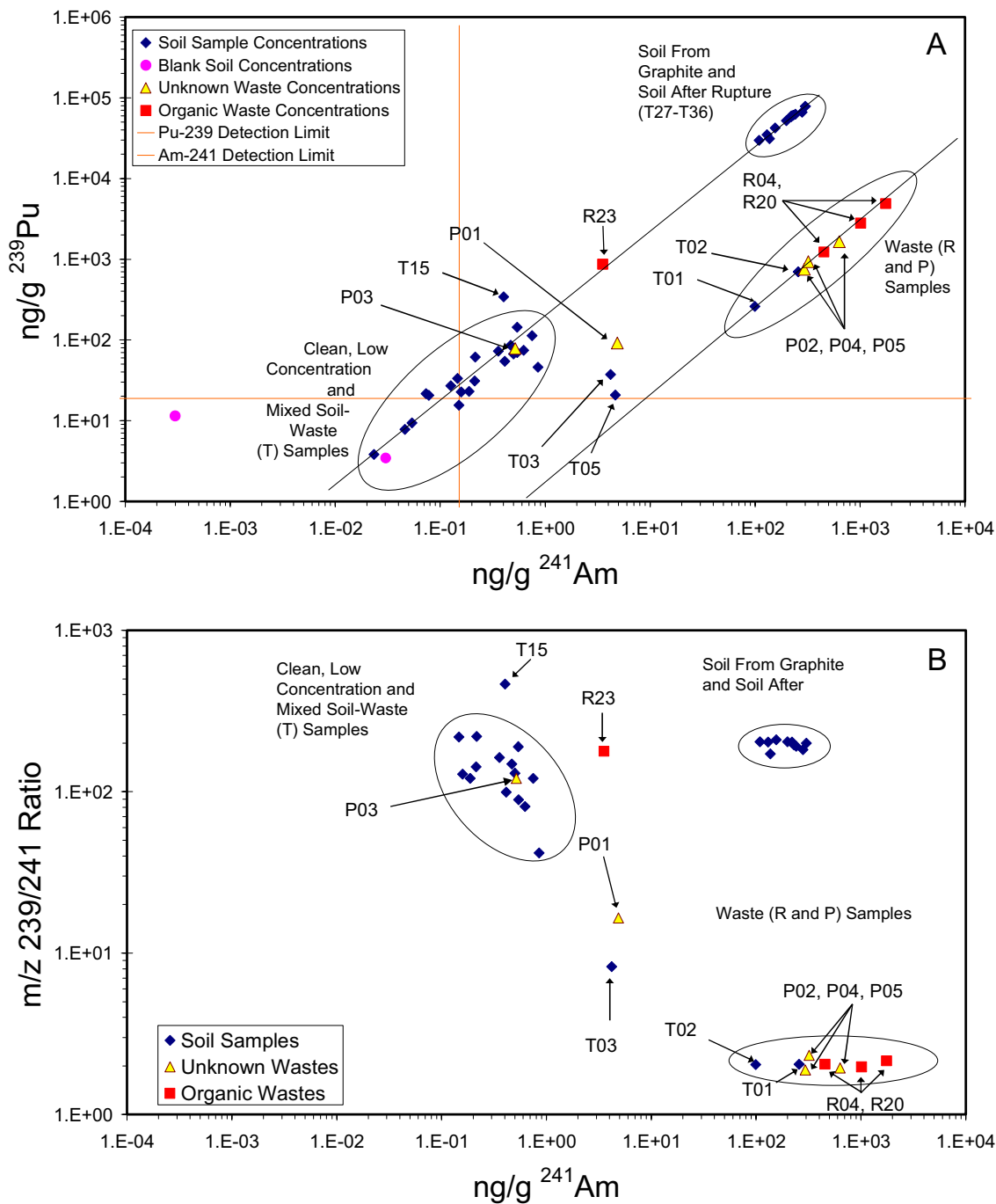


Figure 10. Plots of (A) ^{239}Pu versus ^{241}Am , and (B) the $^{239}\text{Pu}/^{241}\text{Am}$ isotope ratio versus ^{241}Am . Lines have been drawn to highlight the difference in the $^{239}\text{Pu}/^{241}\text{Am}$ ratio for different sample types.

The exception to this behavior was T15, having a significantly higher $^{239}\text{Pu}/^{241}\text{Am}$ ratio compared with any of the soil samples. In fact it has a ratio higher than that measured for any of the high-plutonium soil samples. One of the aliquots of T15 may have contained a small particle of oxide highly enriched in ^{239}Pu , thus perturbing the ratio; recall that this sample also had the highest $^{239}\text{Pu}/^{240}\text{Pu}$ ratio.

Isotope Ratios for Mixed Soil-Waste Samples: T01-07, T17, and T19. $^{232}\text{Th}/^{238}\text{U}$ ratios for samples in this category showed significantly lower values compared to uncontaminated soil. The

$^{238}\text{U}/^{235}\text{U}$ ratios were also lower than that expected for natural abundance uranium. Together, these measurements indicate samples that contained significant contamination by ^{235}U -enriched uranium, consistent with the presence of waste materials mixed with the predominantly soil samples. This is also supported by measurement of ^{232}Th less than natural abundance in these samples.

The $^{239}\text{Pu}/^{240}\text{Pu}$ ratios for samples in this category ranged from 12.4 to 20.8; if sample T02 excluded, the range for the category shrinks to 15.7–20.8, which is what would be expected for weapons-grade plutonium.

The $^{239}\text{Pu}/^{241}\text{Am}$ ratios were scattered in this sample category. T04, T06, T07, T17, and T19 had high values (89–190) consistent with weapons-grade plutonium. On the other hand, T01, T02, T03, and T05 have ratios that range from about 2 to 8, suggesting that these samples appear to be primarily contaminated with waste having other process origins. The ^{239}Pu versus ^{241}Am data points for these soil samples fall on a line defined by several of the waste samples (see Figure 10A); the ratio is on the order of 2×10^1 , indicating that they may have sources of contamination similar to the waste.

Samples T17 and T19 were unique in being permeated with organic material to such an extent that the soil took on a greasy or candied appearance. This phenomenon could only have occurred through soil contact with organic sludge, possibly over an extended period of time. In contrast, samples T03, T05, and probable organic sludge sample R20 are most likely examples of incidental mixing of organic sludge and soil. Incidental mixing leads to dirt encrusted balls of organic material or discrete chunks of organic material clinging to clods of soil. Samples T17 and T19 appeared to be thoroughly mixed, which would not seem to be likely with incidental contact. Thus, these samples may be mixed as a result of other processes not due to actions incidental to the excavation.

Isotope Ratios for Soil Scraped From Graphite (T27) and Soil After Rupture of Graphite Scarfings Jar (T28 through T36). The $^{232}\text{Th}/^{238}\text{U}$ ratios for all of these samples were within normal values for soil; however, the $^{238}\text{U}/^{235}\text{U}$ ratios indicated that the samples contained ^{235}U -enriched uranium. The high concentrations of plutonium in these samples had $^{239}\text{Pu}/^{240}\text{Pu}$ ratios of about 15 to 18, consistent with the presence of weapons-grade plutonium. The ^{239}Pu versus ^{241}Am data points for these samples appear tightly bunched in Figure 10A, where they are contained within the top-most oval. The $^{239}\text{Pu}/^{241}\text{Am}$ ratios were also remarkably precise, ranging from 170 to 210, and in close agreement with values measured for many of the low-contamination soil samples. This latter point is illustrated by extension of a diagonal line derived from the high-plutonium soil samples T27 through T36 (see Figure 10A, circle centered at 2.0×10^2 ng/g on the ^{241}Am x-axis) which extends through the low-contamination soil samples (oval centered at 2.0×10^{-1} ng/g ^{241}Am), and suggests similarity in the process origins of the contamination. The $^{239}\text{Pu}/^{241}\text{Am}$ ratios in the majority of interstitial soil samples, at all concentration levels, implies that most of the plutonium contamination is derived from the highly ^{239}Pu enriched materials.

Isotope Ratios for Unknown Waste Type I: P01, P03. P01 and P03 had lower $^{232}\text{Th}/^{238}\text{U}$ and $^{238}\text{U}/^{235}\text{U}$ ratios, indicating ^{235}U -enriched uranium contamination mixed with little or no soil, which would produce less-than-normal ^{232}Th concentrations. $^{239}\text{Pu}/^{240}\text{Pu}$ ratios were 17 and 24, respectively, consistent with weapons-grade plutonium. $^{239}\text{Pu}/^{241}\text{Am}$ ratios were very different, at 120 for P01 and 17 for P03. The variation is due to a large difference in the ^{241}Am , and points to the difficulty in attempting to categorize waste samples which tend to be extremely heterogeneous. The $^{239}\text{Pu}/^{241}\text{Am}$ ratio for P03 agrees well with that of the majority of the low-contamination soil samples and with the high ^{239}Pu samples; the same ratio for P01, on the other hand, is unique among the samples analyzed in this study.

Isotope Ratios for Unknown Waste Type II: P02, P04 and P05. Like the rest of the waste samples, P02, P04, and P05 were all characterized by low $^{232}\text{Th}/^{238}\text{U}$ ratios; all three samples, however,

had normal or near-normal $^{238}\text{U}/^{235}\text{U}$ ratios, showing that the low $^{232}\text{Th}/^{238}\text{U}$ ratio was principally due to the absence of ^{232}Th , indicating that the samples were mainly waste with little or no soil. The $^{239}\text{Pu}/^{240}\text{Pu}$ ratios for all three samples, ranging from 12.3 to 12.6, were consistently low compared to weapons-grade plutonium. This suggests that the radionuclide contaminants in these samples originate from a process different from those that generated the graphite molds, or the unknown waste type I. The $^{239}\text{Pu}/^{241}\text{Am}$ ratios were the lowest recorded for this set of samples, ranging from 1.9 to 2.3. The low values resulted from high $[^{241}\text{Am}]$ values, which perhaps indicated that this waste was derived from other process origins. The low $^{239}\text{Pu}/^{241}\text{Am}$ ratios were also consistent with organic waste (see below) and with soil samples T01 and T02, which visually contained waste material.

Isotope Ratios for Organic Waste: R04, R20, R23. As expected, the $^{232}\text{Th}/^{238}\text{U}$ ratios were significantly lower than normal soil because very little ^{232}Th was present in these non-soil containing samples. The $^{238}\text{U}/^{235}\text{U}$ ratios were modestly depressed for R04 and R20, but significantly lower for R23 (value of about 26, compared with natural abundance ratio of 131 to 140). Sample R23 was noticeably different from the other two organic waste samples in actinide concentrations, $^{239}\text{Pu}/^{240}\text{Pu}$ ratios, and $^{239}\text{Pu}/^{241}\text{Am}$ ratios. The $^{239}\text{Pu}/^{240}\text{Pu}$ ratios for R04 and R20 ranged from 11.6 to 12.6, which is lower than that expected in material from processes involving weapons-grade plutonium. R23 produced a value of 16, which suggests similarity with material derived from weapons-production processes. In fact, that sample had a $^{239}\text{Pu}/^{241}\text{Am}$ ratio in close agreement with the high- ^{239}Pu soil samples and with the majority of the interstitial soil samples. R04 and R20, on the other hand, had $^{239}\text{Pu}/^{241}\text{Am}$ values ranging from 2.0 to 2.2, in good agreement with the unknown waste samples P02, P04, and P05, and with the mixed soil-waste samples T01 and T02. The relatively large fraction of the ^{241}Am in these samples suggested that they may have other process origins.

Other Isotope Ratios. Three other isotope ratios were also informative, namely $^{239}\text{Pu}/^{237}\text{Np}$, $^{237}\text{Np}/^{241}\text{Am}$, and $^{239}\text{Pu}/^{235}\text{U}$. These ratios were not measured for all sample categories because low abundances precluded calculation in some instances. The three ratios are discussed separately in the following paragraphs.

$^{239}\text{Pu}/^{237}\text{Np}$ Isotope Ratios. A nearly identical plot (see Figure 11) to the one in Figure 10A can be constructed by substituting ^{237}Np for ^{241}Am . There is a direct relationship between the ^{241}Am concentration and the ^{237}Np concentrations for all of the samples and subsamples. This is expected since ^{237}Np is the decay product of ^{241}Am . The relatively short half-life of ^{241}Am ($t_{1/2}=433$ yr) has already given rise to a significant quantity of ^{237}Np ($t_{1/2}=155,000$ yr) in the waste. The concentration of ^{237}Np in the waste will continue to rise with time.

$^{237}\text{Np}/^{241}\text{Am}$ Isotope Ratios. A plot of ^{237}Np concentration versus ^{241}Am concentration further substantiates the direct relationship between two radioisotopes for all of the samples and subsamples (see Figure E-1). As noted above, ^{237}Np concentrations will continue to rise with time: the current m/z 237/241 ratios for organic waste samples and unknown waste samples are 0.0793 ($R^2=0.997$) and 0.0846 ($R^2=0.993$), respectively. Because the waste was buried more than 30 years ago, the high m/z 237/241 ratio for the sludge samples implies that, on a mass basis, the sludge samples initially contained primarily ^{241}Am with little ^{241}Pu .

For the interstitial soil samples, the m/z 237/241 ratio was 0.0585 ($R^2=0.977$). The measurable ^{237}Np and ^{241}Am in these samples were primarily associated with soil from the graphite mold pieces, and soil contaminated by the jar rupture. The much lower m/z 237/241 ratio implies that initially there was much more ^{241}Pu activity than ^{241}Am activity in these samples.

$^{239}\text{Pu}/^{235}\text{U}$ Isotope Ratios. After more than 30 years of interment, a significant portion of the ^{239}Pu would have decayed to ^{235}U (Table 1), and thus a linear relationship between the concentrations of the

two isotopes would be expected: in fact, for the low-contamination soil and the waste samples, this was observed (see Figure E-2A). If that were indeed the case, then uranium should be enriched when significant ^{239}Pu was present, and in fact this was evident in Figure E-2B as the samples with the highest concentrations of ^{239}Pu (high-plutonium soil samples) also had the lowest m/z 238/235 ratios, confirming a significant enrichment in ^{235}U decay product. The waste samples also showed ^{235}U enrichment; however, the m/z 238/235 ratio was only lowered to 100–120 in the waste samples indicating an increase in the total uranium content as well. The exception to this pattern is the R23 organic waste sample which had an m/z 238/235 ratio of 25.5 ± 0.8 , indicating significant ^{235}U enrichment; implications regarding the process origin of R23 are unclear.

A slight but significant difference appears in the $^{238}\text{U}/^{235}\text{U}$ ratio for the organic and unknown waste samples. Most of those samples exhibited either an elevated ^{239}Pu concentration, a lowered m/z 238/235 ratio, or both. In the waste samples, ^{238}Pu may contribute to the ion signal in the ICP-MS at m/z 238, thereby artificially elevating the m/z 238/235 ratio. However, ^{238}Pu could not be confirmed by separating and analyzing the uranium and plutonium fractions. In fact, for weapons-grade plutonium (see Table 1), the ^{238}Pu concentration would be insignificant relative to the quantities of uranium present in the waste or the natural abundance in soil.

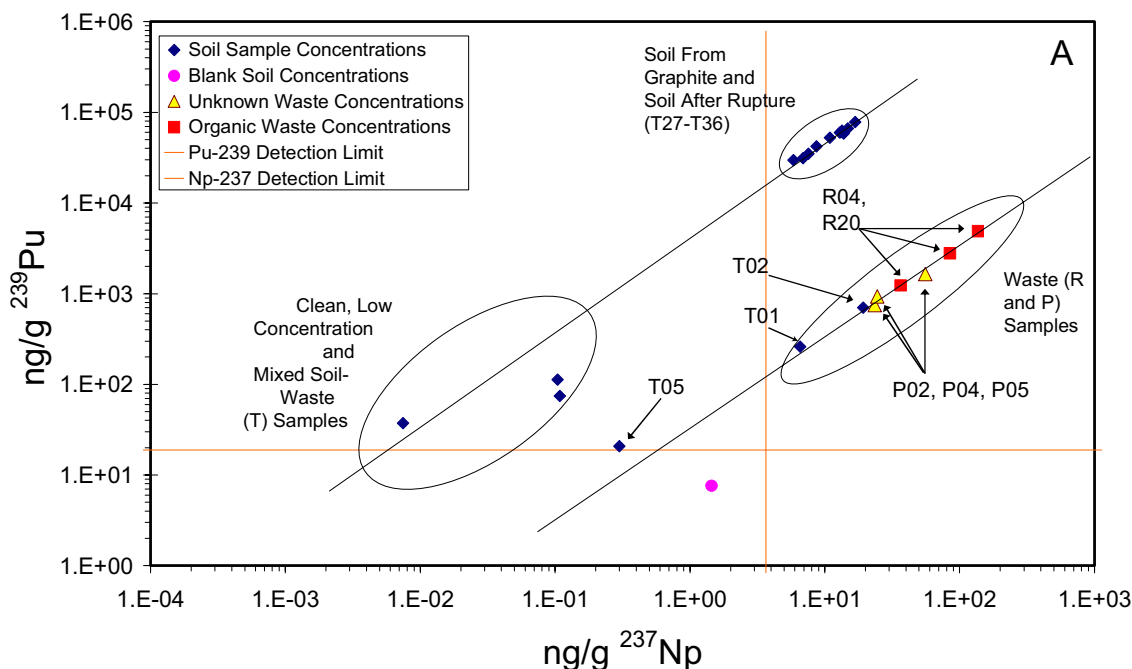


Figure 11. ^{239}Pu concentration versus ^{237}Np concentration in soil and waste samples. Lines have been drawn to highlight the difference in the $^{239}\text{Pu}/^{237}\text{Np}$ ratio for different sample types.

8. LEACHING

The migration potential of contaminants can be related in part to the partition coefficient K_d , which describes the ratio of the concentration of the contaminant sorbed to the concentration in the aqueous phase ($K_d = C_{\text{solid}}/C_{\text{aqueous}}$). Rigorously speaking, the parameter describes an equilibrium partitioning between the aqueous phase and the surface of the solid phase. In dealing with real-world contaminated samples, however, rigorous measurement of K_d values is not possible due to the presence of multiple solid and aqueous species participating in multiple processes. Additionally, the assumption must be made that the contaminants are on the surface of the solids. However, distribution coefficients measured for samples that are necessarily nonhomogeneous (which is referred to here as a K_d) have substantial value in describing the phenomenological partitioning of a contaminant between the solid and aqueous phases. For example, K_d values are used in transport models to parameterize contaminant release from a source term and contaminant readsorption to an adjacent matrix. Large K_d values indicate low partitioning into the aqueous phase, and usually this is correlated with a low probability of mobility. While no such correlation will be made here (because no experiments to explicitly evaluate transport were performed), the operationally defined K_d values measured herein can be used for comparison with values used in transport modeling. Reiterating in the operational context of this study, K_d merely refers to the ratio of the actinide fraction in the solid phase to that dissolved, when a sample is immersed in solution and assumed to reach equilibrium.

Many factors can affect measured K_d values; two of the most important are the pH and the ionic strength (I) of the aqueous solution. Consequently, K_d values were measured in three different ways:

- “Ambient” K_d values were measured using purified H_2O . This experiment was designed to be a simplified simulation of partitioning that would occur when the samples were exposed to a near-neutral aqueous infiltration.
- K_d values were measured as a function of variable pH. In some contaminant/matrix systems, (a) relatively subtle alterations in the leachate pH can have pronounced effects on the contaminant partitioning, and (b) local pH in the burial pit could change as the waste forms continue to degrade. An understanding of the influence of variable pH would enable assessment of the sensitivity of contaminant release to system perturbations.
- K_d values were measured as a function of variable ionic strength I . Aqueous leaching solutions having an elevated ionic strength tend to enhance the solubility of some ionic or otherwise polar species, which would serve to decrease the measured K_d . The motivation for examining K_d versus variable I was the same as for the variable pH leaching study.

The interstitial soil samples were not exhaustively analyzed; instead a subset was down-selected for pH leaching at low ionic strength. The subset of interstitial soil samples selected for pH leaching spanned a range of high to low actinide concentrations and appearance categories (Table 2). They included 24 interstitial soil samples, three organic waste samples, three overburden soil samples (uncontaminated), one unmodified INL blank soil sample, and one plutonium-spiked blank soil sample. The three organic waste samples were selected because variations measured in their americium, plutonium, and uranium concentrations and in their $^{238}\text{U}/^{235}\text{U}$ ratios suggested that variable leaching behavior may be occurring. The blank soil that was examined had been used in previous experiments (Mincher 2003) and the plutonium-spiked blank soil originated from a 2003 program (Mincher 2003). The downselected subset consisted of:

- Clean soil: T13, T22, T24, T26
- Low-contamination soil: T08, T10–13, T14–16, T18
- Mixed soil-waste: T03, T05, T07, T17, T19
- Soil scraped from graphite: T27
- Soil after rupture of graphite scarfings jar: T28, T31–T36
- Organic waste: R04, R20, R23
- Blank soil: W09, W13, W15, and blank INL soil
- Spiked INL soil.

The leaching procedure immersed a 1-g subsample in 10 mL of leaching solution (see Appendix F for a detailed description). After equilibration for 18 hours, the pH was measured, and a 1-mL aliquot was withdrawn and then analyzed using ICP-MS. After reconstituting the volume, the pH was adjusted, and equilibration and analysis were repeated. The pH range covered was <3 to >9.5.

The subset of samples noted above was further reduced for the leaching studies in which *I* was varied. In these studies, leachates that were 100 mM in NaCl were used. The samples identified for the high *I* experiments were:

- Low-contamination soil: T08–T10
- Mixed soil-waste: T03, T07, T17
- Soil scraped from graphite: T27
- Soil after rupture of graphite scarfings jar: T28, T32, T34
- Organic waste: R04, R20, R23
- Blank soil: W09, W13, W15, and blank INL soil
- Spiked INL soil.

K_d values for lead and thorium were measured in addition to uranium, plutonium, americium, and neptunium. Both lead and thorium occur naturally. Lead was included because it is also present in the waste at concentrations that ranged to >15 times the background soil concentration, and because it is the ultimate decay product for most of the radioisotopes of interest. Thorium is useful as a benchmark for radical changes in soil chemistry or composition.

8.1 Distribution Coefficients (K_d) at Ambient pH

When the subsamples were immersed in pH-neutral deionized water, the resulting solutions developed “ambient” pH values and actinide concentrations that reflected the chemistry of the samples and enabled calculation of K_d values. Ranges of values for appearance categories are provided in Table 4, and a complete set of data for the subset of samples is found in Table F-1 of Appendix F. The ambient values are presented separately because they provide insight into the actinide dissolution that might occur on infiltration by ground water having a neutral pH. For all of the soil samples, the ambient pH values ranged from 7.9 through 9.2, with the largest variability found in the samples categorized as mixed soil-waste. K_d values at ambient pH for the actinide elements of interest did vary according to type of sample. For uranium, K_d values in the mid- 10^3 mL/g range were measured for the low-contamination soil

samples; for soil samples contaminated by the rupture of the scarfings jar, values higher by about a factor of two were measured.

²³⁷Np could only be measured above detection limits in the ambient solution in contact with the soil scraped from graphite (T27), and hence this was the only ambient K_d reported for this isotope, at 1,700 mL/g. The wide error bar associated with this sample reflects the imprecision of the low-level measurements.

Ambient plutonium K_d values ranged from about 2×10^3 to 9×10^3 mL/g for most of the low-contamination soil samples examined (T08, T10, T11, T12, T16, T18); however, T14 was unusually low (1×10^3 mL/g), and T15 was unusually high (4×10^4 mL/g). These latter two outstanding values most likely arise from sample heterogeneity, which underscores the difficulty in generalizing partitioning behavior in a diverse matrix. This conclusion was substantiated by the plutonium K_d values measured for the mixed soil-waste samples, which displayed a similar range, from 1.5×10^4 to 3×10^3 mL/g.

Table 4. Ranges of ambient pH and K_d values for categories of down-selected samples. Measurements were conducted using low I leachate solutions. Since there was a single sample for the category “soil scraped from graphite” (T27), the average value was provided with the error bars for that measurement.

	K_d (mL/g)								
	pH	Lead	^{232}Th	^{235}U	^{237}Np	^{238}U	^{239}Pu	^{240}Pu	^{241}Am
Clean Soil									
Range	8.52–8.82	4,580–16,700	56,000–160,000	675–2,860		2,110–4,260			
Low-Contamination Soil									
Range	8.53–9.16	4,190–17,100	13,000–364,000	660–5,300		1,090–8,900	970–43,000	2,177–7,200	910–1,300
Mixed Soil-Waste									
Range	7.97–9.45	7,500–43,000	34,000–450,000	180–11,900		2,250–18,000	2,400–15,000	6,900–10,500	2,020–6,400
Soil Scraped from Graphite									
Range	8.23	32,000 \pm 26,000	430,000 \pm 200,000	1,050 \pm 590	1,700 \pm 1,800	1,950 \pm 760	730,000 \pm 580,000	430,000 \pm 140,000	57,000 \pm 35,000
Soil after Rupture of Graphite Scarfings Jar									
Range	8.53–8.77	9,100–12,400	98,000–240,000	4,080–8,300		4,730–8,830	1,450,000–4,030,000	1,420,000–760,000	22,600–88,000
Organic Waste									
Range	8.90–11.78	9,900–66,000	35,000–74,000	8,500–35,600		21,800–39,000			59,000–68,000
Benchmark soil									
Range	8.45–9.14	45,400–22,000	42,000–430,000	1,500–4,900		5,314–10,500			

The ambient K_d values measured for the high-plutonium soil samples were dramatically higher, signaling much less plutonium dissolution from this type of contamination. The soil scraped from graphite (T27) had K_d values of 7×10^5 and 4×10^5 mL/g for ^{239}Pu and ^{240}Pu , respectively. The values for the soil samples collected after the rupture of the jar were even higher, consistently ranging from about 1×10^6 to 4×10^6 mL/g (samples T28 and T31–T36). These much higher K_d values were surprising because the samples contained much higher plutonium concentrations; the finding strongly suggests different speciation for the plutonium in these samples. Highly insoluble, low-oxidation state plutonium oxides would be a reasonable speciation hypothesis for these samples.

Ambient K_d values for plutonium were not calculated for the organic waste samples because of low-solution plutonium concentrations, which stemmed from small aliquot sizes, low sample concentrations, and probably high K_d values.

^{241}Am ambient K_d values were in the low 10^3 mL/g range for low-contamination soil samples, and ranged to the mid 10^3 mL/g range for mixed soil-waste samples; americium K_d values were not calculated for most of these samples because of low-solution concentrations. In contrast, K_d values ranging from 2×10^4 to 9×10^4 mL/g were calculated for the soil scraped from graphite and in the samples after the jar was ruptured. As in the case of plutonium, partitioning of americium into the aqueous phase was significantly lower from these highly-contaminated samples.

8.2 Distribution Coefficients (K_d) as a Function of pH and I

Examining the ambient K_d data resulted in grouping all interstitial soil samples together because of similarity in the results. The exceptions were those samples containing high ^{239}Pu (T27 through T36). In addition, while organic waste samples R04 and R20 constituted a group, sample R23 was significantly different (both in terms of leaching behavior and $^{238}\text{U}/^{235}\text{U}$ ratio) and warranted a separate plot. Thus, in the following text, graphs of average K_d values versus pH are provided for the elements of interest; each plot contains data for these groupings:

- Low-plutonium soil: T03, T05, T07–T08, T10–T19, T22, T24, and T26
- High-plutonium soil: T27, T28, and T31–T36
- Organic waste: R04 and R20
- Organic waste: R23.

As noted, a more reduced set of the above samples was subjected to leaching using a high-ionic-strength leachate solution consisting of 100 mM NaCl leachate. Thus the plots contain data for both low I leachate (deionized water) and high I leachate (100 mM NaCl).

8.3 Uranium K_d as a Function of pH and I

Uranium (see Figure 12) exhibits multiple speciation forms over the pH range, generating a wide range of K_d values. In the soil samples, the K_d of uranium is in the 10^3 to 10^4 mL/g range when pH is 8–8.5. An important phenomenon applicable to all samples is the large increase in uranium partitioning as the pH drops from 8 to 7. Increases by factors of 10 to 100 times or more can be expected once the pH begins to fall below 8. Most interstitial soil samples, the overburden soils, and RWMC blank soil had nominal pH values in the range 8.45–9.12, with the blank INL soil at pH of 8.45; these values are higher than those expected for INL soil (Hull and Bishop 2004), and are consistent with low uranium solubilization. Samples T07 and T27 had pH values of 7.97 and 8.23, respectively, and correspondingly

displayed two of the lowest ambient K_d values. There tend to be fewer data points in the range where the pH was 6–8, because addition of small quantities of acid produced large changes in pH.

In the low-plutonium soil samples (having sample numbers <T27), K_d values drop to less than 10^2 mL/g at pH of 7. Figure 12 and Figures F-1 and F-2 (Appendix F) indicate an enhancement of aqueous uranium partitioning at about pH of 6, with the K_d peaking at 10^4 mL/g at pH of 4.5. Acid leaching then began to predominate at the lower pH values, and the K_d dropped rapidly with decreasing pH. This trend at the low end of the pH range was consistent for all soil samples, including the overburden and blank INL samples, indicating that under low pH conditions, uranium speciation may be similar to that expected for native uranium. Nearly identical behavior was observed for the high I leaching (see Figure 12), indicating that this parameter does not significantly influence uranium solubilization.

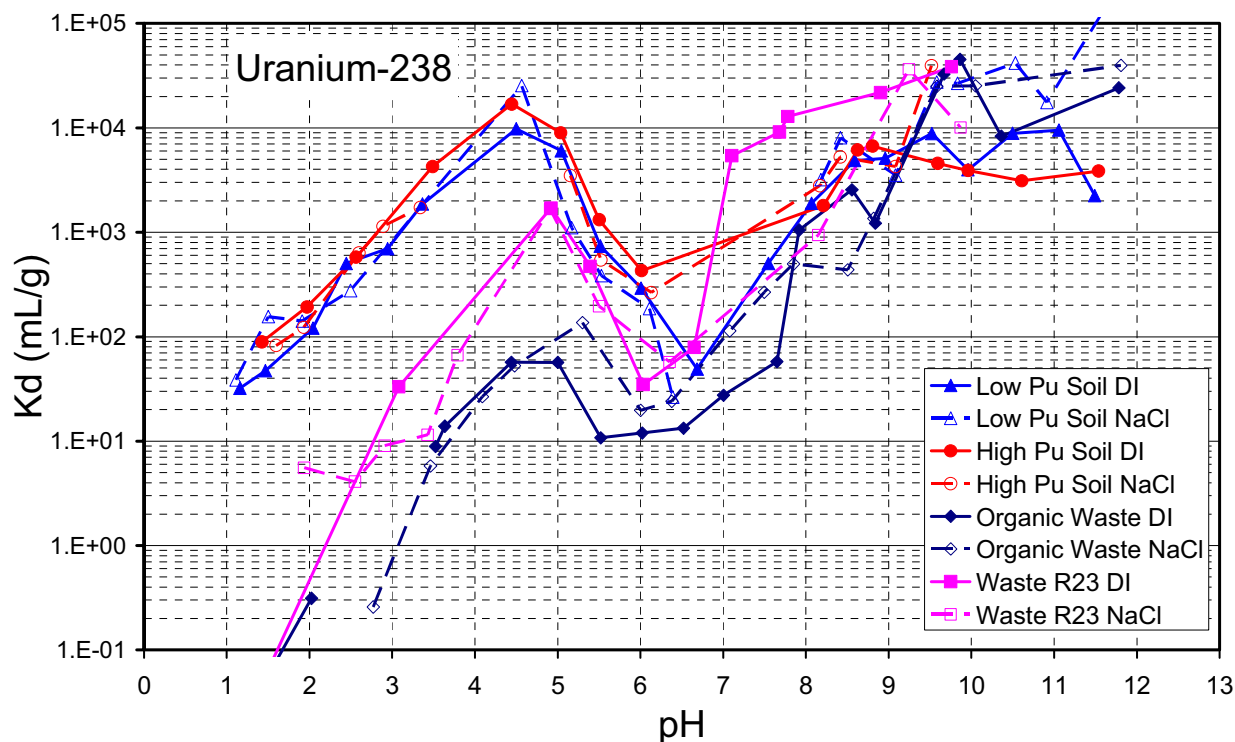


Figure 12. Average K_d values for the leaching of ^{238}U with low-ionic-strength leachate (deionized water) and high-ionic-strength leachate (100 mM NaCl) as a function of pH for interstitial soil samples and organic waste.

Variations in the $^{238}\text{U}/^{235}\text{U}$ ratio as a function of pH suggested that anthropogenic uranium was more readily dissolved than natural uranium from the soil samples at high pH. Overall, the K_d values for ^{235}U were slightly less than those for ^{238}U , and this was particularly the case in the higher pH ranges. Many of these low-plutonium soil samples contained only slightly elevated or normal uranium levels; however, some (T03, T07, T17, and T19) contained ^{235}U significantly above the norm (i.e., 5 to more than 20 times), compared with ^{238}U concentrations that were only modestly elevated (i.e., <4 times the norm). Figure 13 shows the results of low I leaching for T03, which exemplifies this phenomenon. At low pH, where most of the uranium was in the aqueous phase, the $^{238}\text{U}/^{235}\text{U}$ ratio was 10^2 to 10^3 mL/g, but fell regularly to 10^1 mL/g with increasing pH, suggesting that the enriched ^{235}U is more extensively partitioned into the aqueous phase at pH values of 8–11 compared to the native uranium.

The high-plutonium soil samples (T27 through T36) also displayed high uranium K_d values at high pH, and also showed the depression in K_d around pH 6–7 (see Figure 12) before rebounding to about 10^4 mL/g at pH of 4–5. The fraction of dissolved uranium significantly increases at pH values <4 for these

samples. The K_d values are nearly identical to those for the low-plutonium soil samples. In the high-plutonium soil samples, the ^{238}U concentration was not elevated compared with background, whereas in contrast ^{235}U was more than 5 times higher. As in the case of the low-plutonium samples, ^{235}U (presumably originating from the ^{239}Pu decay) appears to be slightly more dissolved at the higher pH values. This is supported by the trend of decreasing $^{238}\text{U}/^{235}\text{U}$ isotopic ratios with increasing pH (see Figure 14), which was observed in both the low I and high I leaching experiments.

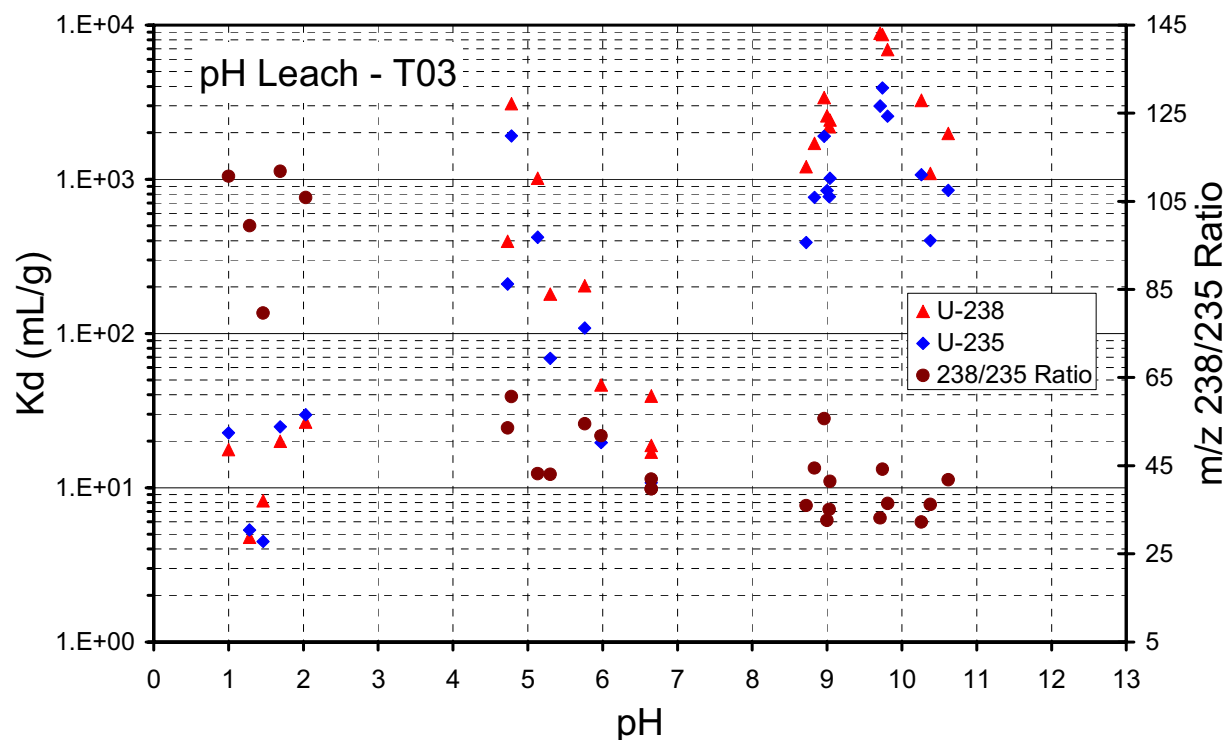


Figure 13. Uranium K_d values (triangular data points, left-hand y axis) and $^{238}\text{U}/^{235}\text{U}$ ratios (square data points, right-hand y axis) as a function of pH for the interstitial soil sample T03.

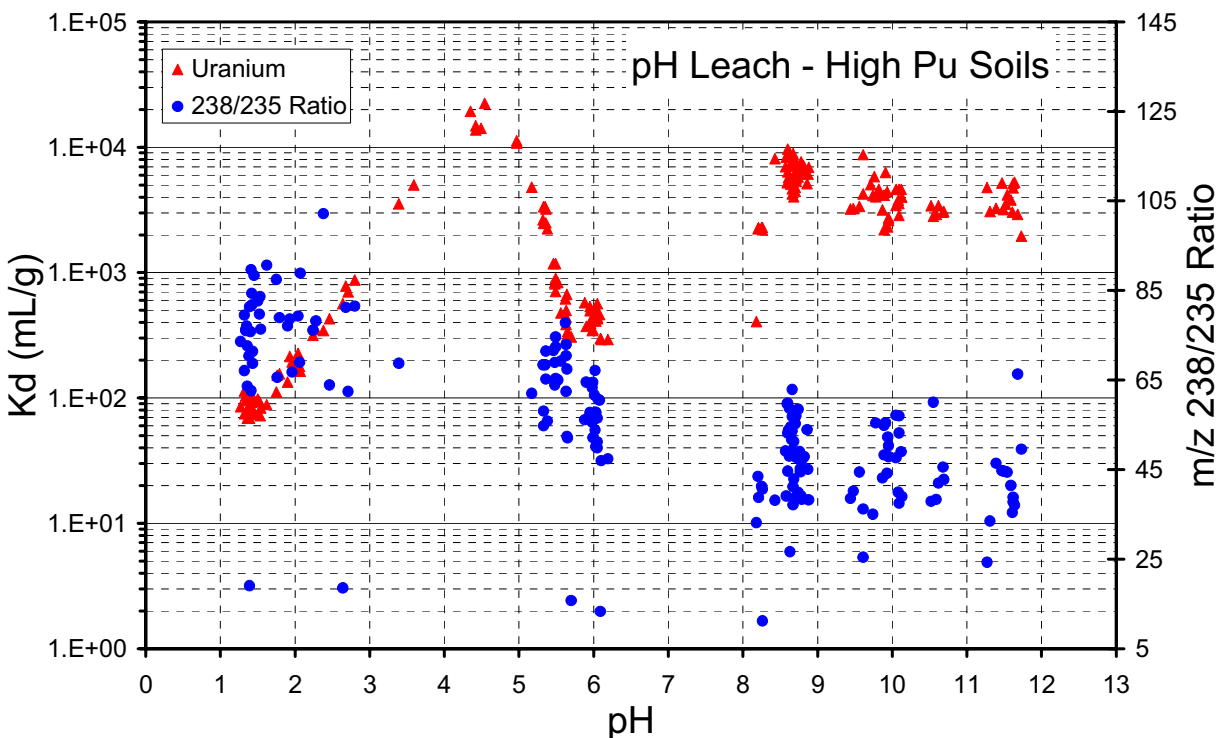


Figure 14. Uranium K_d values (triangular data points, left-hand y-axis) and $^{238}\text{U}/^{235}\text{U}$ ratios (square data points, right-hand y-axis) as a function of pH for the high-plutonium interstitial soil samples.

Similar variations in K_d with pH were observed in leaching uranium from the organic waste samples (see Figure 12). For pH values >9 , K_d values of $>10^4$ mL/g were measured. Markedly increased aqueous partitioning was observed for pH of 6–7 with $K_d < 10^2$ mL/g in this realm. For the pH range 4–5, K_d values increased to $>10^3$ mL/g. Finally, acid leaching became predominant at the lower pH values, where uranium was significantly more dissolved compared to the low-contaminated soil samples (K_d values nearly two orders of magnitude lower). The K_d values determined for the ^{235}U and ^{238}U isotopes are in good agreement with each other, and also track very well with the K_d values determined for the ^{234}U and ^{236}U isotopes (data not shown).

8.4 Plutonium K_d as a Function of pH and I

In contrast to the leaching behavior of the other elements examined, dramatic differences in plutonium leaching were seen when high-plutonium soil samples were compared with low-plutonium soil samples and waste. Figure 15 depicts the K_d values measured for the interstitial soil samples and organic waste samples over the pH range. Overall, plutonium associated with the lightly contaminated soil samples had K_d values from about 10^3 to 10^4 mL/g over the entire pH range of the study; the behavior was consistent with K_d measured for benchmark soil samples spiked with low concentrations of plutonium. In contrast, plutonium associated with the high-plutonium soil samples had K_d values that were 10 to 100 times greater than the low-plutonium soil samples, and were as high as 10^6 mL/g for pH of 5–9. Ionic strength did not have any effect on the leaching behavior of plutonium in any of the samples examined, except for waste R23 (see below).

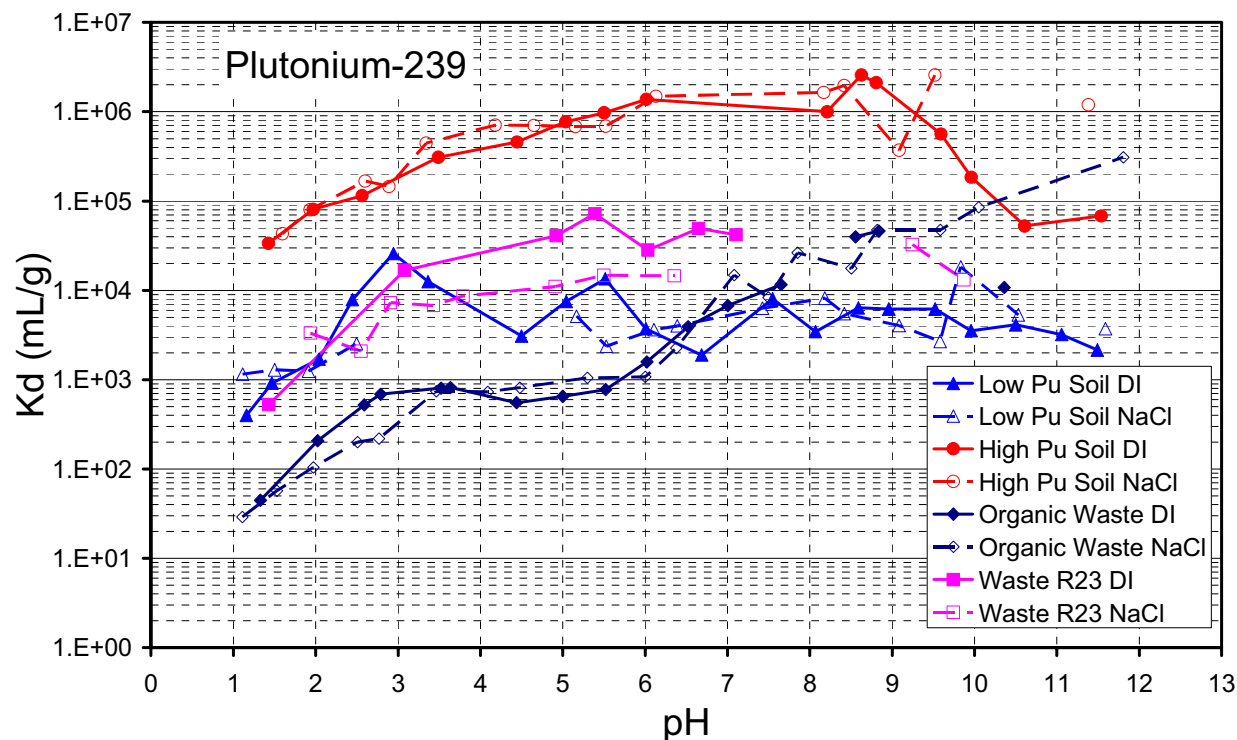


Figure 15. Average K_d values for leaching ^{239}Pu with low-ionic-strength leachate (deionized water) and high-ionic-strength leachate (100 mM NaCl) as a function of pH for interstitial soil samples and organic waste.

The 10- to 100-times difference in the plutonium K_d between the low-plutonium and high-plutonium soil samples suggested a dramatic difference in the plutonium speciation in these samples. As noted previously, the high-plutonium soil samples were in all likelihood contaminated by plutonium directly related to a graphite mold and the dispersal event accompanying the rupture of the jar. While the actual speciation in these samples is unknown, the very low aqueous plutonium partitioning in the high concentration samples is consistent with the presence of highly insoluble Pu(IV) oxide species, which would display very high K_d values.

K_d values for the organic waste samples were substantially lower, which may indicate that these samples may contain plutonium in more soluble Pu(V) or Pu(VI) oxidation states. There appears to be a slight increase in the aqueous partitioning of plutonium from organic waste R23 when using a high-ionic-strength leachate; this sample was the only one for which high ionic strength seemed to augment plutonium dissolution. In all other experiments, the low ionic strength and high ionic strength leaching experiments were indistinguishable within experimental error, indicating that this parameter did not play a significant role in solubilization.

The K_d values by Dicke (1997) for INL surficial sediments and interbeds fall within the range of those determined for the low-plutonium soil samples in this work. However, the K_d values for the high-plutonium soil samples are greater than the K_d values estimated from available K_d data normalized for INL soil composition. Observed agreement between past K_d values and those measured in this study supports use of values in the 10^3 – 10^4 mL/g range for soils, and suggests that even higher values are justified when considering plutonium release from more highly contaminated materials.

8.5 Americium K_d as a Function of pH and I

Like plutonium, americium can exist in multiple oxidation states, but is most commonly encountered as americium (III) in the environment and typically undergoes only limited aqueous partitioning. Previous work (Newman et al. 1996; Fjeld, Coates, and Elzerman 2000; Fjeld et al. 2001) indicated that americium was readily retained by INL sediments and will precipitate from INL groundwater (see also Cleveland and Mullin 1993).

Examining the K_d versus pH for the low-plutonium soil samples (see Figure 16) showed discontinuities in the plot that resulted from large changes in the pH in the neutral range when the samples were acidified. In the pH range of 6–12, K_d values from about 10^2 to 10^4 mL/g were measured. This broad range of values is consistent with the operation of multiple dissolution mechanisms. As pH decreases from 6 to 1, a systematic decrease in K_d in the low I experiment was recorded, minimizing at about 2×10^1 mL/g.

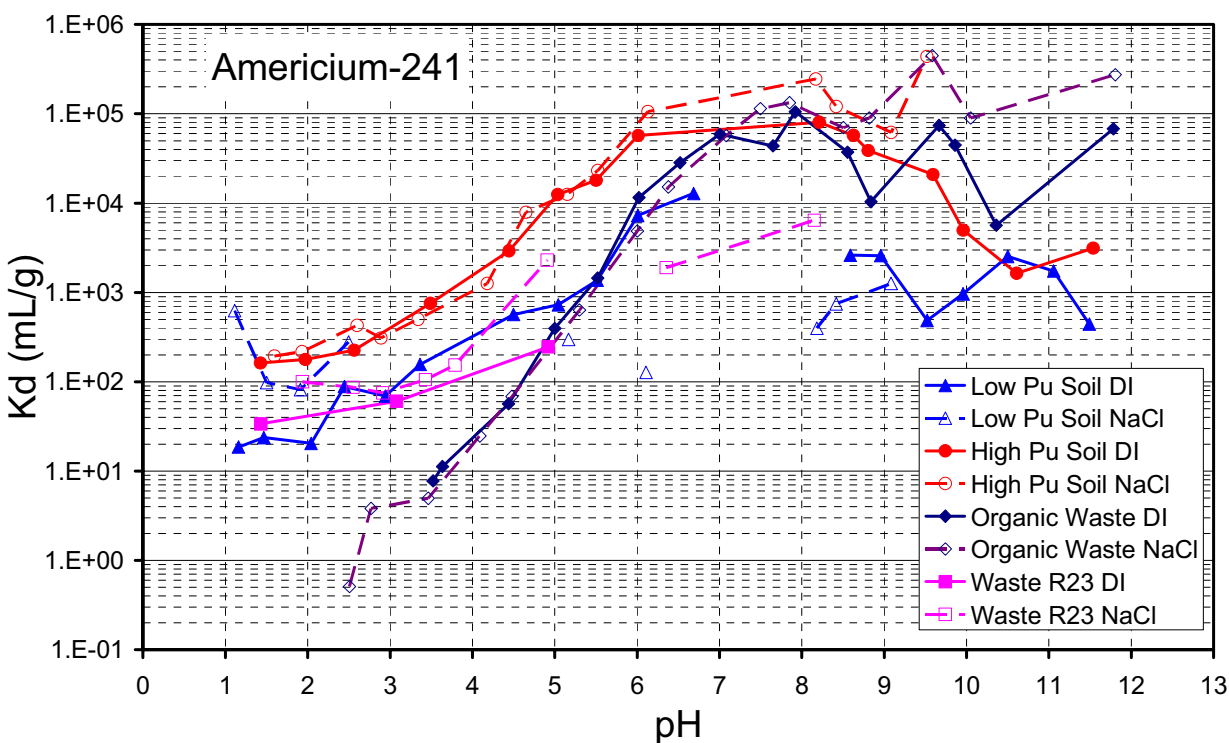


Figure 16. Average K_d values for leaching ^{241}Am with low-ionic-strength leachate (deionized water) and high-ionic-strength leachate (100 mM NaCl) as a function of pH for interstitial soil samples and organic waste samples. Gaps in data sets represent measurements for which ^{241}Am was below detection limits.

More consistent K_d behavior was observed in the leaching experiments of ^{241}Am from the high-plutonium soil samples (see Figure 16). The values maximized at $>10^5$ mL/g in the pH range of 6–9. Above pH 9, the low I leaching experiment showed a decrease into the 10^3 mL/g range, perhaps because of basic dissolution of a part of the silicate matrix. At the acidic end of the pH range, K_d values also decreased; the shape of the curves suggested that a minimum K_d of 2×10^2 mL/g was reached at pH of 2.

Leaching behavior of ^{241}Am from the two organic waste samples R04 and R20 (see Figure 16) were phenomenologically similar to that observed for the high-plutonium soil samples, but significant quantitative differences were seen, particularly at low pH. K_d values $\geq 10^4$ mL/g were measured when the

pH was ≥ 7 , but as pH decreased below this level, K_d values decreased precipitously, falling to values $<10^1$ mL/g. Data were also included for organic waste R23 (see Figure 16). R23 was different from the other two organic waste samples, and in fact displayed some similarity to the low-plutonium soil samples in that scattered K_d values ranging from 10^3 to 10^4 mL/g were measured in the ambient pH range, falling to $<10^2$ mL/g as pH decreased from pH 6 to 1.

8.6 Neptunium K_d as a Function of pH and /

Neptunium was only found in the high-plutonium soil samples and in the organic waste samples R04 and R20. The K_d behavior in the soil samples (see Figure 17) showed plot discontinuities at pH >6 , but nevertheless supported K_d values in the mid 10^2 to mid 10^3 mL/g range. At lower pH values, a modest decrease in K_d was observed to the low 10^2 mL/g range. For neptunium in the soil samples, exposure to caustic solutions ($>\text{pH } 9$) may disrupt the silicon matrix, which would be expected to produce lower K_d values. Generally, neptunium in the ground is believed to exist in the Np(V) oxidation state as the soluble dioxo cation (NpO_2^+ , neptunyl) and have a K_d of about 25 mL/g. However, previous studies (Fjeld, Coates, and Elzerman 2000) have led to the hypothesis that Np(V) can be reduced to Np(IV) in INL soil, which would be consistent with a significantly higher K_d .

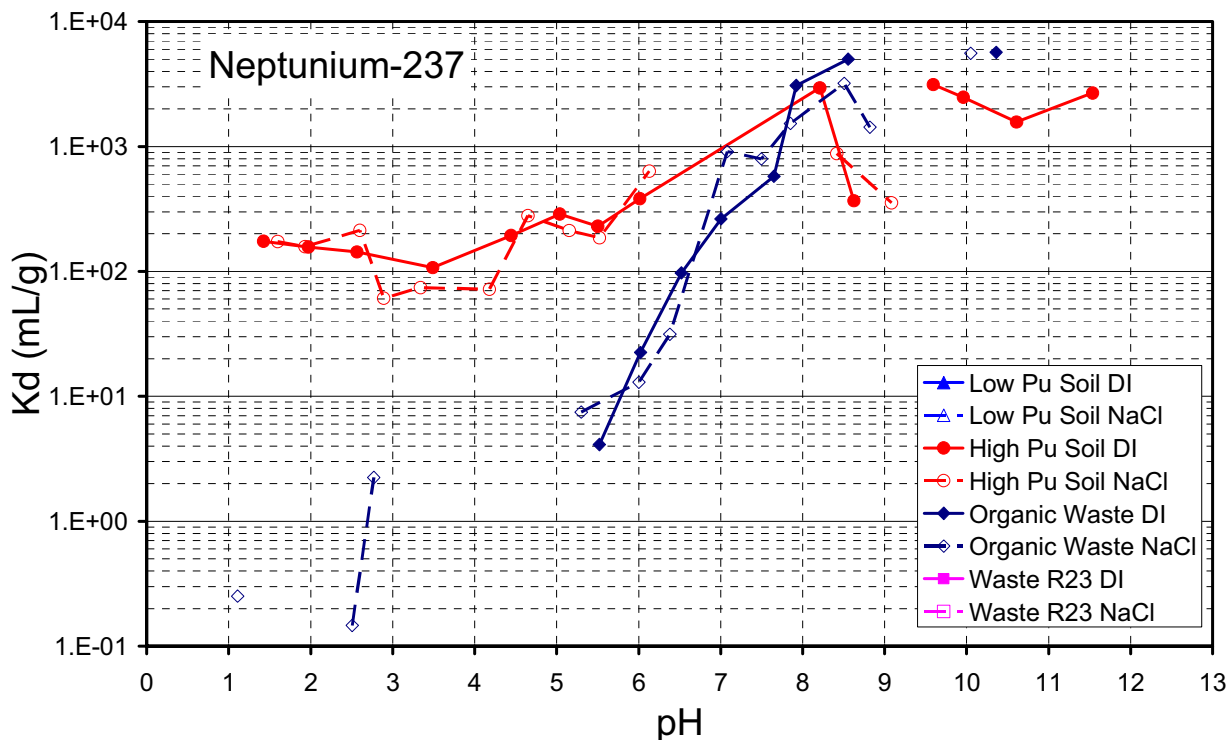


Figure 17. Average K_d values for the leaching of ^{237}Np with low-ionic-strength leachate (deionized water) and high-ionic-strength leachate (100 mM NaCl) as a function of pH for interstitial soil samples and organic waste samples. Gaps in data sets represent measurements for which ^{237}Np was below detection limits.

In the organic waste samples, K_d values between 10^3 and 10^4 mL/g were measured for $\text{pH} > 8$. However, as the pH decreases below this slightly basic value into more neutral and acidic regimes, the K_d values drop sharply, reaching values slightly $< 10^1$ mL/g at pH values < 6 . Thus ^{237}Np will readily partition to the aqueous phase from organic waste in response to very modest increases in solution acidity. While explicit speciation cannot be assigned, a consistent explanation is that Np(V) is present as hydroxide and carbonate salts that would be susceptible to dissolution at near-neutral pH values. Neptunium leaching was not influenced by changes in leachate ionic strength.

8.7 Thorium K_d as a Function of pH and I

Similar thorium leaching behavior was measured for both the low-plutonium (see Figure 18) and the high-plutonium samples; in the neutral to high pH range of 7–11, K_d values of 10^4 mL/g to the mid 10^5 mL/g were calculated. At high pH values, sorption decreased in some of the soil samples, possibly because of the onset of caustic dissolution of the SiO_2 -dominated soil matrix. As pH decreased from 5 to 1, K_d values measured on both categories of soil samples decreased by about 3 orders of magnitude to the 10^2 mL/g range, consistent with acid leaching at low pH values. The experiments showed that ionic strength had a negligible impact on thorium dissolution. In general, the K_d values measured here were much higher than the values predicted for INL soil by Dicke (1997) (200–3,000 mL/g) but were within ranges reported by others (see Table 3 in Dicke 1997). On the other hand, the values measured for the contaminated soil samples were identical to those measured for uncontaminated soil samples. The K_d values measured in this work may be different from those quoted in previous reports because the samples include the native thorium incorporated directly into the crystalline structure of the soil minerals rather than being simply based on thorium sorbed to individual minerals or estimates based on the solubility of thorium compounds.

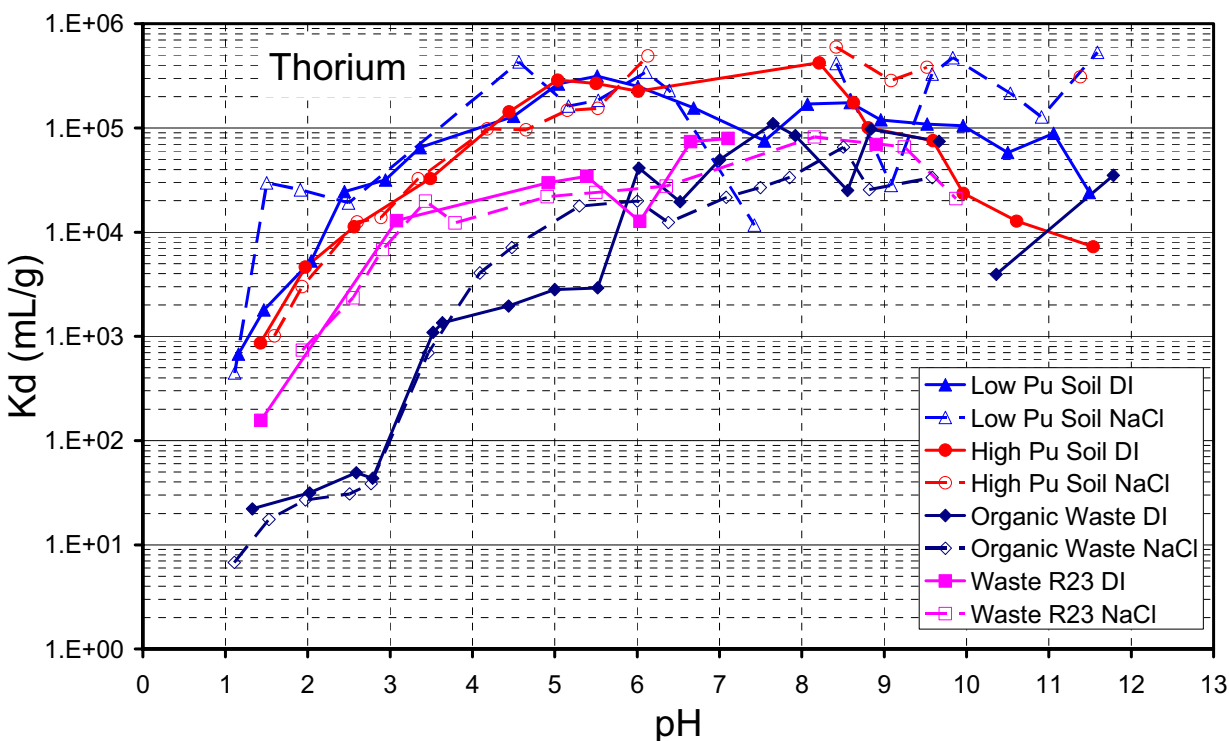


Figure 18. Average K_d values for the leaching of ^{232}Th with low-ionic-strength leachate (deionized water) and high-ionic-strength leachate (100 mM NaCl) as a function of pH for interstitial soil samples and organic waste samples. Gaps in data sets represent measurements for which ^{232}Th was below detection limits.

The K_d values for thorium in the organic waste samples R04 and R20 (see Figure 18) were smaller than those for the soil samples by about a factor of 10 for the pH range of 7–11. However, as pH is decreased, thorium sorption and thus K_d slowly decreased beginning at about pH of 8. At pH of 3, leaching of thorium from the organic waste was more than two orders of magnitude greater than from the soil samples, indicating release of thorium from this matrix is easier. Thorium leaching from organic waste sample R23 was similar to that from other samples at neutral to high pH values, and displayed release behavior intermediate between soil and the other organic waste samples at low pH.

8.8 Lead K_d as a Function of pH and I

Aqueous partitioning of lead was examined because it was a contaminant metal commonly encountered at radioactive burial sites, and because it had mass and concentration values that could be incorporated into the actinide analyses with negligible increases in complexity and cost. As in the case of thorium, the leaching behavior of lead was nearly identical for the two types of soil samples. Low-plutonium samples (see Figure 19) showed K_d values $>10^4$ mL/g for the pH range 5–9. Above pH of 9, lead sorption decreased by an order of magnitude in the low I leaching, and the results were identical for the high-plutonium samples and the low-plutonium soil samples. The pH decrease may be related to dissolution of the soil matrix, as speculated above; however, other processes such as precipitation of lead hydroxide may also be occurring. Below pH of 5, the K_d values for the soil samples drop steadily to the mid- 10^1 mL/g range at pH of 1. Ionic strength had negligible influence on K_d values in these pH ranges regardless of the sample category examined.

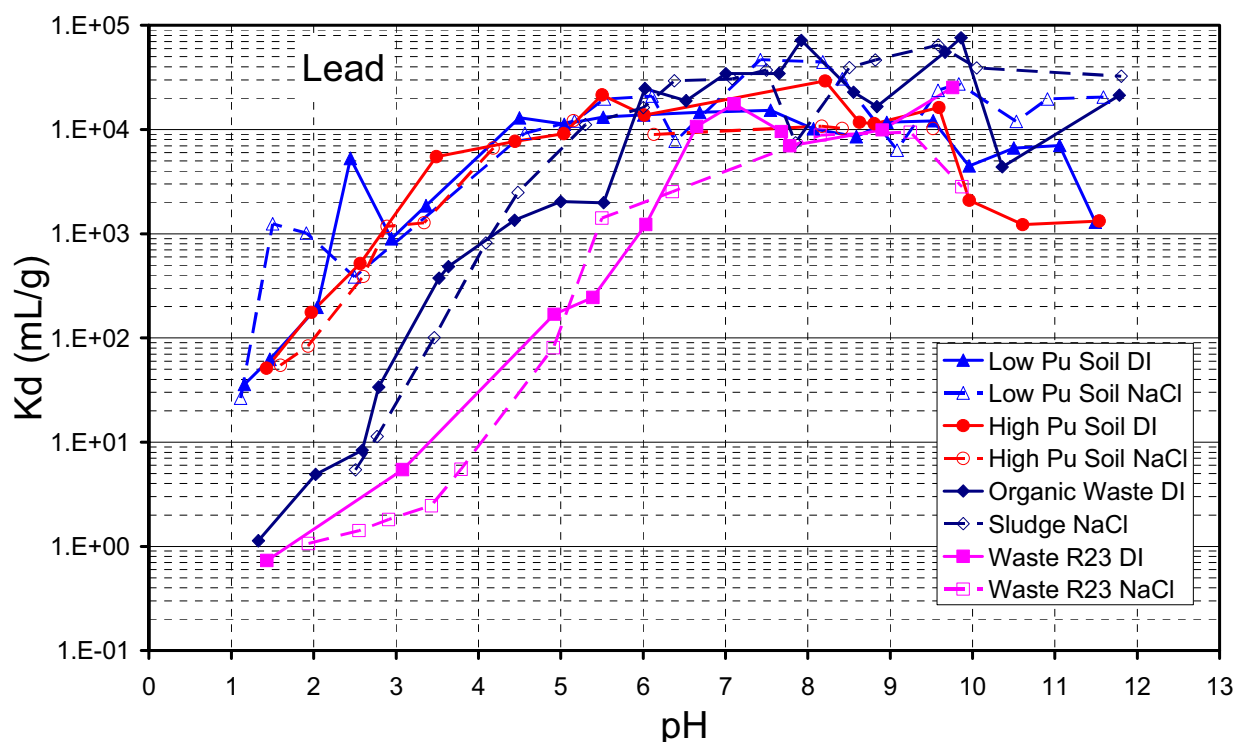


Figure 19. Average K_d values for the leaching of lead with low-ionic-strength leachate (deionized water) and high-ionic-strength leachate (100 mM NaCl) as a function of pH for interstitial soil samples and organic waste samples.

The K_d values measured in soil were somewhat higher than the 30–1,000 mL/g K_d values estimated by Dicke (1997). As before, speciation cannot be inferred, but the pH sensitivity does suggest the

presence of acid-sensitive species. One possibility is the presence of lead carbonate species, which would be largely insoluble at neutral pH values but release lead as the solution becomes acidic.

Leaching of lead from the organic waste samples is similar to that observed from soil above pH of 7; however, the K_d value of lead measured in the organic waste sample R23 (see Figure 19) drops quickly once the pH falls below 6. The K_d value is two orders of magnitude smaller than the values for soil at $\text{pH} \leq 5$. Waste R23 appeared to have a much higher organic content than the other two waste samples, which may be related in some way to the different K_d behavior. On the other hand, the K_d for lead in this sample was more consistent with the range expected from the Dicke (1997) evaluation at lower pH values. The K_d values for the organic waste samples R04 and R20 (see Figure 19) were similar to the other samples at $\text{pH} \leq 7$, falling between those measured for R23 and the soil samples.

9. SEQUENTIAL AQUEOUS EXTRACTION

Trace elements such as plutonium may exist as multiple species in soil that have the potential to strongly influence aqueous partitioning. No methods exist to directly speciate actinides present in concentrations typical for this study, and for this reason sequential aqueous extraction (SAE) is commonly used to operationally define trace metal species. SAE involves contacting the contaminated soil sample with a volume of solution designed to extract the trace metal from a targeted phase of the soil. Many methods have been published; however, the most common SAE procedures are designed to serially remove metals by means of (1) ion exchange, (2) mild acidification, (3) oxidation, (4) reduction, and (5) exhaustive dissolution. The results of SAE studies are normally used to infer solid-phase speciation without direct spectroscopic evidence. The five leaching steps are normally interpreted in terms of the contaminant metals bound to or incorporated in these corresponding target phases: (1) ion exchangeable sites on the soil, (2) carbonates, (3) organic compounds or minerals susceptible to oxidizing agents, (4) iron/manganese amorphous mineral coatings found on most soil particles, or (5) incorporated in silicate or other minerals that are not readily dissolved. The SAE results must be interpreted with caution because (a) the extraction steps may not be specific, and (b) metal readsorption may occur. Nevertheless, the results of SAE experiments provide strong suggestions regarding metal binding to the matrix and further provide explicit insight into chemical perturbations that might cause trace metals to be dissolved. Litaor and Ibrahim's (1996) method was used because it is the only method that has previously been used in the literature for analysis of actinides found in INL soil samples (Ibrahim 1997). Briefly, this SAE method incorporates five primary steps:

1. Exchangeable metal cations are separated with a calcium chloride leach
2. Carbonate-bound metals are released using a pH 5 acetic acid leach
3. Metals bound to oxidizable moieties are released using a hypochlorite (bleach) leach
4. Metals bound to reducible moieties are released using a dithionite leach
5. Residual or strongly bound metals are released by total postextraction soil dissolution using a sodium peroxide fusion, identical to what was used to determine total actinide content (Appendix E).

After each extraction stage, actinides were determined in the leaching solutions using ICP-MS. The procedure is described in detail in Appendix G.

As in the leaching studies, a subset of the samples was selected for the SAE investigations. Samples in the SAE subset were selected to span a range of sample categories and contaminant concentrations. These included

- Low-contamination soil: T08, T09, T10
- Mixed soil-waste: T03, T05, T07, T17
- Soil scraped from graphite: T27
- Soil after rupture of graphite scarfings jar: T32, T34
- Organic waste: R04, R20, R23
- Blank soil: overburden soil W09, W13, and W15, and blank INL soil
- Spiked INL soil.

SAE results are presented in the following sections on an element-by-element basis. The results are summarized in graphical fashion, and complete data sets are found in Appendix G, Table G-1.

9.1 Operational Speciation of Uranium

The speciation of uranium in uncontaminated INL soil samples (i.e., the overburden and blank soil samples) and in a plutonium-spiked soil was examined to provide a baseline for comparison of samples from the waste zone. INL blank soil was acquired from an area close to the SDA (referred to as Spreading Area B), and provided a benchmark that was not intimately associated with Pit 9 (in contrast to the overburden). The plutonium-spiked soil (see Section 9.2) was included because infiltration with another actinide element may cause redistribution of uranium into other phases. These SAE studies only compared ^{238}U because the low concentration of ^{235}U in the blank and plutonium-spiked soil presented experimental challenges. The majority of ^{238}U , between 70 and 80%, was found in the residual fraction of this soil, with small but measurable quantities in the other fractions as shown in Figure 20. Error bars shown correspond to one standard deviation, and can be quite large, but are not atypical for SAE results for actinides from environmental samples and simply are a reflection of soil chemistry heterogeneity. Very similar results for uranium were obtained when plutonium-spiked INL soil was examined.

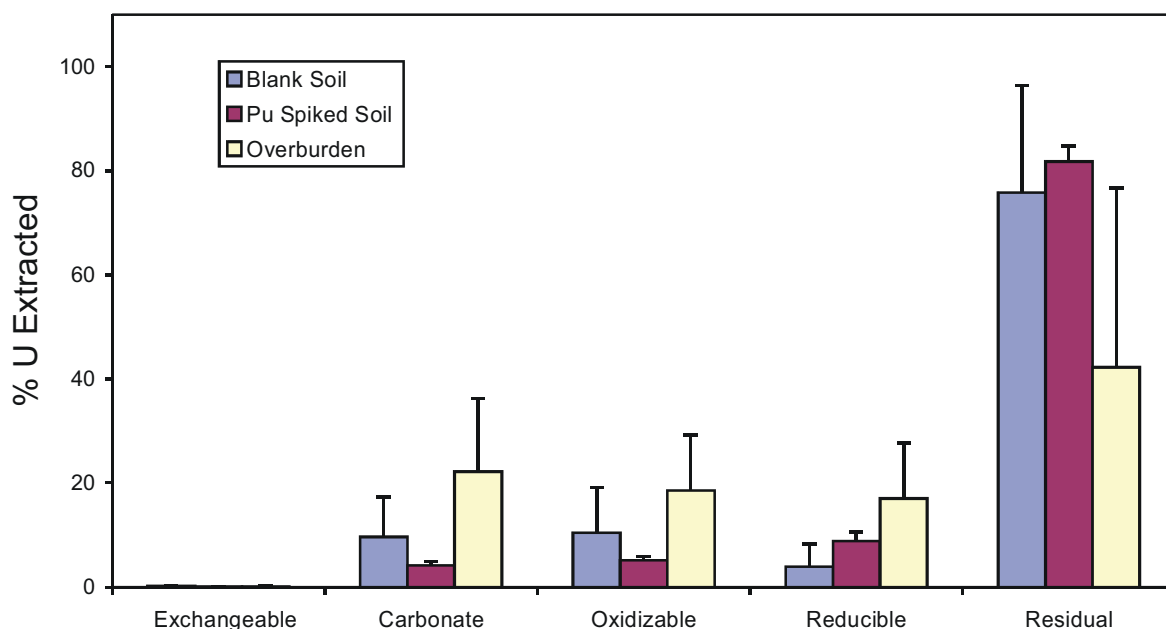


Figure 20. SAE dissolution profile for ^{238}U present in blank INL soil plutonium-spiked blank, and an average of overburden soil samples W09, W13, and W15.

SAE results for the three overburden soil samples showed significantly more uranium partitioning into the carbonate, oxidizable, reducible fractions, with correspondingly less ^{238}U partitioned into the residual fraction (42%). This difference was unexpected since the overburden was considered to be very similar to INL blank soil samples; the reason for the difference is not known.

For low-contamination soil samples T08 and T10, about 70% of the ^{238}U was associated with the residual phase (see Figure 21), and in general behaved like naturally occurring uranium in the overburden and uncontaminated INL soil. In contrast, in sample T09, only about 20% of the ^{238}U was in the residual fraction; the majority of the uranium was in the oxidizable fraction. The discrepancy between T08 and T09 was unexpected, since the two soil samples were retrieved from the same transfer cart and were both visibly clean on inspection in the lab. T09 showed no indication of incidental cross-contamination or ^{235}U

enrichment. The fact that those two apparently identical, clean soil samples have markedly different ^{238}U -SAE dissolution profiles suggested chemical alteration occurring in sample T09 that had not occurred in sample T08 or sample T10. This reflected redistribution of the natural ^{238}U from the residual phase to a potentially more mobile phase susceptible to dissolution in the presence of oxidizing agents.

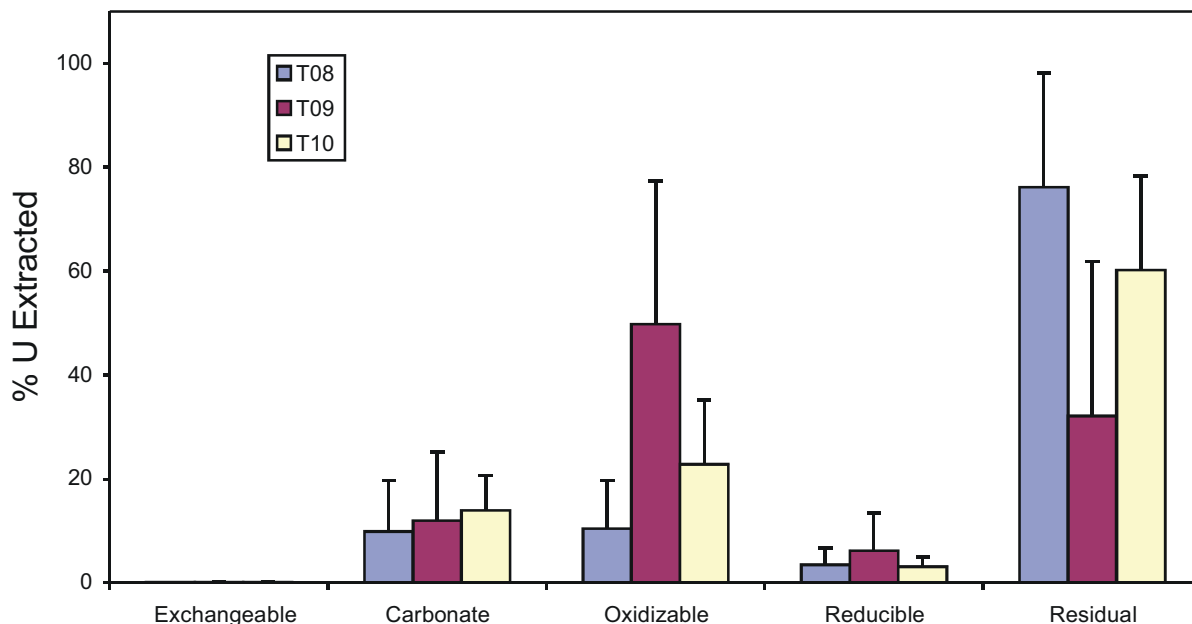


Figure 21. SAE dissolution profile for ^{238}U present in low-contamination soil samples T08, T09, and T10.

Samples analyzed by SAE that were categorized as “mixed soil-waste” were T03, T05, T07, T17. The results showed significant variability in their operational speciation, which is consistent with the high level of heterogeneity in these samples (see Figure 22). All of these samples contained ^{238}U concentrations that were about 1.5 to 3.7 times greater than the uncontaminated soil samples, and ^{235}U concentrations that were between 2.8 and 8 times higher.

SAE results for both ^{238}U and ^{235}U isotopes were in agreement within experimental error for samples T03, T07, and T17, but the samples themselves differed radically from each other. T17 uranium speciation was similar to that of background soil, with 80–90% of the uranium in the nonleachable residual phase. However, the residual phase accounted for only 20–40% in T03 and T07; in these samples uranium was also partitioned into the carbonate, oxidizable, and to a lesser extent reducible phases. Clearly uranium speciation in these samples is different. For T03 and T09, uranium partitioning into the carbonate and oxidizable fractions is consistent with soil that was incidentally mixed with waste during excavation. SAE profiles are similar to organic waste R04, R20, and R23 (see Figure 22). SAE profiles for T17 are more consistent with soil that has contained uranium for an extended period of time, perhaps reflecting the unique nature of this sample.

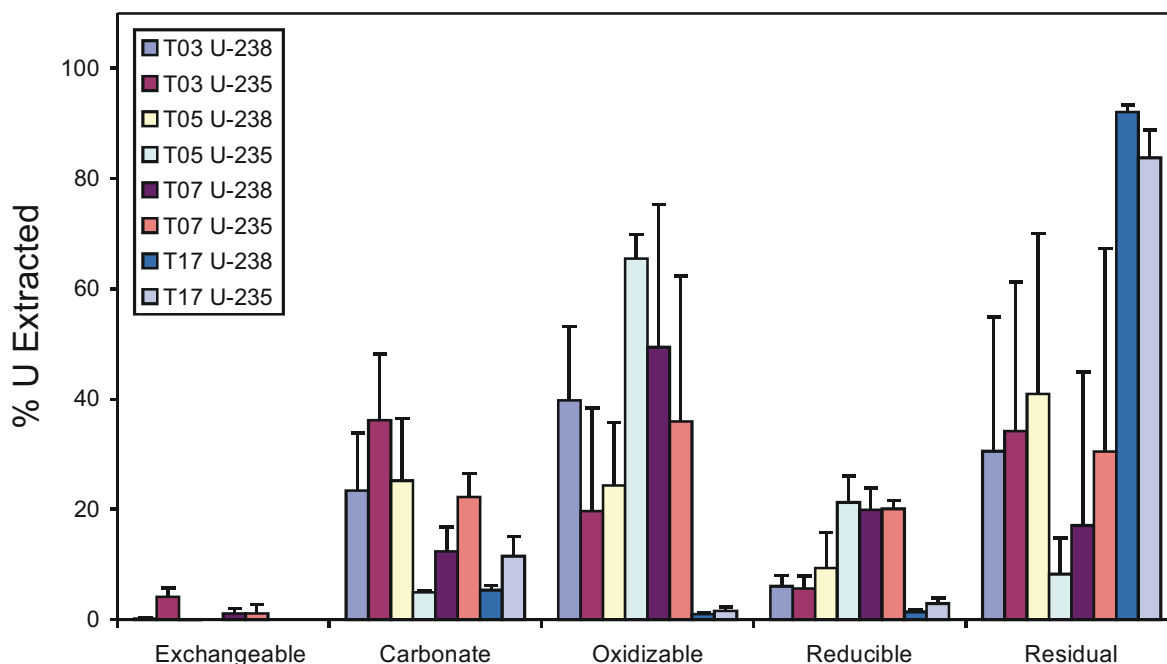


Figure 22. SAE dissolution profile for ^{238}U and ^{235}U present in interstitial soil samples T03, T05, T07, and T17.

Note that the SAE profile for ^{238}U in T05 was markedly different from that of ^{235}U . ^{238}U is evenly partitioned between the carbonate, oxidizable, and residual fractions, in contrast with ^{235}U , which appears prominently in the oxidizable fraction. This phenomenon, also seen in organic waste R23, is interpreted in terms of uranium from two different process origins having different operational speciation. ^{235}U susceptibility to solubilization on treatment with an oxidizing agent is normally interpreted in terms of organometallic complexation. There are alternative explanations for release upon oxidation; reduced uranium species may oxidize, forming soluble U(VI) species, or reduced metal binding sites may be destroyed. These possibilities cannot be differentiated at this time.

Interstitial samples having high-plutonium contamination, and elevated ^{235}U were T27, T32, and T34; as concluded above, T27 was different from T32 and T34 in that it was scraped from graphite fragments, while the latter two were contaminated from the rupture of the jar containing scarfings. In all three samples, the ^{235}U concentrations were about 3.5 to 4 times greater than the overburden and blank soil samples. In contrast, the ^{238}U concentrations in those samples were within levels typically accepted as natural ^{238}U background.

The SAE results show that agreement is good between the ^{235}U and ^{238}U isotopes in T27 and T32. In these samples, most (70–90%) of the uranium was concentrated in the nonleachable residual fraction (see Figure 23). The SAE results from those samples also show elevated levels of anthropogenic ^{235}U , which may be consistent with the presence of high levels ^{239}Pu , since ^{235}U is formed by alpha decay of the plutonium isotope. In this case the mineral containing both elements may be similar.

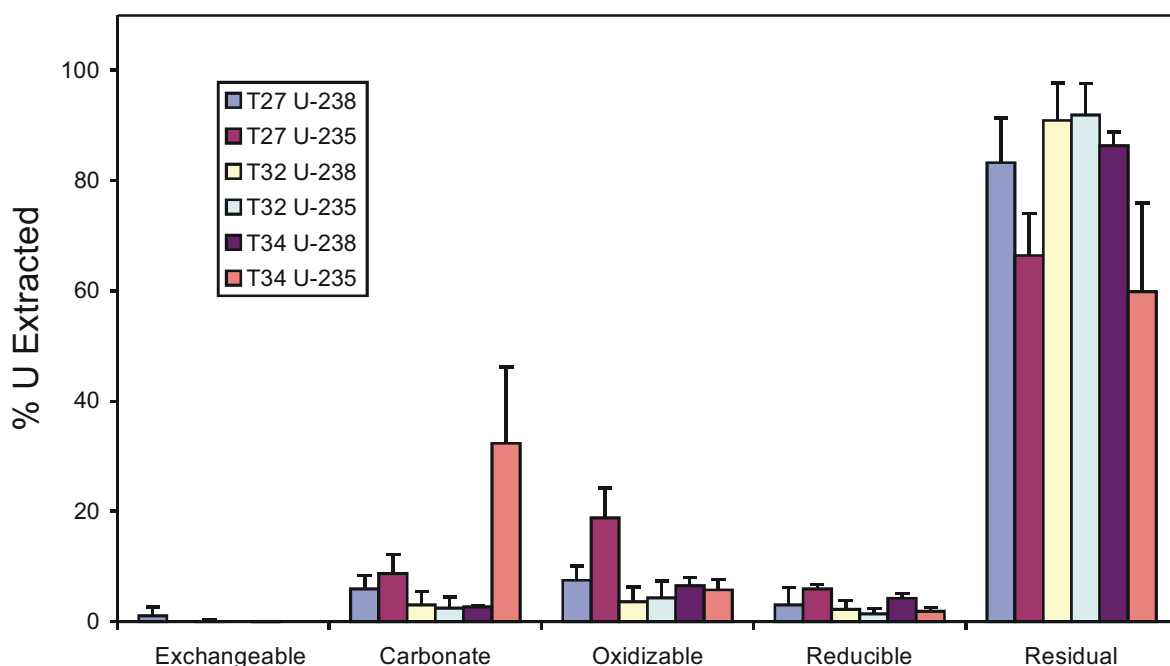


Figure 23. SAE dissolution profile for ^{238}U and ^{235}U present in the highly plutonium-contaminated interstitial soil samples.

Uranium in sample T34 was also predominantly localized in the residual fraction; however, 30–40% of the ^{235}U was partitioned into the carbonate fraction. ^{238}U did not do this, which suggests that ^{235}U was deposited in the sample by precipitation from aqueous solution.

The probable organic waste samples R04, R20, and R23 showed variable uranium-SAE dissolution results, consistent with the expected heterogeneous nature of the material (see Figure 24). R04 was similar to soil, with most (70–80%) of the uranium in the residual phase consistent with mostly soil and visible chunks of probable organic sludge. Agreement was good between the ^{238}U and ^{235}U isotopes for this sample and for R20. However, in R20 the uranium was evenly partitioned between the carbonate, oxidizable, and residual fractions, strongly pointing to the presence of multiple species in this material as manifested in highly varied leaching behavior.

Significant isotopic differences were seen in the SAE results for R23: most of the ^{238}U was present in that sample was in the residual phase >90%. In contrast, 30–40% of the ^{235}U appeared in the oxidizable fraction. As in the case of mixed soil-waste sample T05, this strongly suggests the presence of uranium from two different sources having different isotopic compositions, different molecular speciation, and consequently different aqueous partitioning behavior.

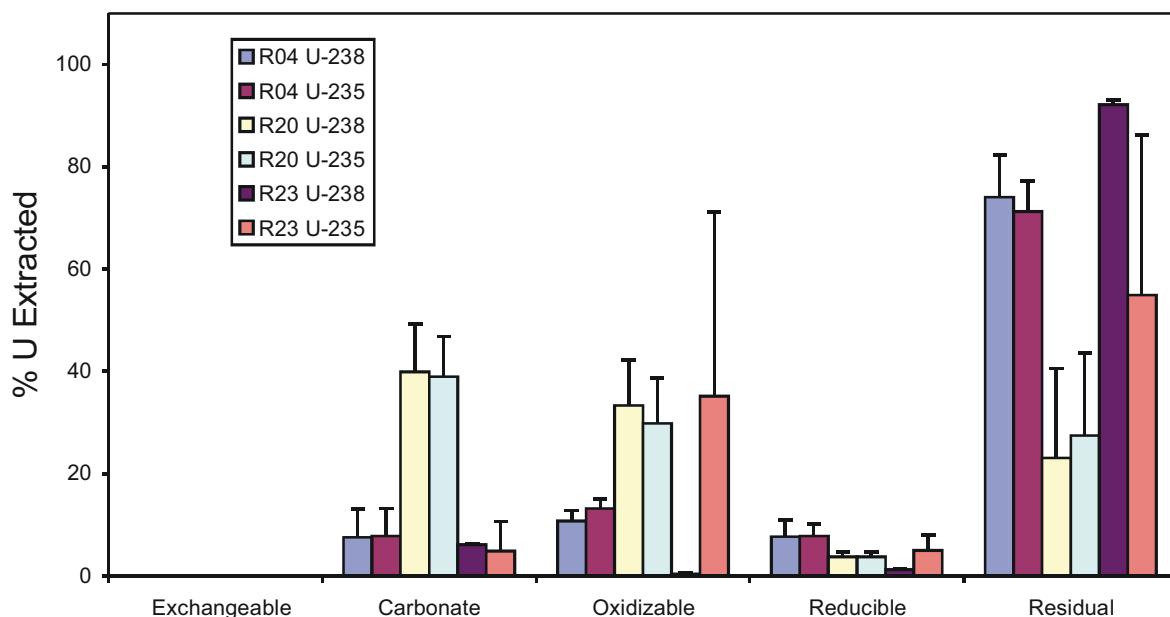


Figure 24. SAE dissolution profile for ^{238}U and ^{235}U present in probable organic waste samples R04, R20, and R23.

9.2 Operational Speciation of Plutonium

SAE results for plutonium are important to this study because the dissolution data suggestive of plutonium speciation are necessary for assessing long-term potential for mobilization. Adequate benchmark behavior is also necessary to compare with contaminated soil and waste samples, and since plutonium is not encountered in uncontaminated soil, plutonium-spiked soil samples were used for this purpose. Uncontaminated INL soil from Spreading Area B—previously spiked with ^{239}Pu and ^{240}Pu in November of 2003—was used as the plutonium-SAE benchmark. The experiments showed that most of the plutonium was recovered from the oxidizable fraction (73%, Figure 25), perhaps due to oxidation of surface-adsorbed Pu(IV) to Pu(V) or Pu(VI), which is generally more desorbable than Pu(IV). Almost all of the remainder was in the reducible fraction. The implication of this result is that exposure to plutonium solutions results in species that are leachable, at least after a period of 1 year.

SAE experiments for the low-contamination soil samples, which contained ^{239}Pu concentrations ranging from 2 to 3 times greater than the overburden, showed that the largest percentage of the plutonium was contained in the oxidizable fraction. Each sample also had 20–30% of the plutonium associated with the reducible fraction. As in the case of uranium, a significant percentage of the plutonium in T08 and in T10 was partitioned into the residual fraction, which was not observed in T09, indicating that these samples were less susceptible to chemical attack. On the other hand, the plutonium SAE profile for T09 was identical to that of the plutonium-spiked soil. A possible explanation is that both samples were exposed to plutonium in the same fashion (e.g., by floodwater contaminated with plutonium).

Samples categorized as mixed soil-waste (T03, T05, T07, and T17) also showed SAE behavior with considerable variability (see Figure 26). This is in part consistent with the variable composition of the samples, which contained ^{239}Pu concentrations ranging from 0.8 to 4.5 ng/g.

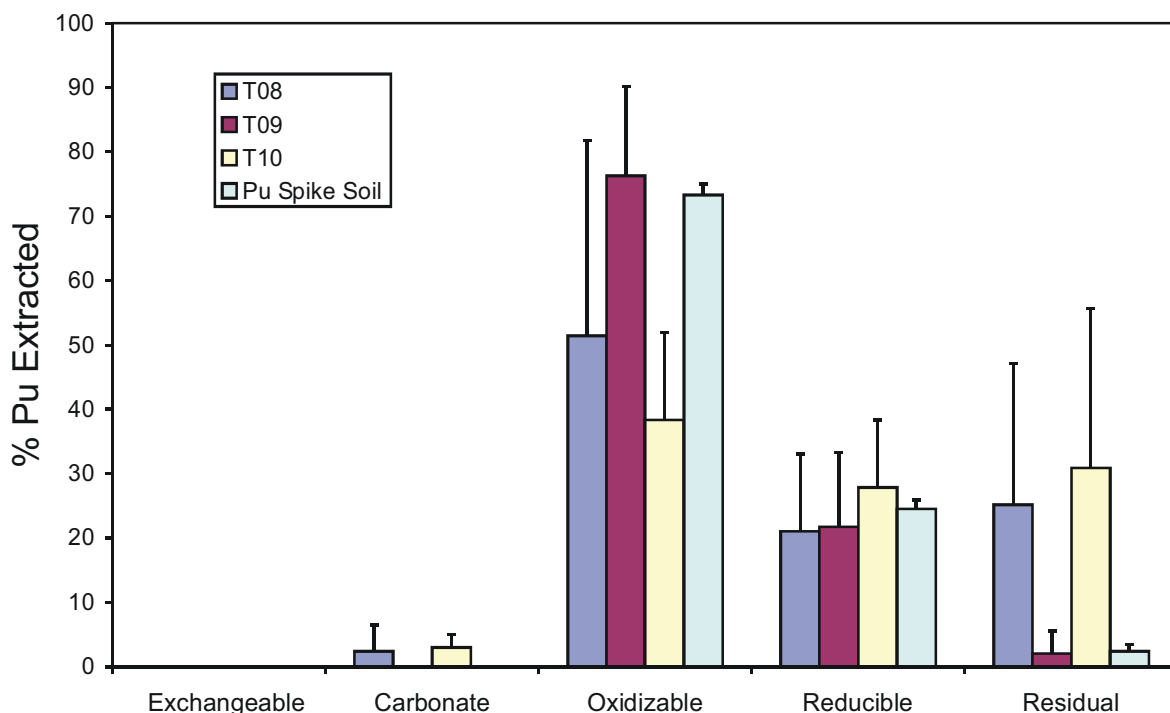


Figure 25. Plutonium-SAE dissolution profiles for the spiked soil, and the low-contamination soil samples T08, T09, and T10. Data are plotted together with data from SAE analysis of plutonium-spiked INL blank soil.

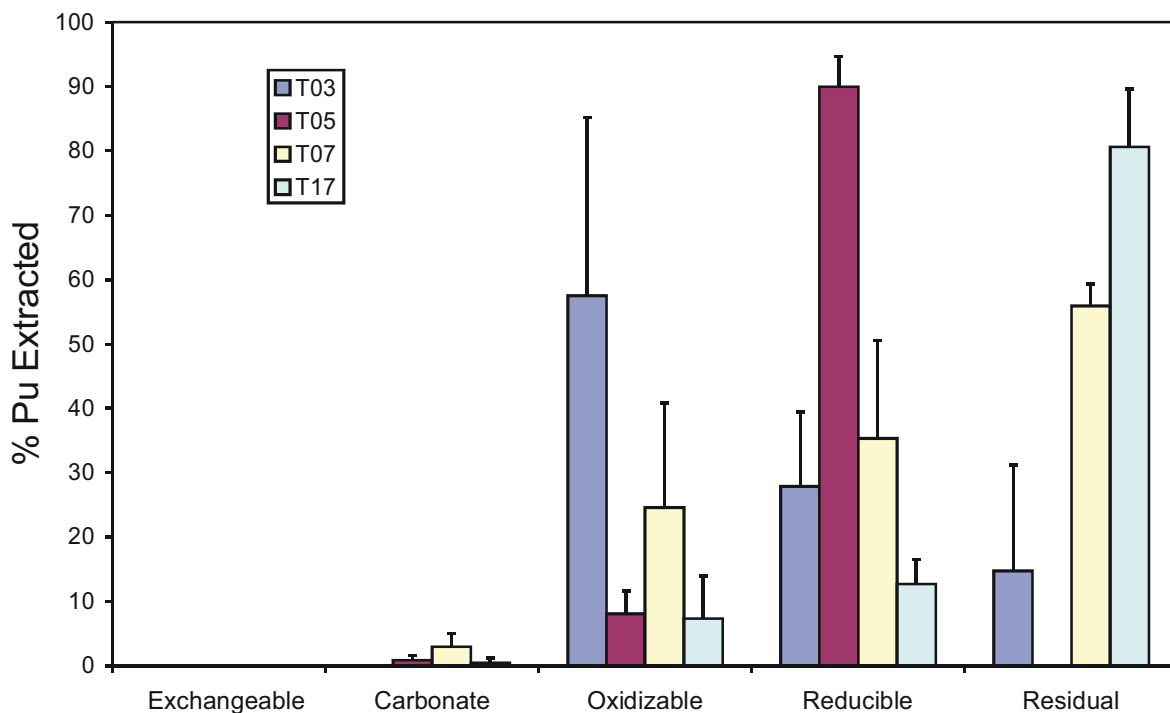


Figure 26. Plutonium-SAE dissolution profiles for mixed soil-waste samples T03, T05, T07, and T17.

As in the case of uranium, 70–80% of the plutonium in T17 was partitioned into the residual fraction, and the majority of the plutonium in T07 was also in this phase. Thus the behavior for these two samples is very different from that noted for the low-contamination soil samples and the plutonium-spiked soil, where the percentages of plutonium in the residual phases ranged from negligible to <30%.

For the other two mixed soil-waste samples T03 and T05, more than 50% of the plutonium was partitioned into the oxidizable and reducible fractions, respectively. A textbook interpretation of these observations would be that oxidizable plutonium in T03 is tied up with organic material, which would be conceivable given that bacteria, cellulosic material, and chelating agents exist in the SDA. A more defensible explanation is that the plutonium is surface-bound as an insoluble Pu(IV) species, which is susceptible to oxidation to more soluble Pu(V) or Pu(VI) forms as shown for spiked soil (see Appendix G, Table G-2, and Figure 25). The high percentage of plutonium in the reducible fraction in T05 suggests binding to iron sesquioxides, which is possible since there are rusting barrels and naturally occurring iron in Pit 9.

The high-plutonium soil samples (30–80 ppm) collected from the graphite scrapings (T27) and after the jar rupture (T32 and T34) had plutonium-SAE dissolution profiles in which most of the ^{239}Pu was associated with the residual phase (i.e., was highly leach resistant) (see Figure 27). For the two soil samples collected after the rupture, the residual fraction accounted for about 70–80% of the total plutonium contamination, with other fractions accounting for 10% or less. The soil scraped from graphite T27 was also dominated by the residual fraction, but also had a fairly significant percentage of oxidizable plutonium (30–40%). These results suggest that for the highly contaminated plutonium soil samples, little plutonium dissolution would be anticipated, particularly if oxidizing conditions were excluded.

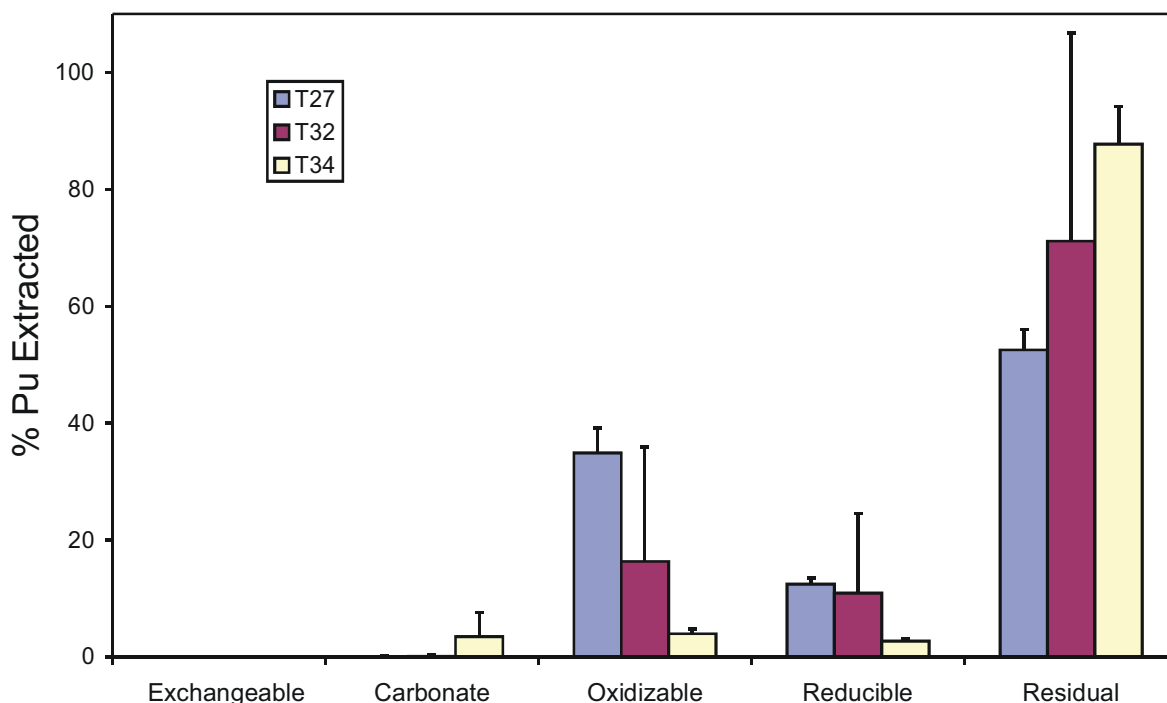


Figure 27. Plutonium-SAE dissolution profiles for high-plutonium soil samples.

Plutonium-SAE dissolution results for the organic waste samples show that for R04 and R20, most of the plutonium (80–90%) is confined to the residual phase (see Figure 28), and in this feature these samples resemble the operational speciation observed in the high-plutonium soil samples. As noted previously, R23 is distinct from the other two putative waste samples, with large percentages of plutonium in the carbonate (about 20%), oxidizable (about 20%), and reducible (about 50%) fractions. The leaching behavior of this sample could be considered to be intermediate between that of the highly contaminated soil samples and the low-contamination soil samples, which would be a reasonable description of the sample.

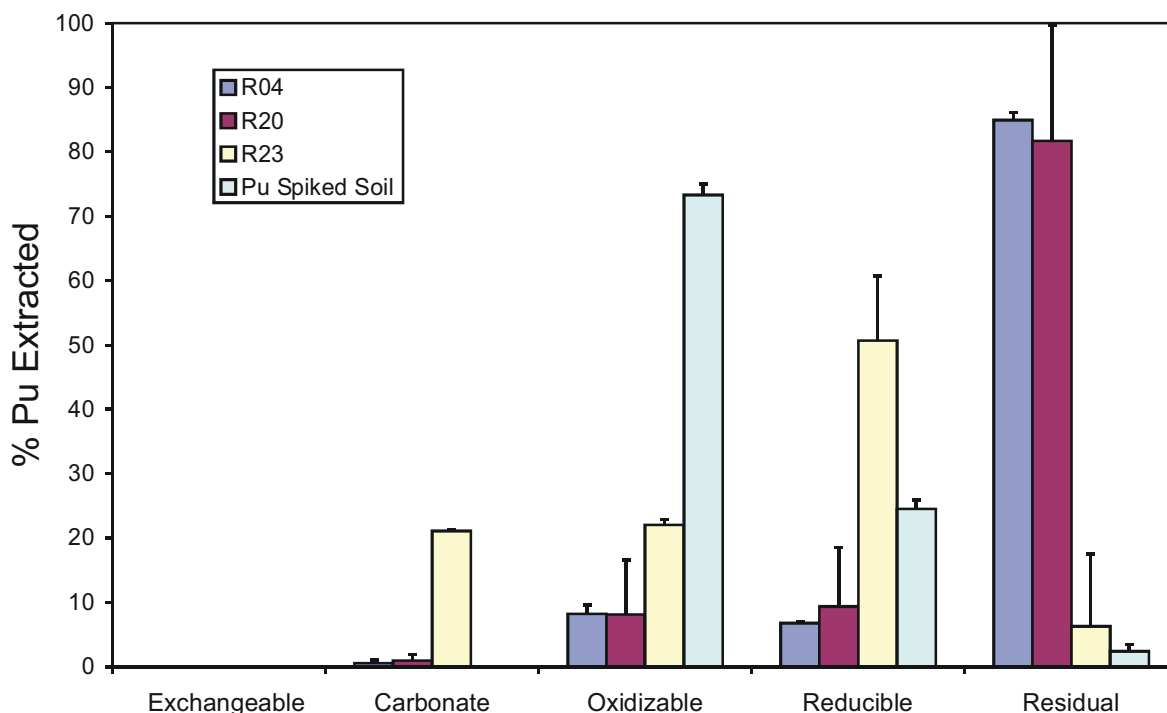


Figure 28. Plutonium-SAE dissolution profiles for probable organic sludge samples R04, R20, and R23.

9.3 Operational Speciation of Americium

SAE results were generated only for ^{241}Am for the high-plutonium soil samples and the organic waste samples because ^{241}Am was not detected in the clean overburden soil samples, INL blank soil samples, or low-contamination soil samples (T08, T09, and T10). For the mixed soil-waste samples (T03, T05, T07 and T17), ^{241}Am was either not detected or the concentrations were too low for SAE profiles to be calculated.

The plutonium-spiked INL soil showed that americium was distributed across the carbonate, oxidizable, and reducible fractions, with a smaller percentage in the residual (see Figure 29). This distribution of americium is typical for near-term americium contamination. The soil scraped from graphite (T27) showed that 60–70% of the americium was unextractable, with 10–20% in both the oxidizable and reducible fractions.

In contrast to the soil scraped from graphite, SAE of soil samples contaminated by the jar rupture (T32 and T34) showed that the ^{241}Am was predominantly tied up in the residual fraction, similar to the behavior observed for uranium and plutonium in these samples.

Like the soil samples, SAE results for americium in the organic waste samples (R04 and R20) showed that the element was concentrated in the residual fraction (88% and 75%, respectively), with smaller but significant amounts partitioned to the sesquioxide fraction (see Figure 30). Americium was not found in organic waste sample R23 in sufficient concentrations to allow SAE profiles to be calculated.

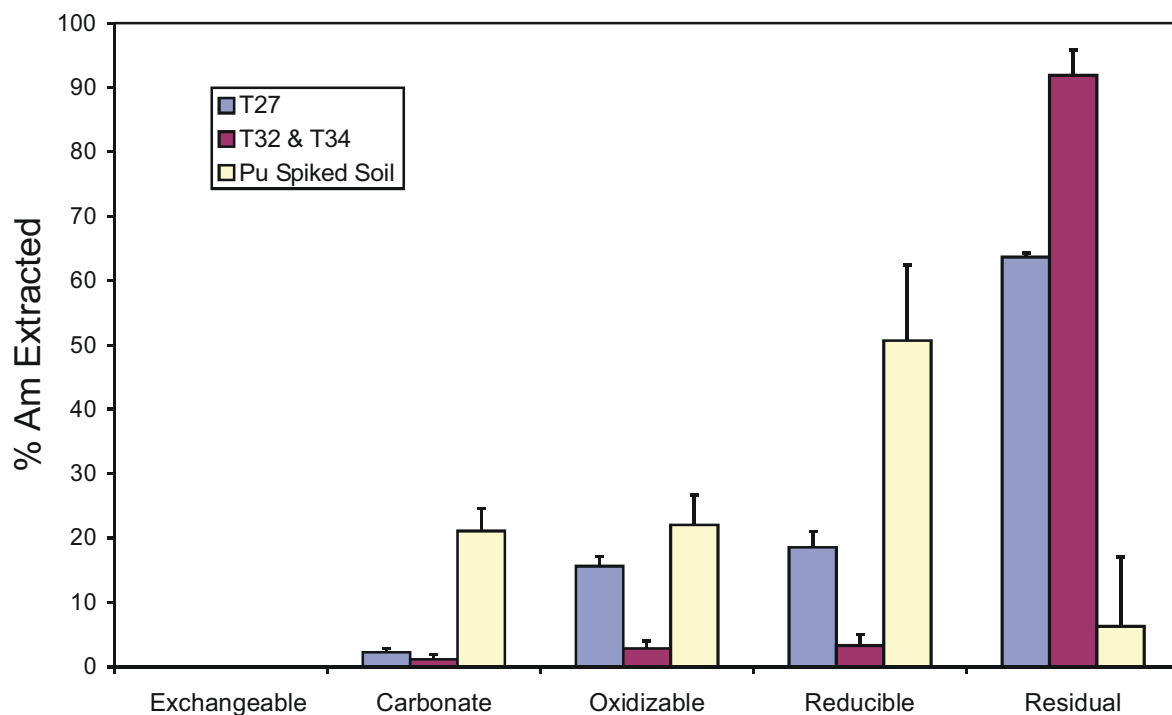


Figure 29. Americium-SAE dissolution profiles for interstitial soil samples T27, T32, and T34.

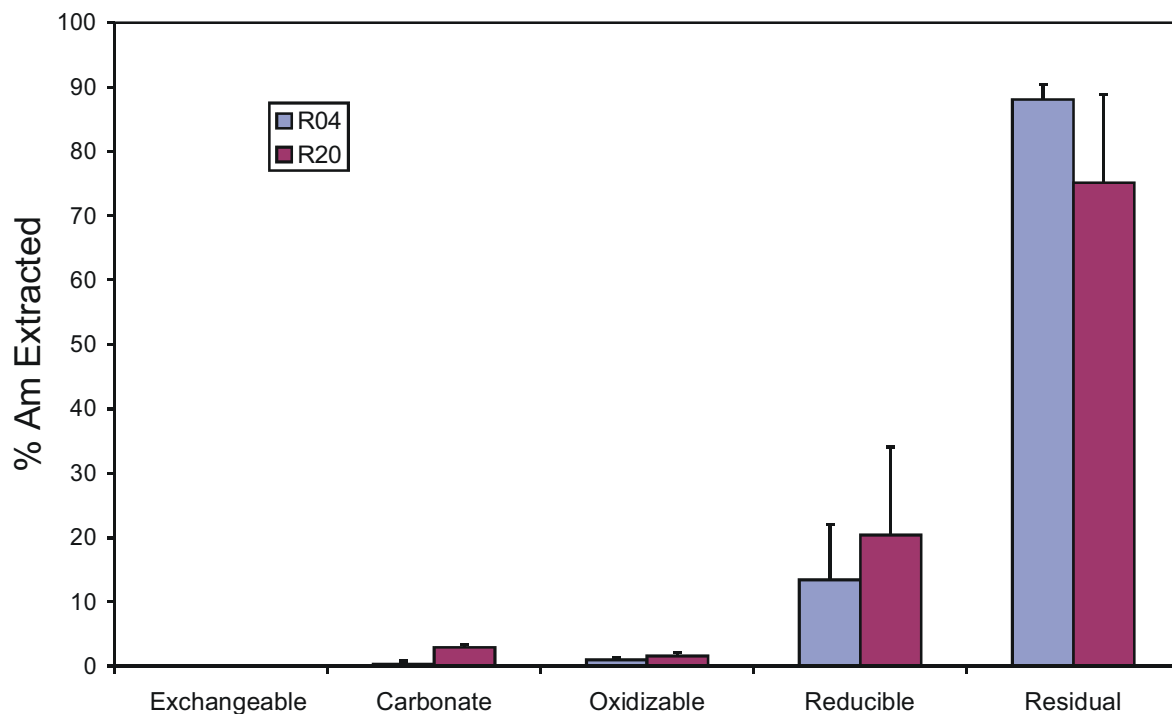


Figure 30. Americium-SAE dissolution profiles for probable organic sludge samples R04 and R20.

9.4 Operational Speciation of Neptunium

^{237}Np SAE results are scarce because of the overall low concentrations of this radionuclide in the soil and waste samples. The results suggest that when ^{237}Np was above detection limits, it was predominantly partitioned into the oxidizable fraction (about 70%) with a significant percentage in the carbonate fraction (20–30%). This behavior is illustrated by the soil scraped from graphite (T27) and by organic waste sample R20 (see Figure 31). ^{237}Np was observed in other soil and waste samples; however, concentrations were not adequate to generate statistically significant SAE distributions. In those SAE fractions where ^{237}Np was detected, it appeared in the carbonate and oxidizable fractions, consistent with the results for T27 and R20. The fact that neptunium dissolution is observed upon oxidation suggests that a fraction of the neptunium is either reduced, existing as Np(IV) insoluble oxides or hydroxides on the matrix surface, or are complexed with unidentified organic material.

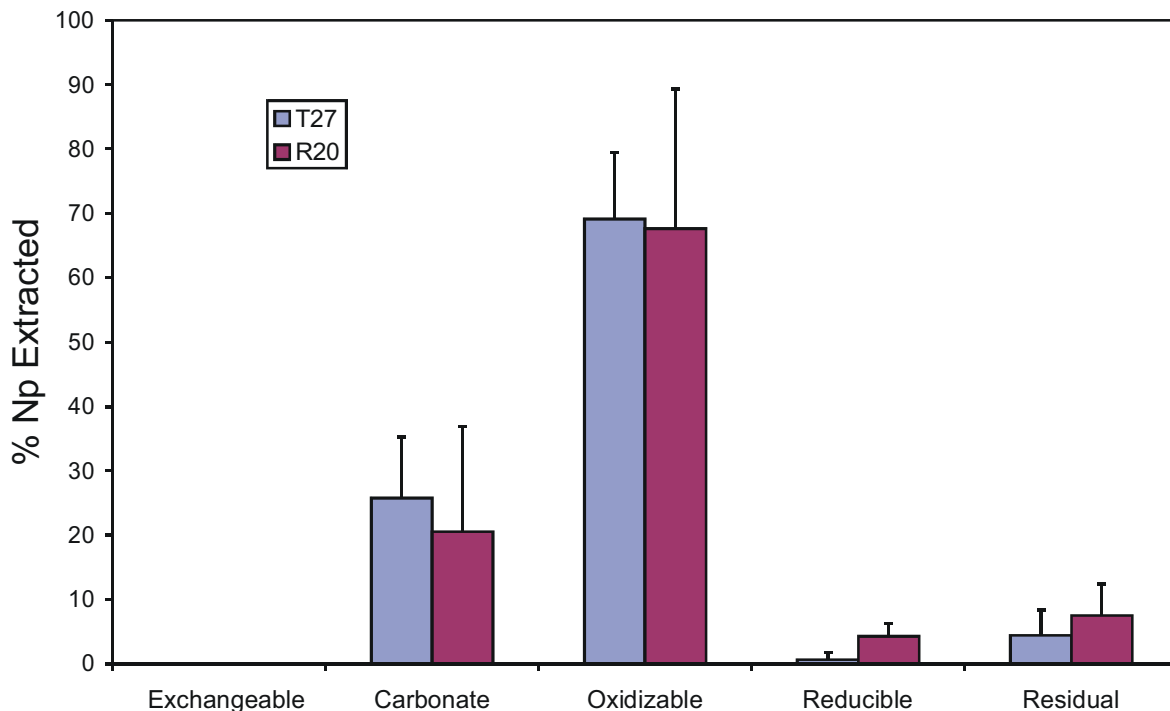


Figure 31. Neptunium-SAE dissolution profiles for probable organic sludge sample R20 and interstitial soil sample T27.

10. SURFACE CHARACTERIZATION

The surfaces of all the samples were screened using secondary ion mass spectrometry (SIMS), providing insight into the surface chemistry of the top-most molecular layer of the samples. SIMS is very surface sensitive and therefore surface contamination can affect results, but SIMS can provide valuable insight into the nature of the matrix and adsorbed contaminants. A detailed description of the instrumentation and approach are provided in Appendix H.

10.1 Negative Ion SIMS spectra

The most illuminating analyses were derived from the negative ion SIMS analyses of the organic waste samples, because they clearly showed that in one instance high nitrate and silicate were present. The negative spectrum of soil showed silicate anions typical of what has been observed in many other studies (i.e., hydroxylated SiO_2 oligomers), which have a tendency to hydrate. In fact, both silicate and aluminosilicate materials qualitatively produce the same pattern, because $(\text{Al} + \text{H})$ has the same mass and valence as does Si; thus for any of the compositions listed on Figure 32, $(\text{Al} + \text{H})$ maybe substituted for Si. The benchmark overburden soil samples in this study showed spectral properties similar to those in Figure 32a, which presents an average of the overburden soil samples in the present study.

When the organic waste samples R20 and R23 were analyzed (see Figure 32b), ion abundances were markedly depressed, which was consistent with the higher organic signature evident in the positive ion spectra (see below). The silicate pattern was observed, but the signal was much less intense and the observed patterns were less obvious. Overall, this is consistent with a high organic content in these samples; empirically, it was observed that when the samples contained high organic ion abundances in the positive ion mode, the negative ion spectrum had a significantly depressed overall abundance.

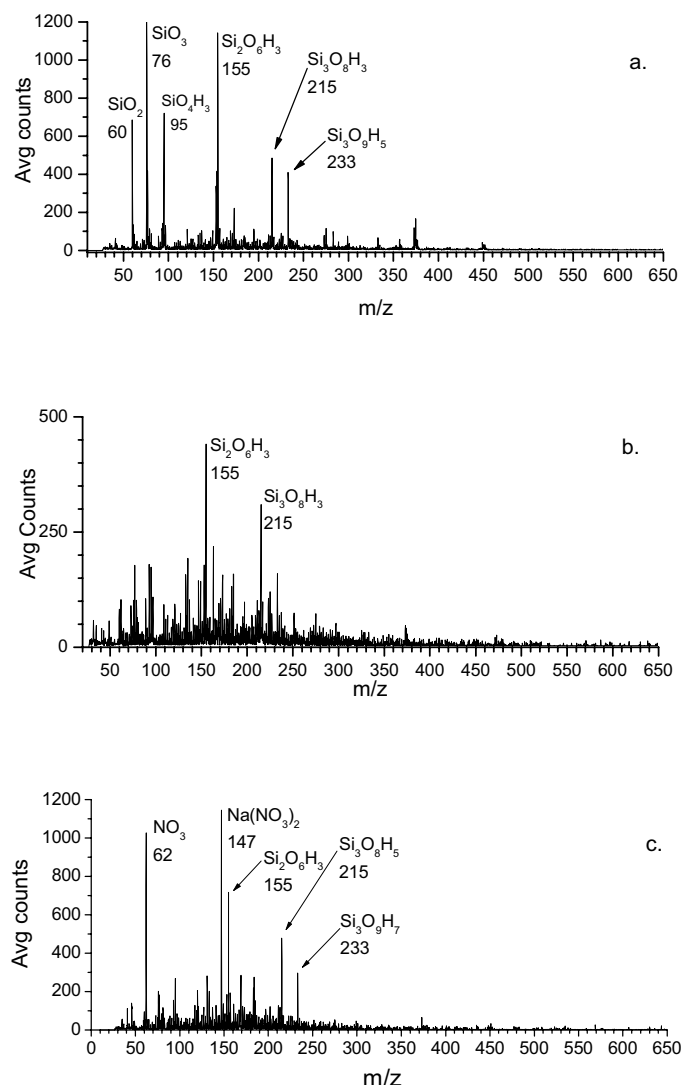


Figure 32. Averaged negative ion SIMS spectra: (a) overburden soil samples, (b) organic waste samples R20 and R23, (c) organic waste sample R04.

Organic waste sample R04 produced a negative ion spectrum (see Figure 32c) different from R20 and R23, and also different from the soil samples. The silicate pattern was observable superimposed with abundant ions indicative of a lot of sodium nitrate in the sample. A relatively organic-free subsample was picked for SIMS analysis, producing the high-nitrate/high-silicate pattern observed. Notable similarities were observed when this result was compared with the negative ion spectra of the unknown waste samples P01–P05 (see Figure 33). In these spectra, high nitrate (NO_3) was observed in all instances except for P01, together with the silicate signature in each case. A number of intriguing anions were not identified, most notably m/z 153, which shows up in every sample, and m/z 145, which appears in P02. A more determined mass spectrometry study could produce better insight into the surface composition of these samples.

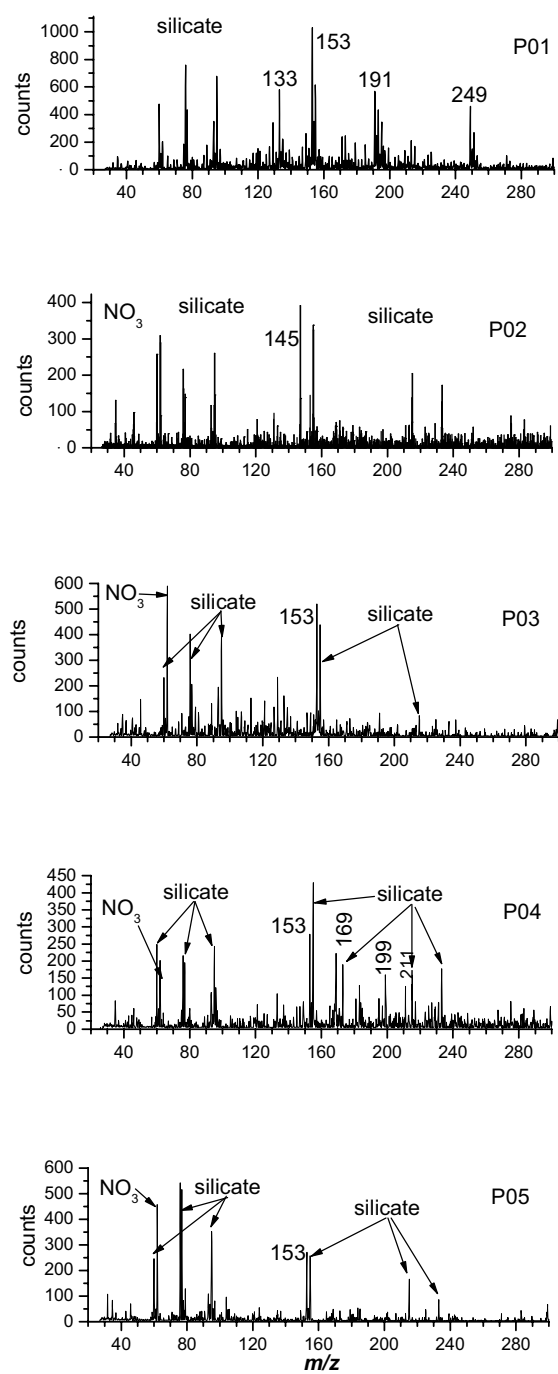


Figure 33. Anion spectra of unknown waste samples P01, P02, P03, P04, and P05.

10.2 Positive Ion SIMS Spectra

The positive ion spectra of the soil and waste samples were less informative because a layer of organic molecules covers all natural surfaces. In spite of this, the positive spectra suggested chemical differences on the surfaces consistent with the appearance categorizations derived earlier, and enabled development of empirical categorization approach that may be useful in situations where categorization of a very small sample is needed.

The average positive spectrum for soil showed peaks arising from hydrocarbons containing different numbers of carbon atoms. These hydrocarbon “envelopes” are grouped by the number of C atoms (see Figure 34a); within a given envelope, ion formulas are generally C_nH_{2n+1} , C_nH_{2n-1} , C_nH_{2n-3} , C_nH_{2n-5} . Differences in ion abundances between selected ions within a given envelope and between ion envelopes can be used to categorize types of materials. For example, ions in the C_8 and C_9 envelopes are significantly more prominent in the spectrum of organic waste generated from the average of R20 and R23 (see Figure 34b) than they are in soil. In addition, the more unsaturated ions (e.g., C_nH_{2n-1} , C_nH_{2n-3}) tended to be more abundant than the saturated ions (C_nH_{2n+1}) in the organic waste samples. These observations are consistent with the presence of hydrocarbon oils in the organic waste materials. One final difference between the organic waste samples and the soil samples was that the ratio of the C_7H_7 cation at m/z 91 to the abundant ion at m/z 95 was in general greater in the soil samples than in the waste samples. This can be used for differentiating soil from waste samples.

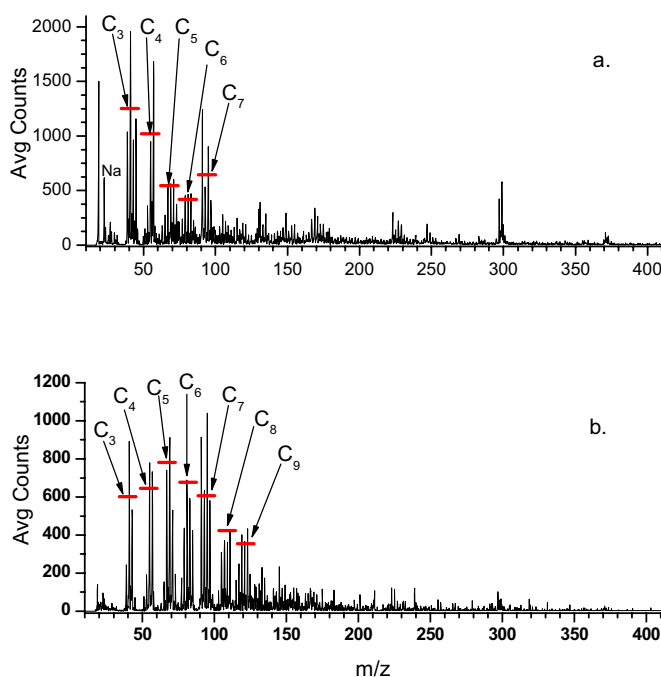


Figure 34. Averaged positive ion SIMS spectra of (a) overburden soil samples and (b) organic waste samples R20 and R23.

10.3 Development of Empirical Method for Identification of Sample Type

The development of an empirical method for identifying the sample type is described in detail in Appendix H. The results of the sample categorization using this approach were very similar to those based on the appearance, gamma spectroscopy, and total actinide content. The majority of the samples were categorized similarly using both approaches (see Table H-3, Appendix H for categorization using surface analysis). The principal exceptions were T01 and T02 (identified as soil by surface analysis, but mixed soil-waste by appearance), and T14, T15, T16, and T18 (identified as waste by surface analysis, but as low-contamination soil samples by appearance). These samples were noted to have significant heterogeneity, which could explain the discrepancies in categorization.

11. SUMMARY OF PROJECT SAMPLE MANAGEMENT

This section describes of the management practices for the unaltered sample material and the sample waste generated during the Retrieved Waste and Soil Characterization (RWSC) Project. This information will aid in future planning decisions on waste characterization and management of unaltered sample material.

11.1 Handling of Retrieved Waste and Soil Characterization Project Samples

At the completion of the RWSC Project unaltered sample material and sample waste were handled according the Waste Management Plan (Hanson et al. 2003). Sample material that was unaltered during testing and characterization was classified as “unaltered sample material” and packaged for proposed research activities according to best management practices. Details of the RWSC unaltered samples from laboratory characterization methods are provided in Appendix I. Table I-1, I-2 and I-3 lists the container identification numbers used for sample repackaging. Sample information may be traced to the individual drum for (1) sample identification number, (2) sample container type, and (3) approximate amount. Detailed sample characterization may be found within this report. The figures below show sample P9GT04016G (i.e., approximately 63 grams) (see Figure 35, left), which was wrapped in a radioactive material handling sack (see Figure 35, right) and placed in a 10-gal container #1 (see Figure 36). There are three 10-gal (container #1, #2 and #3) DOT Type A 7A containers (UN 1A2/Y1.2/100/04/USA/M4035; UN 1A2/X100/S/04/USA/M4035; QA# 105395) containing double-bagged Glovebox Excavator Method samples placed in one 30-gal drum that is currently stored within the RWMC. Table I-4 lists the radioactivity at contact and 1-m (3.3-ft) radiological dose rate measurements for each of the three individual containers placed in the 30-gal drum to be temporarily stored.



Figure 35. Photograph of RWSC sample P9GT04016G (left), wrapped in radioactive material handling sack (right).



Figure 36. Photograph of Drum #1 contents (left) and lid (right) before shipment to storage facility.

11.2 Handling of Retrieved Waste Soil Characterization Project Sample Waste

Waste streams were generated from the RWSC tests as anticipated in the *Waste Management Plan* (Hanson et al. 2003). Waste from total actinide content, leachability studies, and sequential aqueous extractions were disposed of using the existing radiological waste stream for the Reactor Technologies Complex. Unanticipated liquid waste was generated due to the closure of the warm drains at the Reactor Technologies Complex. Table I-5 lists the radioactivity at contact and 1-m (3.3-ft) radiological dose rate measurements for the drum shipped to INTEC 1617. Liquid waste will be shipped to Permafix for treatment and disposal. Solid waste was shipped to INTEC 1617 for disposal by Waste Generator Services of INL.

12. SUMMARY

A total of 44 samples (250-mL each) of soil and waste were collected during the Glovebox Excavator Method excavation of Pit 9 at the SDA and were visually categorized, analyzed for total actinide content, evaluated for solubilization, and tested for operational speciation. Samples were initially grouped into three categories when they were collected: 36 interstitial soil samples, three organic sludge samples, and five inorganic sludge samples. Photographic inspection and chemical analyses showed that the samples were significantly more diverse than indicated by the initial categorizations. Soil samples were subcategorized into clean, mostly clean, mixed soil-waste, and soil scraped from graphite mold fragments. The rupture of a jar containing graphite scarfings resulted in high actinide contamination of visually clean samples that compelled creation of a fifth category: Soil after Rupture of Graphite Scarfings Jar. The three samples categorized as organic sludge had chemical characteristics that in many cases forced them to be considered separately; however, they did share some visual and physical similarities and the original grouping was maintained. The five samples initially grouped and identified as inorganic sludge were subsequently judged not to be inorganic sludge in the context of material expected from RFP. Chemical analyses suggested that these could be grouped into two categories, designated Inorganic Waste Type I and Inorganic Waste Type II.

Throughout the following summary, note that the sample categorization and grouping is somewhat arbitrary; however, the grouping is critical because it enables the results to be distilled to a manageable size. The alternative would be to discuss each sample separately, which to some degree would be warranted given the extreme heterogeneity of the burial site, but would be functionally impractical.

12.1 Caveats Related to Sample Collection

The Glovebox Excavator Method Project excavation was performed using a backhoe in an enclosure designed to contain particulate radioactive contamination. Utilization of a backhoe to excavate a highly heterogeneous burial site could, and in most cases did result in mixing of waste materials before sample collection. Conclusions regarding mechanism of contamination must be tempered by this caveat. Actinide-contaminated soil could have been, and in some instances was generated by actinide dissolution and movement from the waste materials to adjacent clean soil during periods of water infiltration. However, the excavation approach was undeniably responsible for cross-contamination of some samples, and cannot be unequivocally excluded as a contamination mechanism.

12.2 Actinide Contamination

Four soil samples were identified as “clean,” based on their appearance and actinide concentrations that were either less than the detection limits, or in the case of uranium, close to background levels and isotopic distributions expected in nature. The exception to this generalization was the presence of very low levels of ^{240}Pu just above background in three of the four samples. The error bars (1σ) overlap the detection limits for ^{240}Pu , underscoring the tenuous nature of these measurements for any one of these samples; yet the fact that ^{240}Pu was observed repeatedly in three of the four “clean” samples, and all other soil samples, but not observed in any of the benchmark samples strongly suggests that the measurements are real. This low-level contamination notwithstanding, these “clean” or “very nearly clean” soil samples strongly suggest that samples uncontaminated by gross mixing from the excavation were acquired.

Thirteen soil samples were categorized as “mostly clean” on the basis of appearance, and consideration of the actinide concentrations suggested that a designation of “low-contamination” was more appropriate. Eleven of the thirteen had ^{239}Pu concentrations above detection limits, and (with one exception) ranged from not detected to about 90 ng/g. The exception had a ^{239}Pu concentration of

340 ng/g, and probably should have been categorized as a mixed soil-waste sample. ^{240}Pu was detected in all thirteen, and ^{241}Am was above detection limits in nine of thirteen. The uranium concentration was slightly elevated compared to the natural background in about half of these samples, and a slight decrease in the $^{238}\text{U}/^{235}\text{U}$ ratio was measured, consistent with ^{235}U enrichment.

The $^{239}\text{Pu}/^{240}\text{Pu}$ isotope ratios for the low-contamination soil samples ranged from 16 to >50 , which were consistent with weapons-grade plutonium derived from RFP process waste. The $^{239}\text{Pu}/^{241}\text{Am}$ ratio was more diagnostic; while the range of 100 to 500 was quite broad, it was consistent with those measured for soil scraped from graphite and soil contaminated from the rupture of the graphite scarfings jar. Contamination in both of these latter soil samples certainly originated from RFP process waste. The $^{239}\text{Pu}/^{241}\text{Am}$ ratios were distinct from those measured for waste materials.

Nine of the interstitial soil samples were categorized as mixed soil-waste; actinide concentrations for these samples displayed significantly greater variability. For example, ^{239}Pu ranged from not detected in one instance to 700 ng/g. Elevated uranium (with a depressed $^{238}\text{U}/^{235}\text{U}$ ratio), ^{240}Pu , and ^{241}Am were measured in each of these samples. The $^{239}\text{Pu}/^{240}\text{Pu}$ ratio ranged from 12 to 20, indicating in general weapons-grade plutonium. The $^{239}\text{Pu}/^{241}\text{Am}$ ratio, on the other hand, had more of a bimodal distribution: five of the samples had ratios ranging from 90 to 190, consistent with RFP scarfings as noted above for the low-contamination soil samples. However, three samples had $^{239}\text{Pu}/^{241}\text{Am}$ ratios <10 , which was more in accord with that measured for five of the eight waste samples. This suggested a different process origin for the contamination in these materials.

One soil sample was caked to graphite mold fragments, and scraped directly into a sample container. This occurred before the rupture of the graphite scarfings jar, and thus this sample is an invaluable benchmark of contaminated soil found close to a graphite fragment. The ^{239}Pu concentrations measured for multiple subsamples were exceptionally high and were highly variable, ranging from 31,000 to 78,000 ng/g. The sample did not contain elevated ^{238}U , but did contain significant ^{235}U , ^{236}U , ^{237}Np , ^{240}Pu , ^{241}Am , and ^{242}Pu . However, note that ^{239}Pu was by far the most abundant actinide isotope: $^{239}\text{Pu}/^{240}\text{Pu}$ ratios were consistently about 16, in agreement with RFP plutonium isotopic distributions. The $^{239}\text{Pu}/^{241}\text{Am}$ isotope ratios were about 200 in this sample.

Nine soil samples having a clean appearance were collected after the rupture of the graphite scarfings jar, and in most respects were analytically indistinguishable from the soil scraped from the graphite. Concentrations of 30,000–63,000 ng/g were measured for ^{239}Pu , and similar results were recorded for the other isotope concentrations and ratios measured for the sample of soil scraped from graphite. This suggests that contamination in the soil scraped from graphite and contamination in the soil after rupture of graphite scarfings jar have similar origins.

The actinide content of the samples identified as waste was also highly variable. All three of the organic waste samples had significantly elevated concentrations of the isotopes of interest (^{237}Np was not detected in any of them), with ^{239}Pu at nearly 5,000 ng/g for one sample. For two of the organic sludge samples, the $^{239}\text{Pu}/^{240}\text{Pu}$ ratio was about 12, indicating that this was not entirely weapons-grade plutonium. This view was supported by very low $^{239}\text{Pu}/^{241}\text{Am}$ ratios for these samples (about 2), suggesting that these samples were derived from other process origins. The third organic sludge had $^{239}\text{Pu}/^{240}\text{Pu}$ and $^{239}\text{Pu}/^{241}\text{Am}$ ratios consistent with soil scraped from graphite, although the plutonium concentrations in this sample were much lower.

Three of the waste samples originally categorized as inorganic waste had ^{239}Pu concentrations, $^{239}\text{Pu}/^{240}\text{Pu}$, and $^{239}\text{Pu}/^{241}\text{Am}$ ratios that were very similar to those of the two high-plutonium organic waste samples, despite their physical appearance being markedly different. A fourth unknown waste sample had actinide concentrations and isotope ratios that were very similar to the low concentration

interstitial soil samples. The fifth unknown waste sample had low but significant concentrations of ^{239}Pu and ^{241}Am , but displayed isotope ratios that were unlike any of the other categories. This again emphasizes the variability that can be encountered.

12.3 Aqueous Partitioning of Actinide Contaminants

Distribution coefficients (K_d) were measured across a range of pH and ionic strength (I) values for the actinide isotopes, for a subset of samples. These studies provided a quantitative assessment of actinide dissolution from the waste materials, and subsequent adsorption to the adjacent soil. Commonality observed between the different actinide elements were:

- K_d values decrease significantly as the pH of the leachate solution becomes acidic
- K_d values for organic waste samples are much more sensitive to decreased pH than are soil samples
- In the pH range typical of INL soil (about 8), K_d values are not significantly affected by small changes in pH
- At high pH ranges, K_d values frequently undergo modest decreases, thought to be due to dissolution of the matrix.

Uranium partitioning displayed complex behavior. K_d values of 10^3 to 10^4 mL/g were measured in the pH 8–12 range for all samples. Below pH 8, K_d values dropped sharply, reaching local minima at about pH 6 that were one to two orders of magnitude lower than those at high pH. The K_d minimum at pH 6 indicates a significant alteration in the chemistry of the system, which is reversed at mildly acidic pH values where K_d values once again rise. Increases in partitioning coefficients in the pH range 4–5 are dramatic (to about 10^4 mL/g) for the soil samples, but more modest for the waste samples. Finally at very acidic pH regimes, K_d drops to between 10^1 and 10^2 mL/g for the soil samples, where uranium is essentially dissolved from the waste samples. Generally, I had little effect on K_d values for uranium.

The partitioning of anthropogenic uranium (e.g., ^{235}U enriched) at high pH is somewhat greater than that of naturally occurring uranium. This conclusion is based on the observation that the $^{238}\text{U}/^{235}\text{U}$ ratio in the leachate drops regularly as pH increases.

In contrast to uranium, plutonium partitioning varies more regularly and depends greatly on the solid matrix. For organic waste samples exposed to pH <3, K_d values as low as the mid 10^1 mL/g range are measured. The K_d rises to 10^3 mL/g at pH 3–7, and then rises to the 10^5 mL/g range at higher pH. For low-contamination soil samples, plutonium K_d values as low as 10^3 mL/g were measured at pH 1, but rise steadily to about 10^4 mL/g by pH 3, and hover between 2×10^3 mL/g and 2×10^4 mL/g over the remainder of the pH range studied.

Plutonium partitioning was markedly lower in the soil scraped from graphite and in soil acquired after the rupture of the jar. At low pH, K_d values in the mid 10^4 mL/g range were measured, but as pH rose to ambient pH levels (5–10), K_d for plutonium increased to 10^6 mL/g. At the highest pH ranges, a modest decrease in K_d was observed, which may signal some dissolution of the silicate matrix.

Americium partitioning in the ambient-to-high pH range (about 6–12) is described by K_d values that range from 10^4 to 10^5 mL/g; low-contamination soil samples display somewhat lower values at very high pH due to dissolution of the silicate matrix. Beginning at pH 6, K_d for the soil samples begins to decrease as the pH is lowered, finally reaching about 10^2 mL/g at pH 2. The decrease with decreasing pH

is even sharper for organic sludge samples. $K_d < 10^1$ mL/g were recorded at pH values just slightly less than 4 for organic waste samples.

Neptunium partitioning from soil samples was characterized by a K_d of about 10^2 mL/g at low pH, rising to about 10^3 mL/g as pH increases to about 7. Similar values were measured for the waste samples at high pH; however, in these samples, K_d drops sharply with decreasing pH, reaching a value of less than 10^1 mL/g by pH 5, and probably achieving complete dissolution at lower pH values.

12.4 Operational Speciation

Sequential aqueous extraction studies showed susceptibility of the actinide elements to dissolve under perturbed chemical conditions and also provided insight into the operational speciation within the solid sample matrix. Uranium in soil samples tended to reside predominantly in the residual fraction (i.e., it would not leach under the SAE conditions imposed). Depending on the particular sample being studied, smaller percentages of uranium were partitioned into carbonate, oxidizable, and reducible fractions, with oxidizable being second in importance behind residual. These tendencies were even more pronounced in the high-plutonium soil samples from the graphite scarfings, in which bias toward the residual fraction was even more exaggerated. Uranium operational speciation in organic waste samples tends to be more evenly partitioned among the residual, oxidizable, and carbonate fractions, which reflects the more heterogeneous nature and less aggressive binding of this matrix.

Plutonium in the low-concentration soil samples tends to be fairly evenly partitioned between the oxidizable and reducible fractions. The speciation of plutonium in the oxidizable fraction is probably due to oxidizable plutonium that is present as insoluble Pu(IV) oxides or hydroxides that are susceptible to oxidation, forming more soluble Pu(V) or Pu(VI) species, or perhaps to destruction of binding sites on the matrix upon oxidation. This conclusion is supported by the fact that the largest percentages of plutonium were measured in the oxidizable fraction from SAE of plutonium-spiked soil that contained almost no organic matter. Plutonium in the reducible fractions is commonly attributed to metal bound with iron sesquioxide minerals: these are certainly present on the surfaces of silicate soil particles or as rusted barrel debris within the burial site.

For the highly contaminated samples scraped from graphite or that were contaminated by the jar rupture, the plutonium distribution is shifted strongly toward the residual fraction, which is consistent with the very high K_d values measured for these samples. Similar patterns were observed for the waste samples: plutonium tends to reside in the residual or nonleachable fraction.

Operational speciation of americium was only studied in the highly plutonium-contaminated soil samples and in the organic waste samples. A significant difference was observed when americium partitioning in the soil scraped from graphite was contrasted with the soil after rupture of graphite scarfings jar: in the soil scraped from graphite, the largest percentage of americium was in the reducible fraction, and there were also significant percentages in the oxidizable and carbonate fractions; this was similar to americium behavior in the plutonium-spiked soil samples. In sharp contrast, americium in the soil samples contaminated by the rupture resided almost exclusively in the residual fraction, again suggesting that americium is unlikely to leach from this material. Similarly, the largest percentage of americium in the organic sludge samples was found in the residual fractions.

Neptunium operational speciation could only be assessed for two samples, the soil scraped from graphite, and one organic sludge. In both instances, the largest percentage of neptunium was found in the oxidizable fraction, with the carbonate also significant. This suggests that sorbed neptunium may be present in a reduced form.

13. REFERENCES

- ACMM-3993, 2005, "Gamma Spectrometry Using the Sun Sparcstation 2," Rev. 8, *Analytical Chemistry Methods Manual, Vol. II*, B. Storms, Idaho National Laboratory.
- Asbury, S. M. L., S. P. Lamont, and S. B. Clark, 2001, "Plutonium Partitioning to Colloidal and Particulate Matter in an Acidic, Sandy Sediment: Implications for Remediation Alternatives and Plutonium Migration," *Environmental Science & Technology*, Vol. 35, pp. 2295–2300.
- Bartholomay, Roy C., LeRoy L. Knobel, and Linda C. Davis, 1989, *Mineralogy and Grain Size of Surficial Sediment from the Big Lost River Drainage and Vicinity, with Chemical and Physical Characteristics of Geologic Materials from selected Sites at the Idaho National Engineering Laboratory, Idaho*, USGS Open File Report 89-384, U.S. Department of Energy Idaho Operations Office DOE/ID-22081, U.S. Geological Survey.
- Bartholomay, R. C., 1990, *Mineralogical Correlation of Surficial Sediment from Area Drainage with Selected Sedimentary Interbeds at the Idaho National Engineering Laboratory, Idaho*, USGS Water-Resources Investigations Report 90-4147, U.S. Department of Energy Idaho Operations Office DOE/ID-22092, U.S. Geological Survey.
- Bartholomay, R. C., B. R. Orr, M. J. Liszewski, and R. G. Jensen, 1995, *Hydrologic Conditions and Distribution of Selected Radiochemical and Chemical Constituents in Water, Snake River Plain Aquifer, Idaho National Engineering Laboratory, Idaho*, 1989 through 1991, USGS Water-Resources Investigations Report 95-4175, U.S. Geological Survey.
- Beasley, T. M., J. M. Kelley, L. A. Bond, W. Rivera, Jr., M. J. Liszewski, and K. A. Orlandini, 1998, *Heavy Element Radionuclides (Pu, Np, U) and ¹³⁷Cs in Soils Collected from the Idaho National Engineering and Environmental Laboratory and Other Sites in Idaho, Montana, and Wyoming*, Environmental Measurements Laboratory Report, EML-599, Los Alamos National Laboratory.
- Becker, B. H., T. A. Bensen, C. S. Blackmore, D. E. Burns, B. N. Burton, N. L. Hampton, R. M. Huntley, R. W. Jones, D. K. Jorgensen, S. O. Magnuson, C. Shapiro, and R. L. VanHorn, 1996, *Work Plan for Operable Unit 7-13/14 Waste Area Group 7 Comprehensive Remedial Investigation/Feasibility Study*, INEL-95/0343, Rev. 0, Idaho National Laboratory.
- Becker, B. H., J. D. Burgess, K. J. Holdren, D. K. Jorgensen, S. O. Magnuson, and A. J. Sondrup, 1998, *Interim Risk Assessment and Contaminant Screening for the Waste Area Group 7 Remedial Investigation*, DOE/ID-10569, Rev. 0, U.S. Department of Energy Idaho Operations Office.
- Carlson, J., J. Bardsley, V. Bragin, and J. Hill, 2005, *Plutonium Isotopics - Non-Proliferation and Safeguards Issues*, Rocky Flats Environmental Test Site.
- Cleveland, M. J. and A. H. Mullin, 1993, *Speciation of Plutonium and Americium in Ground Waters from the Radioactive Waste Management Complex, Idaho National Engineering Laboratory, Idaho*, USGS-Water-Resources Investigation Report 93-4035, U.S. Geological Survey.
- Dicke, C. A., 1997, *Distribution Coefficients and Contaminant Solubilities for the Waste Area Group 7 Baseline Risk Assessment*, INEEL/EXT-97-00201, Rev. 0, Idaho National Laboratory.

- DOE/RFP-CO, 2003, *Radionuclide Air Emissions Annual Report, Appendix A—Radioactive Materials Associated with Rocky Flats*, Department of Energy Rocky Flats Plant-Colorado Operations Office, January 18, 2005, accessed at <http://www.rfets.gov/eddie/>.
- DOE-ID, 1991, *Federal Facility Agreement and Consent Order for the Idaho National Engineering Laboratory*, Administrative Docket No. 1088-06-29-120, U.S. Department of Energy Idaho Operations Office; U.S. Environmental Protection Agency, Region 10; Idaho Department of Health and Welfare.
- DOE-ID, 2004, *Remedial Action Report for the OU 7-10 Glovebox Excavator Method Project*, DOE/NE-ID-11155, Rev. 0, U.S. Department of Energy Idaho Operations Office.
- Eisenbud, M. and T. Gesell, 1997, *Environmental Radioactivity From Natural, Industrial and Military Sources*, 4th Ed., San Diego, CA: Academic Press.
- Fjeld, R. A., J. T. Coates, and A. W. Elzerman, 2000, *Final Report, Column Tests to Study the Transport of Plutonium and Other Radionuclides in Sedimentary Interbed at INEEL*, INEEL/EXT-01-00763, Rev. 0, Clemson University, Department of Environmental Engineering and Science, Clemson, South Carolina, for the Idaho National Laboratory.
- Fjeld, R. A., T. A. DeVol, R. W. Goff, M. D. Blevins, D. D. Brown, S. M. Ince, and A. W. Elzerman, 2001, "Characterization of the Mobilities of Selected Actinides and Fission/Activation Products in Laboratory Columns Containing Subsurface Material from the Snake River Plain.," *Nuclear Technology*, Vol. 135, pp. 92–108.
- Fox, R. V. and B. J. Mincher, 2003, "Supercritical Fluid Extraction of Plutonium and Americium from Soil Using Beta-Diketone and Tributyl Phosphate Complexants," *Supercritical Carbon Dioxide: Separations And Processes*, edited by Aravamudan S. Gopalan, Chien M. Wai, and Hollie K. Jacobs, Washington: American Chemical Society, ACS Symposium Series No. 860, pp. 36–49.
- Geslin, J. K., P. K. Link, J. W. Riesterer, M. A. Kuntz, and C. M. Fanning, 2002, "Pliocene and Quaternary Stratigraphic Architecture and Drainage of the Big Lost River Trough, Northeastern Snake River Plain, Idaho," edited by P. K. Link and L. L. Mink, *Geology, Hydrogeology, and Environmental Remediation: Idaho National Laboratory, Eastern Snake River Plain, Idaho, Boulder, Colorado*, Geologic Society of America Special Paper 353, pp. 11–26.
- Hanson, Duane J., Brent N. Burton, Gary S. Groenewold, Steve L. Lopez, Gretchen E. Mattern, and Jeffrey C. Messaros, 2003, *Waste Management Plan for Operable Unit 7-13/14 Preremedial Design, Retrieved Waste and Soil Characterization, and Environmental Management Science Program Tests*, INEEL/EXT-03-00554, Idaho National Laboratory.
- Hardy, E. P., P. W. Krey, and H. L. Volchok, 1973, "Global Inventory and Distribution of Fallout Plutonium," *Nature*, Vol. 241, February 16, 1973, pp. 444–445.
- Hill, S., 2003, "Receive, Section, and Subsample Underburden Core Samples from the OU 7-10 Glovebox Excavator Method Project," ACLP-0.80, Rev. 1, Analytical Chemistry Laboratory Procedure, Idaho National Laboratory.
- Hill, S., 2004, "Receiving and Subsampling Samples from the OU 7-10 Glovebox Excavator Method Project and OU 7-13/14 Projects," ACLP-0.81, Rev. 2, Analytical Chemistry Laboratory Procedure, Idaho National Laboratory.

- Holdren, K. Jean, Bruce H. Becker, Nancy L. Hampton, L. Don Koeppen, Swen O. Magnuson, T. J. Meyer, Gail L. Olson, and A. Jeffrey Sondrup, 2002, *Ancillary Basis for Risk Analysis of the Subsurface Disposal Area*, INEEL/EXT-02-01125, Rev. 0, Idaho National Laboratory.
- Hull, L. C. and C. W. Bishop, 2004, "Fate of Brine Applied to Unpaved Roads at a Radioactive Waste Subsurface Disposal Area," *Vadose Zone Journal*, Vol. 3, No. 1, pp. 190–202.
- Ibrahim, S. A. and R. C. Morris, 1997, "Distribution of Plutonium among Soil Phases near a Subsurface Disposal Area in Southeastern Idaho, USA," *Journal of Radioanalytical and Nuclear Chemistry*, Vol. 226, Nos. 1-2, pp. 217–220.
- Komosa, A., 1999, "Migration of Plutonium Isotopes in Forest Soil Profiles in Lublin Region (Eastern Poland)," *Journal of Radioanalytical and Nuclear Chemistry*, Vol. 240, pp. 19–24.
- Komosa, A., 2002, "Study on Geochemical Association of Plutonium in Soil Using Sequential Extraction Procedure," *Journal of Radioanalytical and Nuclear Chemistry*, Vol. 252, pp. 121–128.
- Liszewski, M. J., J. J. Rosentreter, and K. E. Miller, 1997, *Strontium Distribution Coefficients of Surficial Sediment Samples from the Idaho National Engineering Laboratory, Idaho*, Water-Resource Investigations Report 97-4044, U.S. Geological Survey.
- Liszewski, M. J., J. J. Rosentreter, K. E. Miller, and R. C. Bartholomay, 1998, *Strontium Distribution Coefficients of Surficial and Sedimentary Interbed Sediment Samples from the Idaho National Engineering Laboratory, Idaho*, Water-Resource Investigations Report 98-4073, U.S. Geological Survey.
- Litaor, M. I. and S. A. Ibrahim, 1996, "Plutonium Association with Selected Solid Phases in Soils of Rocky Flats, Colorado, Using Sequential Extraction Technique," *Journal of Environmental Quality*, 1996, Vol. 25, pp. 1144–1152.
- Litaor, M. I., G. Barth, E. M. Zika, G. Litus, J. Moffitt, and H. Daniels, 1998, "The Behavior of Radionuclides in the Soils of RFP, Colorado," *Journal of Environmental Radioactivity*, Vol. 38, No. 1, pp. 17–46.
- LMITCO, 1998, *OU 7-10 Staged Interim Action Project System Requirements Document*, INEEL/EXT-98-00310, Rev. 1, Idaho National Laboratory.
- Miller, J. C. and J. N. Miller, 1988, *Statistics for Analytical Chemistry*, 2nd ed., Chichester, West Sussex, UK: Ellis Horwood Limited.
- Mincher, Bruce J., Robert V. Fox, D. Craig Cooper, and Gary S. Groenewold, 2003, "Neptunium and Plutonium Sorption to Snake River Plain, Idaho Soil," *Radiochimica Acta*, Vol. 91, No. 7, pp. 397–401.
- Mincher, Bruce J., Robert V. Fox, Catherine L. Riddle, D. Craig Cooper, and Gary S. Groenewold, 2004, "Strontium and Cesium Sorption to Snake River Plain, Idaho Soil," *Radiochimica Acta*, Vol. 92, No. 1, pp. 55–61.
- Myasoedov, B. F. and F. I. Pavlotskaya, 1989, "Measurement of Radioactive Nuclides in the Environment," *Analyst*, Vol. 114, pp. 255–263.

- Newman, Meredith E., Indrek Porro, Rick M. Scott, Frank W. Dunnivant, Russell D. Goff, Matthew M. Blevins, Steve D. Ince, John A. Leyba, Timothy W. DeVol, Alan Elzerman, and Robert A. Fjeld, 1996, *Evaluation of the Mobility of Am, Cs, Co, Pu, Sr, and uranium through INEL Basalt and Interbed Materials: Summary Report of the INEL/Clemson University Laboratory Studies*, INEL-95/282, EDF-ER-WAG7-82, Idaho National Laboratory, Clemson University, Clemson, South Carolina.
- Olson, Gail, 2004, *OU 7-13/14 Field Representative GEM Logbook-Glovebox Book*, ER-038-2004, Rev. 0, Idaho National Laboratory, January 20, 2004 – February 20, 2004.
- Rightmire, C. T. and B. D. Lewis, 1987, *Hydrogeology and Geochemistry of the Unsaturated Zone, Radioactive Waste Management Complex, Idaho National Engineering Laboratory, Idaho*, USGS Water-Resources Investigations Report 87-4198, U.S. Department of Energy Idaho Operations Office DOE/ID-22073, U.S. Geological Survey.
- Rosentreter, J. J., R. Nieves, J. Kalivas, J. P. Rousseau, and R. C. Bartholomay, 1999, *The Use of Chemical and Physical Properties for Characterization of Strontium Distribution Coefficients at the Idaho National Engineering and Environmental Laboratory, Idaho*, Water-Resources Investigations Report 99-4123, U.S. Geological Survey.
- Salomon, Hopi, Daryl R. Haefner, Beth A. McIlwain, Jila Banaee, Jeffrey J. Einerson, and Anna K. Podgorney, 2003, *Field Sampling Plan for the OU 7-10 Glovebox Excavator Method Project*, INEEL/EXT-02-00542, Rev. 2, Idaho National Laboratory.
- Ullman, N. R., 1972, *Statistics: An Applied Approach*, Lexington, MA: Xerox College Publishing, Xerox Corporation.
- Vejvoda, Edward, 2005, *Summary of Rocky Flats Waste Buried in the Subsurface Disposal Area*, ICP/EXT-04-00717, Idaho Completion Project.